Lessons 19 and 20

- **First results from High Energy Astrophysical Neutrino Telescope (like BAIKAL, AMANDA, ANTARES, IceCube, KM3NeT…)**
- **Multimessenger searches: the GW-ν connection**
- **Other physics items of study for Neutrino Telescopes**
    - **Neutrino oscillations**
    - **Neutrino mass hyerarchy**
    - **Indirect search for Dark Matter**
    - **….**
- **New techniques for larger detectors for higher energies (acoustic detectors, radio detectors)**

Multi-messenger approach: Gravitational Waves and ν

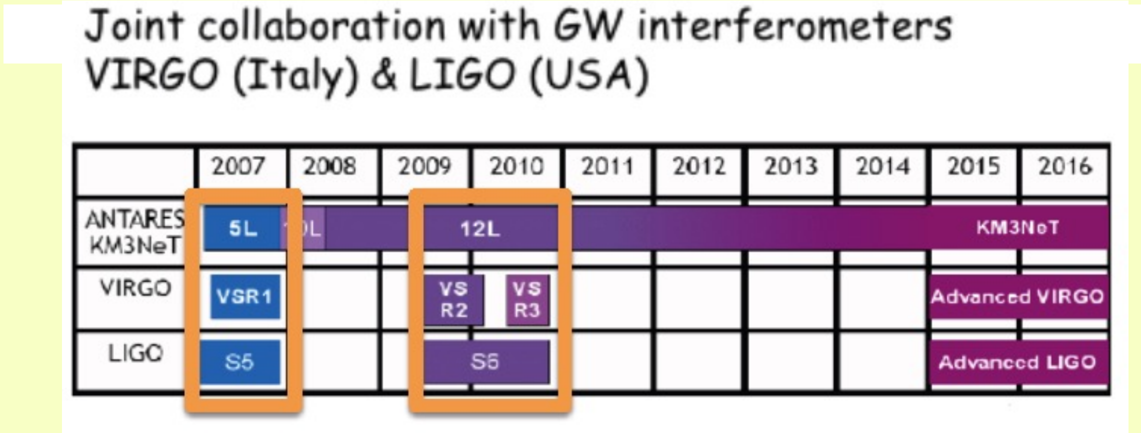

High Energy Neutrino Astrophysics

- Possible common sources: (GRB-core collapse into BH; SGR – powerful magnetars; hidden sources)
- Sky regions in common
- Expected low signals, coincidences increase chances of detection
- GW & HEN is a must
- First analysis completed with 2007 concomitant dataset: no coincidence found -> exclusion distance on common GW/HEN possible sources: *ANTARES & LIGO & VIRGO Coll., JCAP 06 (2013) 008*
- Analysis of 2009-2010 dataset ongoing

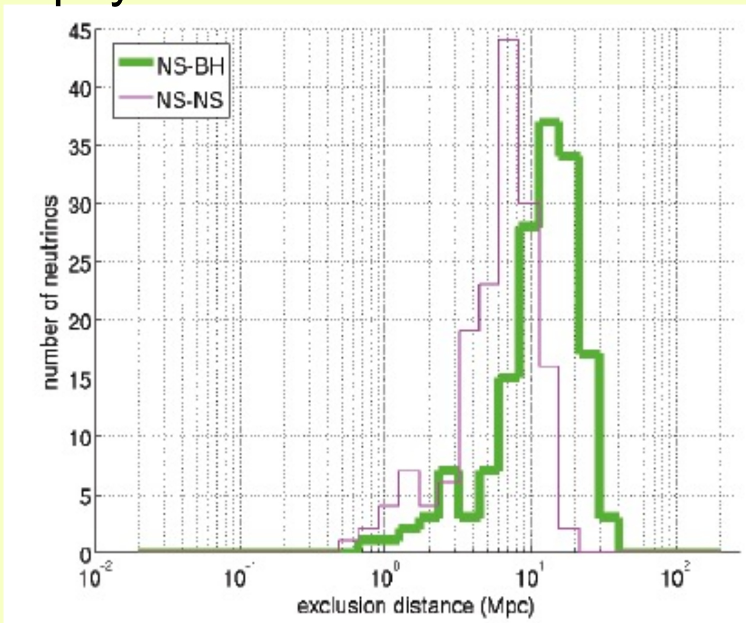

Dal Cosmo ci aspettiamo anche le onde gravitazionali

Interferometro di Michelson: due fasci di luce laser, provenienti dai due bracci, vengono ricombinati in opposizione di fase su un rivelatore di luce in maniera che, normalmente, non arrivi luce sul rivelatore. Un'onda gravitazionale varia la lunghezza dei "bracci". La variazione del cammino ottico, causata dalla variazione della distanza tra gli specchi che varia, produce un piccolissimo sfasamento tra i fasci e quindi un'alterazione dell'intensità luminosa osservata, proporzionale all'ampiezza dell'onda gravitazionale.

Interferometro Virgo, costruito a Càscina, nei pressi di Pisa.

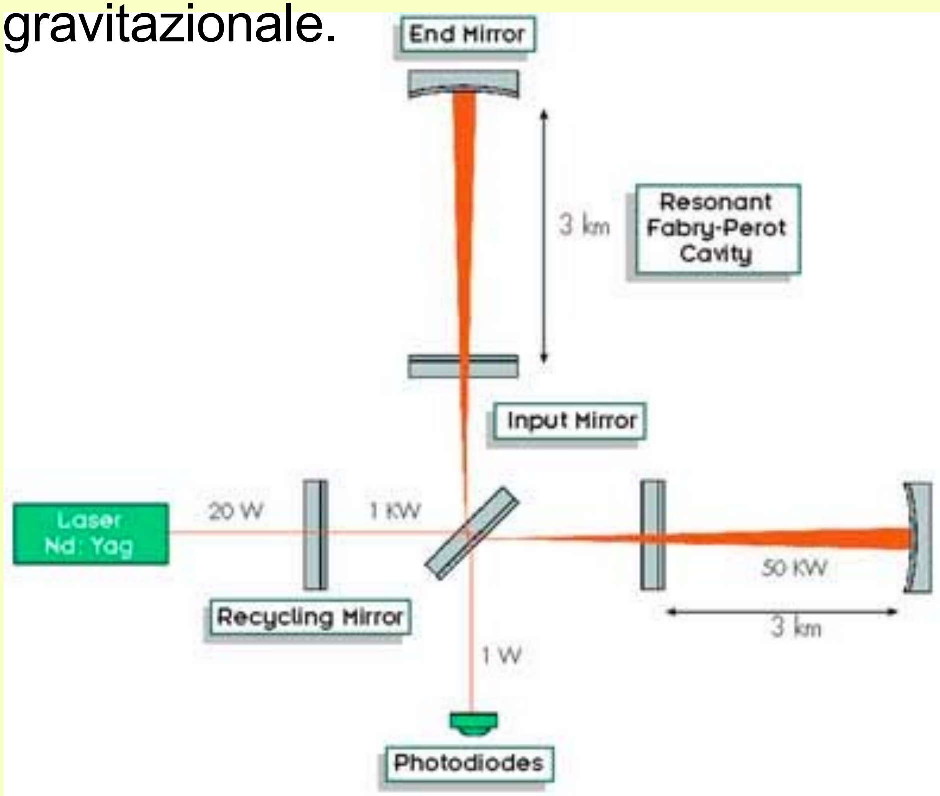

ANTARES sensitivity

For binary neutron star systems of (1.35-1.35) M_{Sun} and black hole-neutron star systems of (5-1.35) M_{Sun} typical distance limits are 5Mpc and 10Mpc respectively.

For the sine-Gaussian waveforms with $E_{GW} = 10^{-2}\ M_{sun}\ c^2$ we find typical distance limits between 5Mpc and 17Mpc in the low-frequency band and of order 1Mpc in the high-frequency band.

For other E_{GW} the limits scale as $D_{90\%} \propto (E_{GW}/\ 10^{-2}\ M_{Sun}\ c^2)^{1/2}$. For example, for $E_{GW} = 10^{-8}\ M_{Sun}\ c^2$ (typical of core-collapse supernovae) a signal would only be observable from a Galactic source.

Febbraio 2016: annunciata la prima osservazione di onda gravitazionale, GW150914

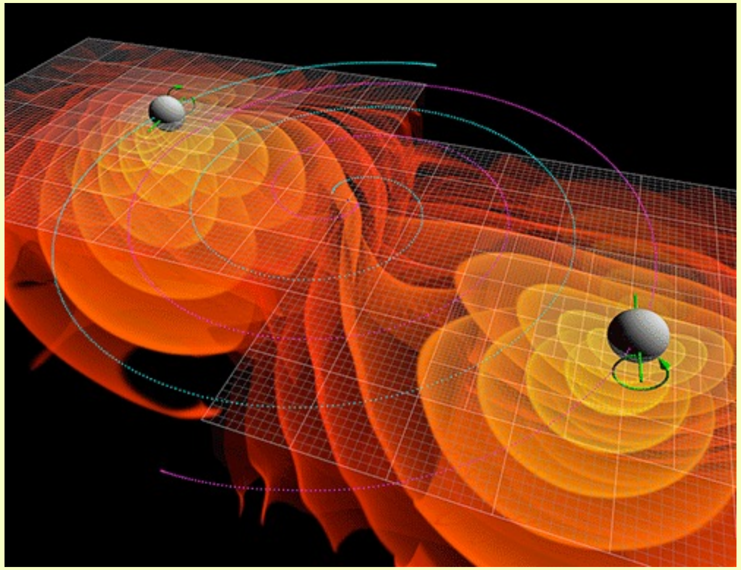

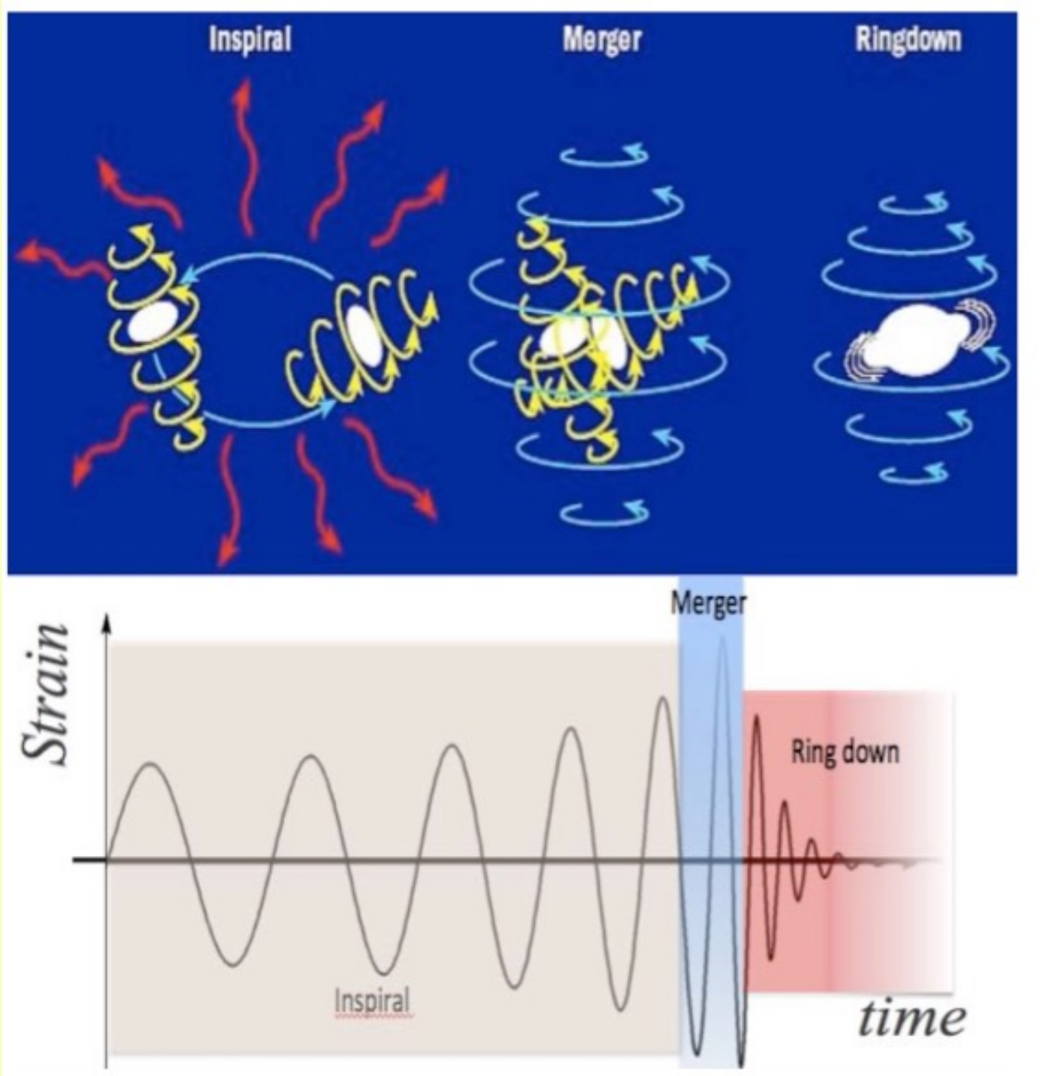

Avvicinamento, e mescolamento di due "buchi neri": la rivelazione dell'onda gravitazionale così generata ha aperto la strada ad una nuova epoca di osservazioni astronomiche

Il primo evento "GW" osservato

L'apparato LIGO è composto da due interferometri in due distanti località.
GW150914 è stata osservata in contemporanea dai due interferometri.

GW150914: il primo evento osservato il 14/09/2015

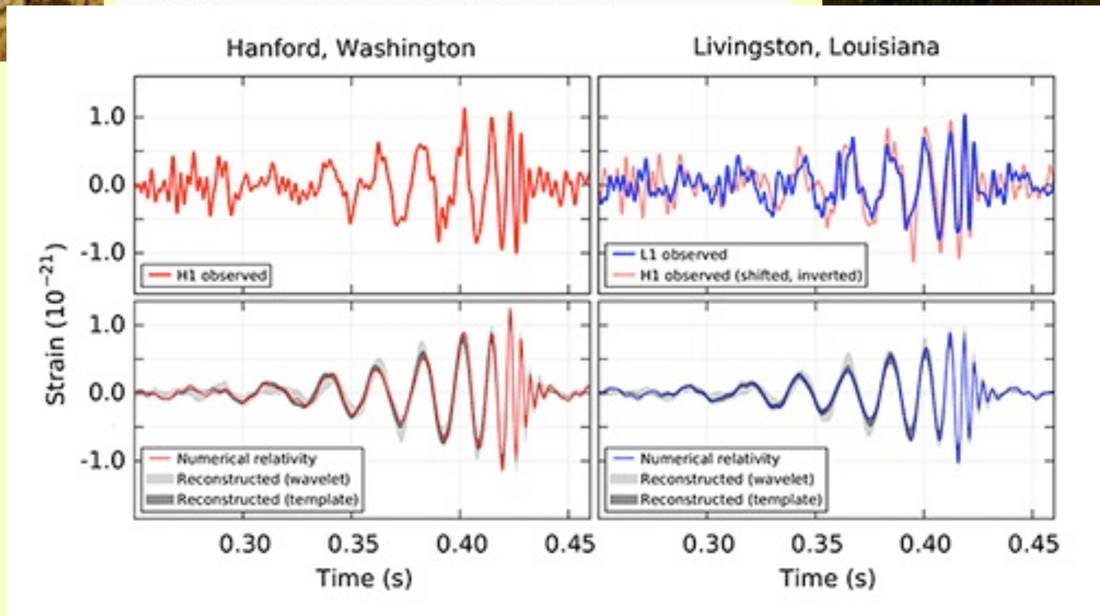

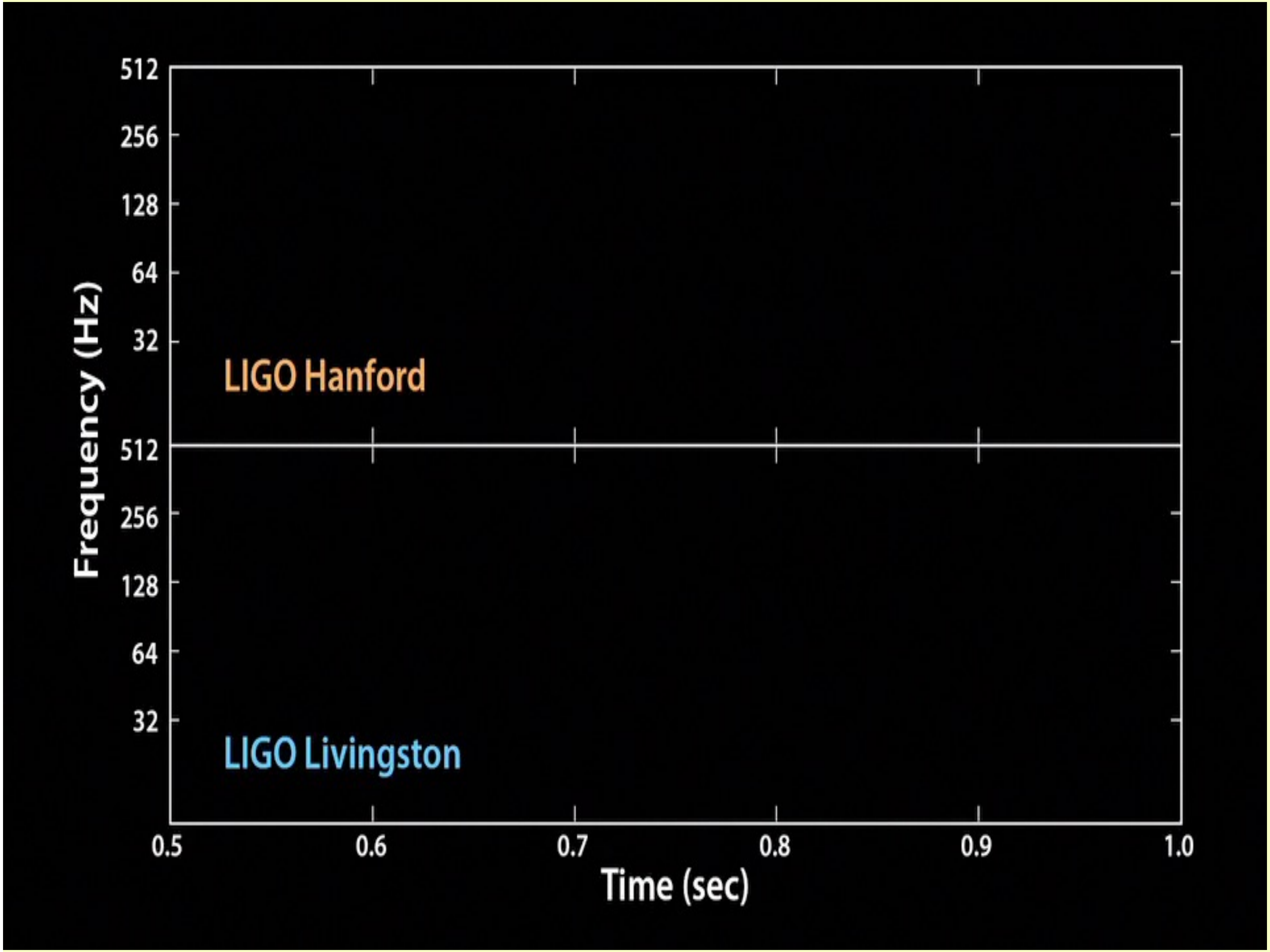
512
256
128
64
32
LIGO Hanford
512
256
128
64
32
LIGO Livingston
Frequency (Hz)
0.5
0.6
0.7
0.8
0.9
1.0
Time (sec)

ANTARES Multi-messenger program
ν follow-up of GW sources - 1

3 alerts sent by LIGO during the run 01 (2015/09 → 2016/01):

- GW150914: merging of 2 BHs (M= 36/29 M_{Sun} - 410 Mpc - 5.1σ)
- LVT151012: merging of 2 BHs (M= 23/13 M_{Sun} -1000 Mpc - 1.7σ)
- GW151226: merging of 2 BHs (M= 14/7 M_{sun} - 440 Mpc -> 5σ)

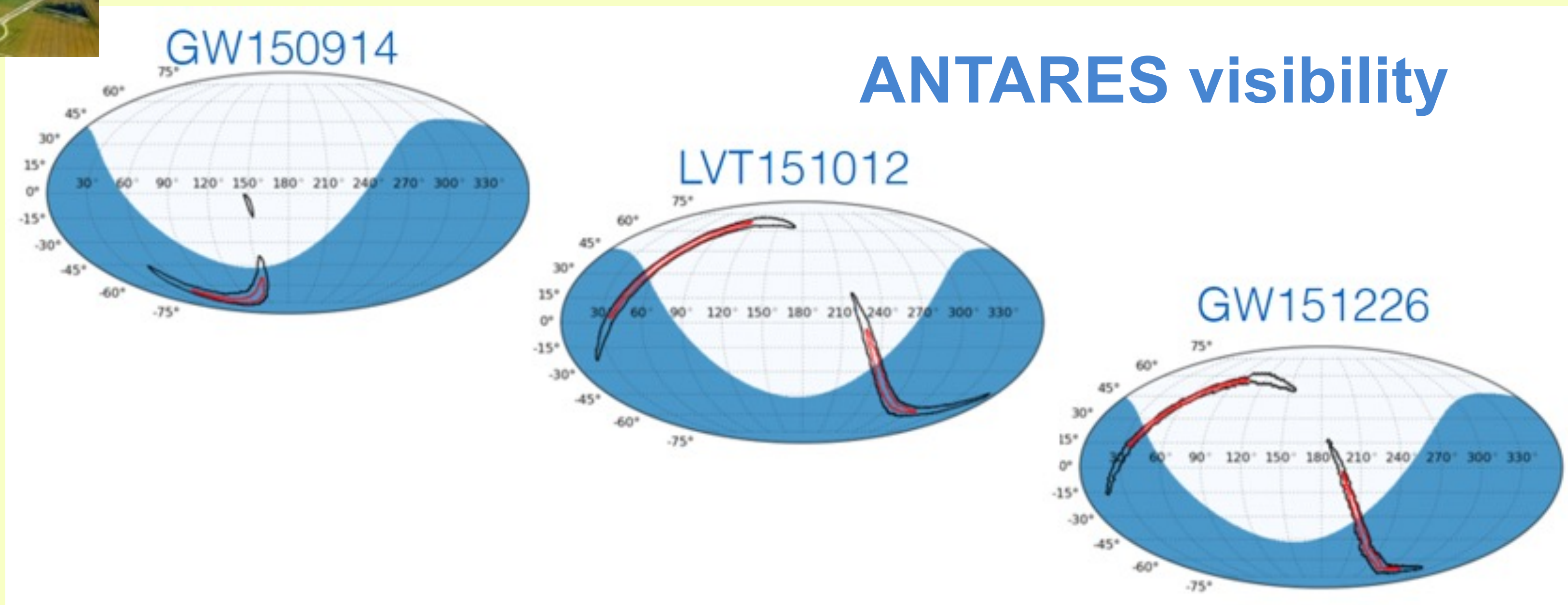

ANTARES Multi-messenger program
ν follow-up of GW sources - 2

The LIGO event GW170104 during run 02 (Nov. '16 – Aug. '17):

- GW170104: merging of 2 BHs (M= 31/19 M_{Sun} - 880 Mpc)

ANTARES visibility for up-going tracks includes 51% of LIGO/Virgo error box

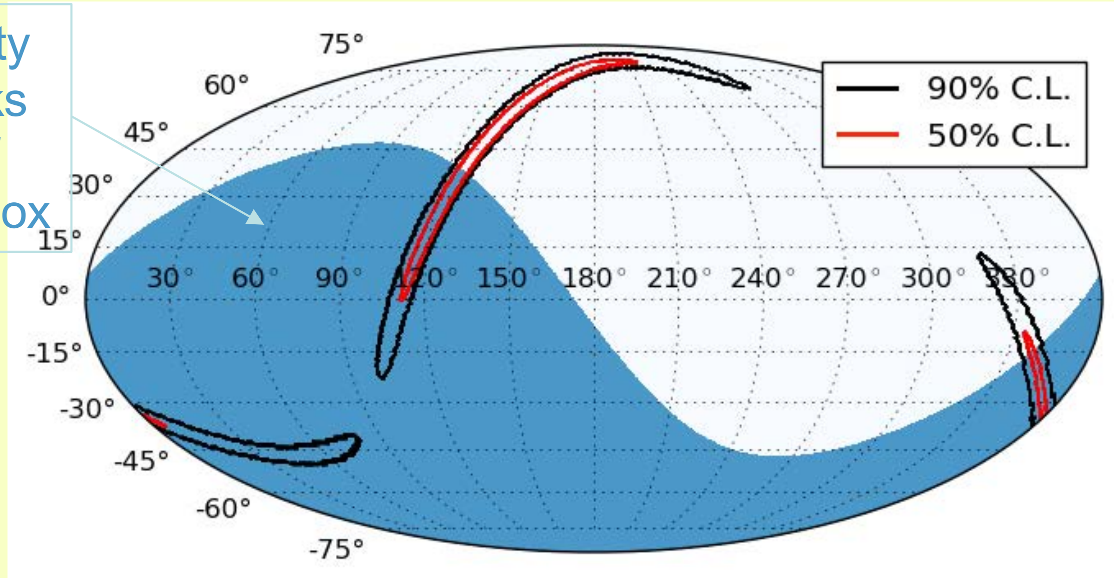

No neutrino candidates were found within ±500 s around the GW event time (result in <24h after the alert) nor any time clustering of events over an extended time window of ±3months.

ANTARES Multi-messenger program
ν follow-up of GW sources - 3

The search for neutrinos over $\pm$3 months around the GW170104 alert was performed by looking for time clustering of up-going neutrino events.
No events observed.

The non-detection is used to constrain isotropic-equivalent high-energy neutrino emission from GW170104 to less than $4 \cdot 10^{54}$ erg for a E^{-2} spectrum.

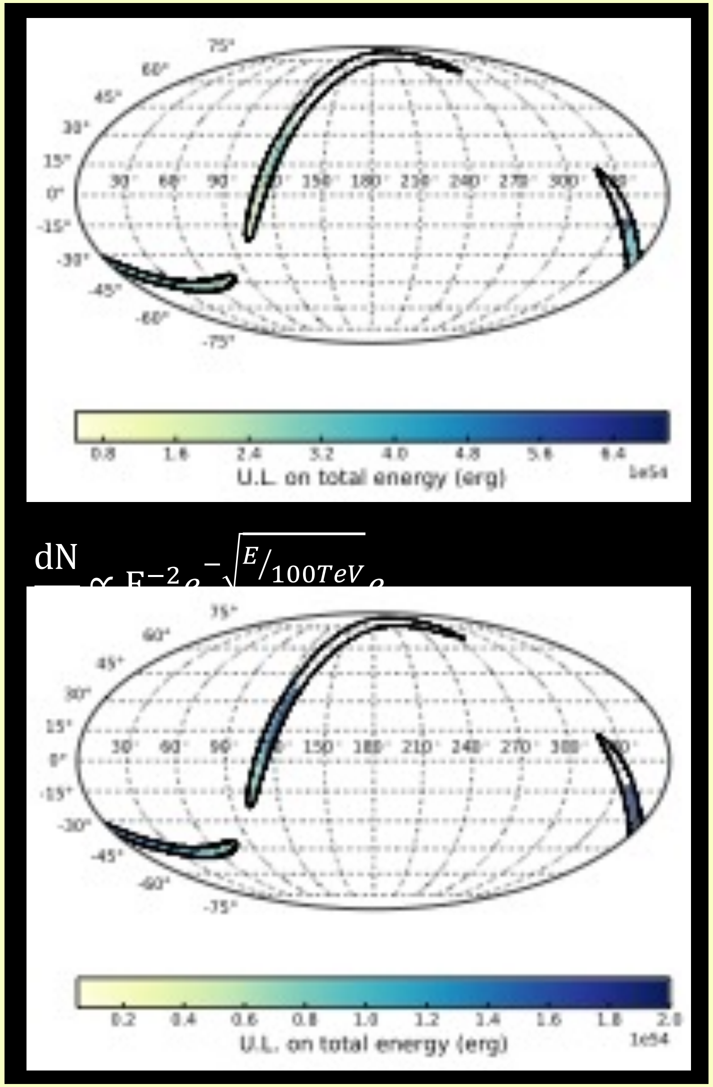

The most wanted object: NS-NS (NS-BH) GW

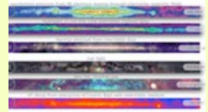

- A rich variety of phenomena in the case of NS-NS merging
- GW standard “siren”
- Neutrinos ν
- EM counterpart
  - Fast emission (GRB)
    - Beamed emission
    - Afterglow (X-ray,…)
  - Kilonova (*)
    - Isotropic emission
    - Neutron-rich ejecta
  - Radio emission
- UHECR’s acceleration?

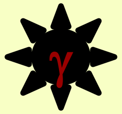

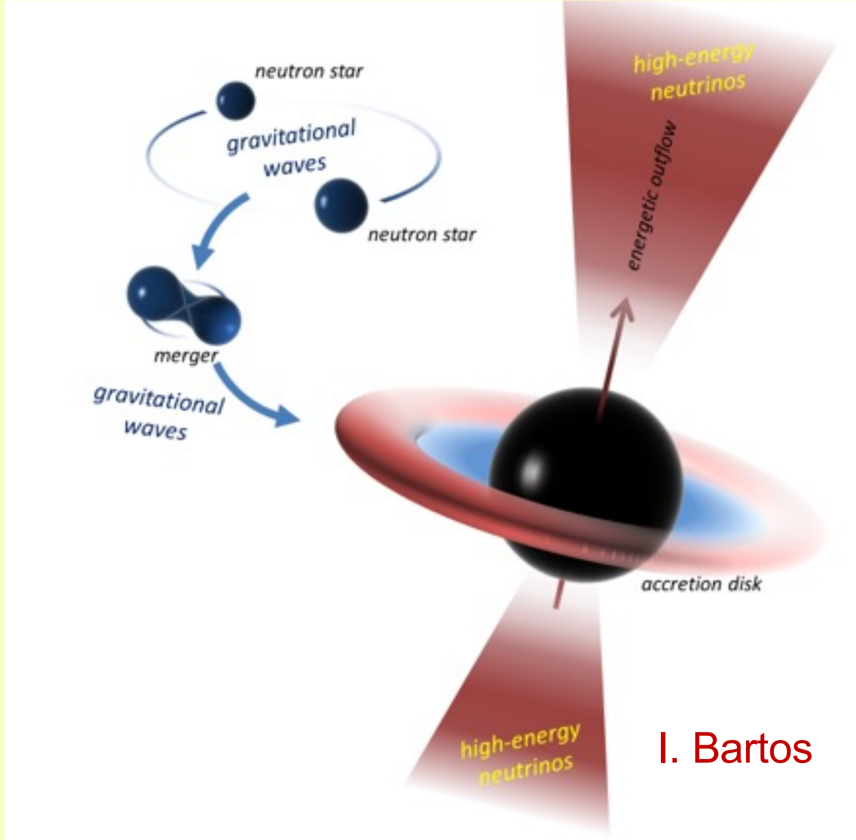

(*) By radioactive decay of heavy elements produce via r-process nucleosynthesis in the neutron-rich merger ejecta

17 August 2017: NS-NS cohalescence

A joint ANTARES/IceCube/LigoSC/Virgo/Auger analysis performed as "Neutrino follow-up" of GW170817

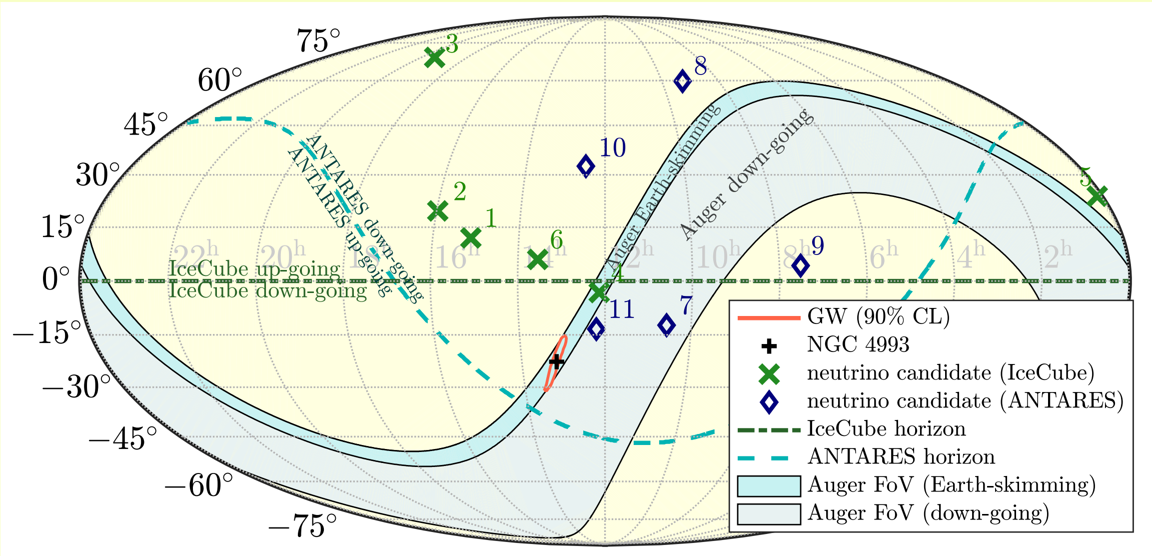

The location of this source was nearly ideal for Auger.
It was well above the horizon for IceCube and ANTARES for prompt observations.
IceCube and ANTARES sensitivity is then limited for neutrinos with E_ν < 100 TeV.

- A **short gamma-ray burst** (GRB) that followed the merger of this binary system was **recorded by the Fermi-GBM** (E_{iso} ~$4 \cdot 10^{46}$ erg) and **INTEGRAL.**
- Advanced LIGO and Advanced Virgo observatories reported **GW170817**
- Optical observations allowed the precise localization of binary neutron star inspiral in **NGC4993** at ~ **40Mpc**.
- **ANTARES**, **IceCube**, and **Pierre Auger Observatories** searched for high-energy neutrinos from the merger in the **10^{11} eV–10^{20} eV** energy range .
- **IceCube** detector is also sensitive to outbursts of **MeV neutrinos** via a simultaneous increase in all photomultiplier signal rates.

A joint ANTARES/IceCube/LigoSC/Virgo/Auger analysis performed as "Neutrino follow-up" of GW170817

- **No neutrinos** directionally coincident with the source were **detected within ±500 s** around the merger time**.**
- Additionally, **no MeV neutrino burst signal was detected (in IceCube) *coincident with the merger*.**
- In **Pierre Auger Observatory no** inclined showers passing the Earth-skimming selection (**neutrino candidates**) **were found in the time window ±500 s** around the trigger time of GW170817**.**
- **No neutrino found in an extended search in the direction within the 14-day period following the merger.**
- **GRB170817A's** observed **prompt gamma-ray emission**, as well as Fermi-GBM's luminosity constraints for extended gamma-ray emission, are **significantly below typical values for observed short GRBs**. One possible explanation for this is the **off-axis observation of the GRB**.

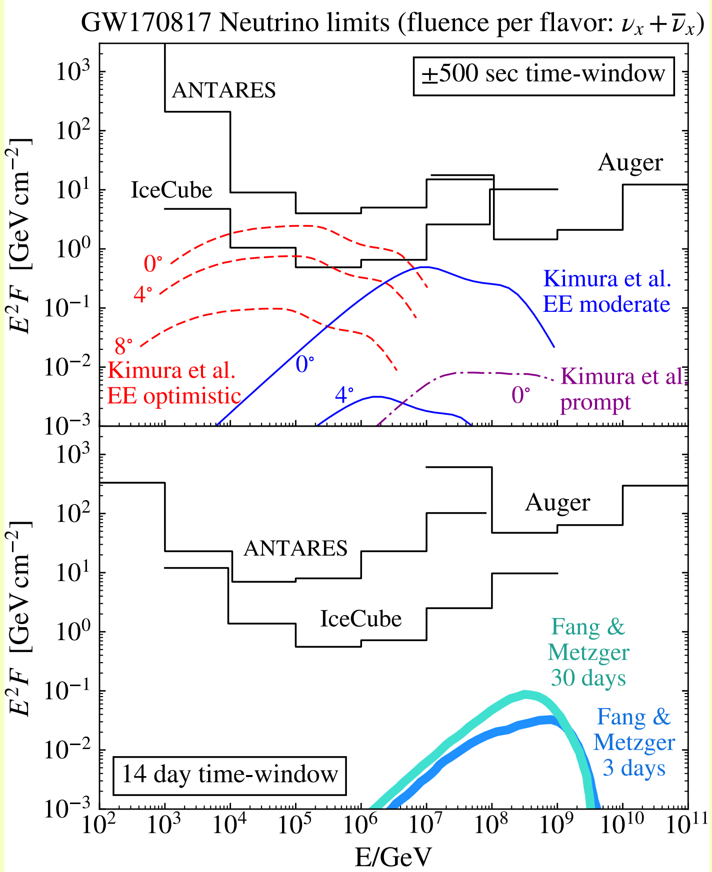

- The non observation of neutrinos allow to put limits both extended emission (EE) and prompt emission (scaled to a distance of 40 Mpc): limits are shown for the case of on-axis viewing angle (0) and selected off-axis angles to indicate the dependence on this parameter.

… not only neutrino astrophysics…

… also open problems in particle physics …

- Dark Matter searches:
  - Neutralino annihilation in Sun, Earth, Galactic Center
- Magnetic Monopoles
- Particle acceleration mechanisms
- Multi-messenger searches
- Neutrino Oscillations
- Search for Sterile Neutrinos
- …

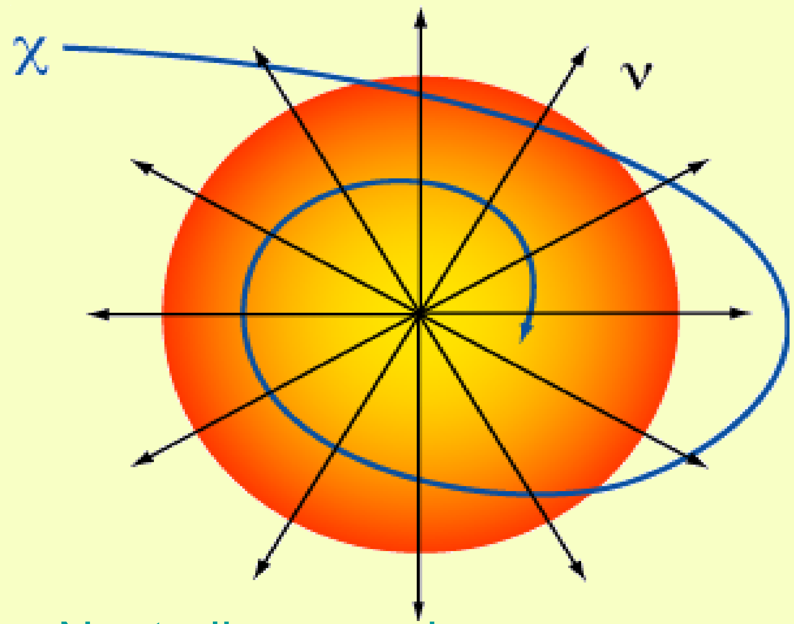

Neutralino search: $\chi\chi \rightarrow \nu + \ldots$

Neutrino oscillations

We have calculated the "oscillation probability" in the case of 2 mass-eighenstates neutrinos(ν_1 and ν_2) considering the neutrinos eighenstates of weak interactions (ν_α and ν_β) as their linear combination

$$\begin{pmatrix} \nu_\alpha \\ \nu_\beta \end{pmatrix} = \begin{pmatrix} \cos\theta & \sin\theta \\ -\sin\theta & \cos\theta \end{pmatrix} \begin{pmatrix} \nu_1 \\ \nu_2 \end{pmatrix}$$

time ←

Interaction of the neutrino as a "weak interaction" state ν_β

Propagation in space-time of the superposition of state ν_1 e ν_2

Creation of the state ν_α

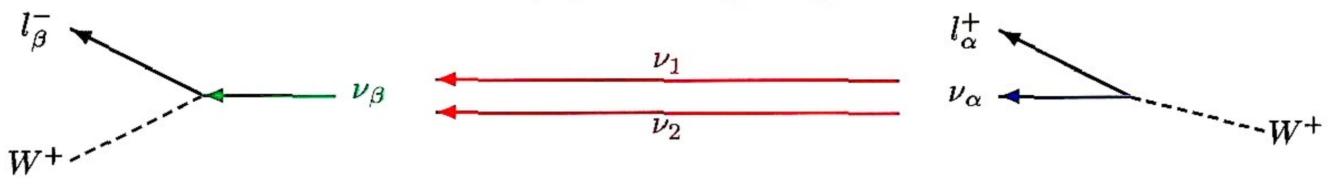

$$P(\nu_\alpha \to \nu_\beta) = \left| \begin{pmatrix} 0 \\ 1 \end{pmatrix} \begin{pmatrix} \cos\theta & \sin\theta \\ -\sin\theta & \cos\theta \end{pmatrix} \begin{pmatrix} e^{-i(E_1 t - p_1 L)} & 0 \\ 0 & e^{-i(E_2 t - p_2 L)} \end{pmatrix} \begin{pmatrix} \cos\theta & -\sin\theta \\ \sin\theta & \cos\theta \end{pmatrix} \begin{pmatrix} 1 \\ 0 \end{pmatrix} \right|^2$$

$$= \sin^2(2\theta) \cdot \sin^2\left(\frac{\Delta m^2 \cdot L}{4E}\right) \qquad \text{with } \lambda_{osz} = \frac{4\pi \cdot E}{\Delta m^2} = 2.5\, km \cdot \frac{E[GeV]}{\Delta m^2[eV^2]}$$

$$\text{relative phase: } \Delta\Phi(L,t) = \Delta E t - \Delta p L = \frac{\Delta m^2 \cdot t}{E_1 + E_2} + \Delta p \cdot \underbrace{\left(\frac{p_1 + p_2}{E_1 + E_2} t - L\right)}_{\approx 0} \approx \frac{\Delta m^2 \cdot t}{2E}$$

Neutrino oscillations

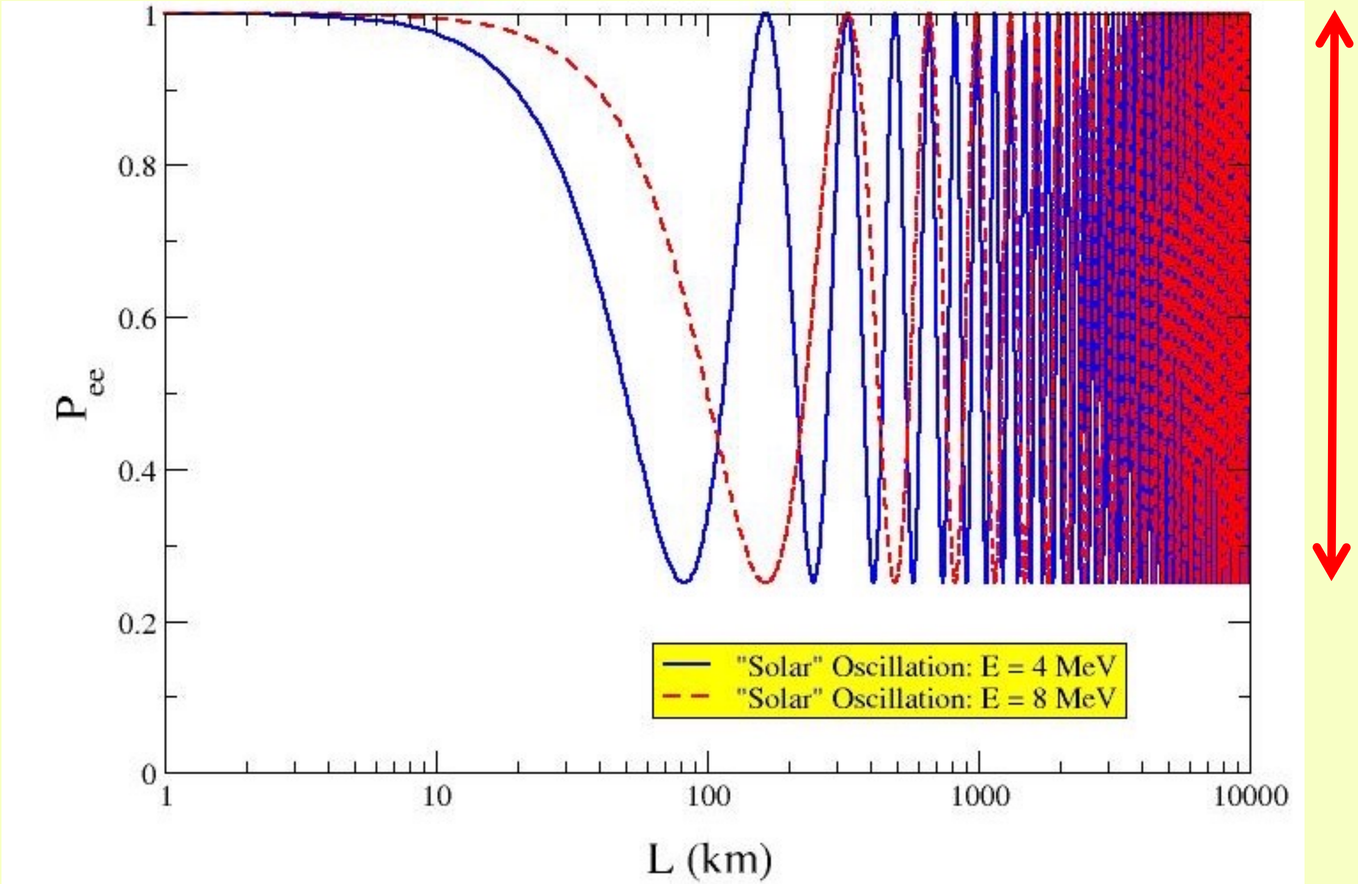

$\sin^2(2\theta)$

$$P_{ee} = 1 - \sin^2 2\theta \cdot \sin^2 k\Delta m^2 L/E$$

$$k = 1.27\ \text{MeV}/(\text{m}\cdot\text{eV}^2)$$

Atmosferic Neutrinos

The expected value of the relationship between different types of atmospheric neutrinos is

$$\nu_\mu / \nu_e \sim 2$$

– π production and decay responsible for this value
- k production and decay contribute mainly to ν_e flux

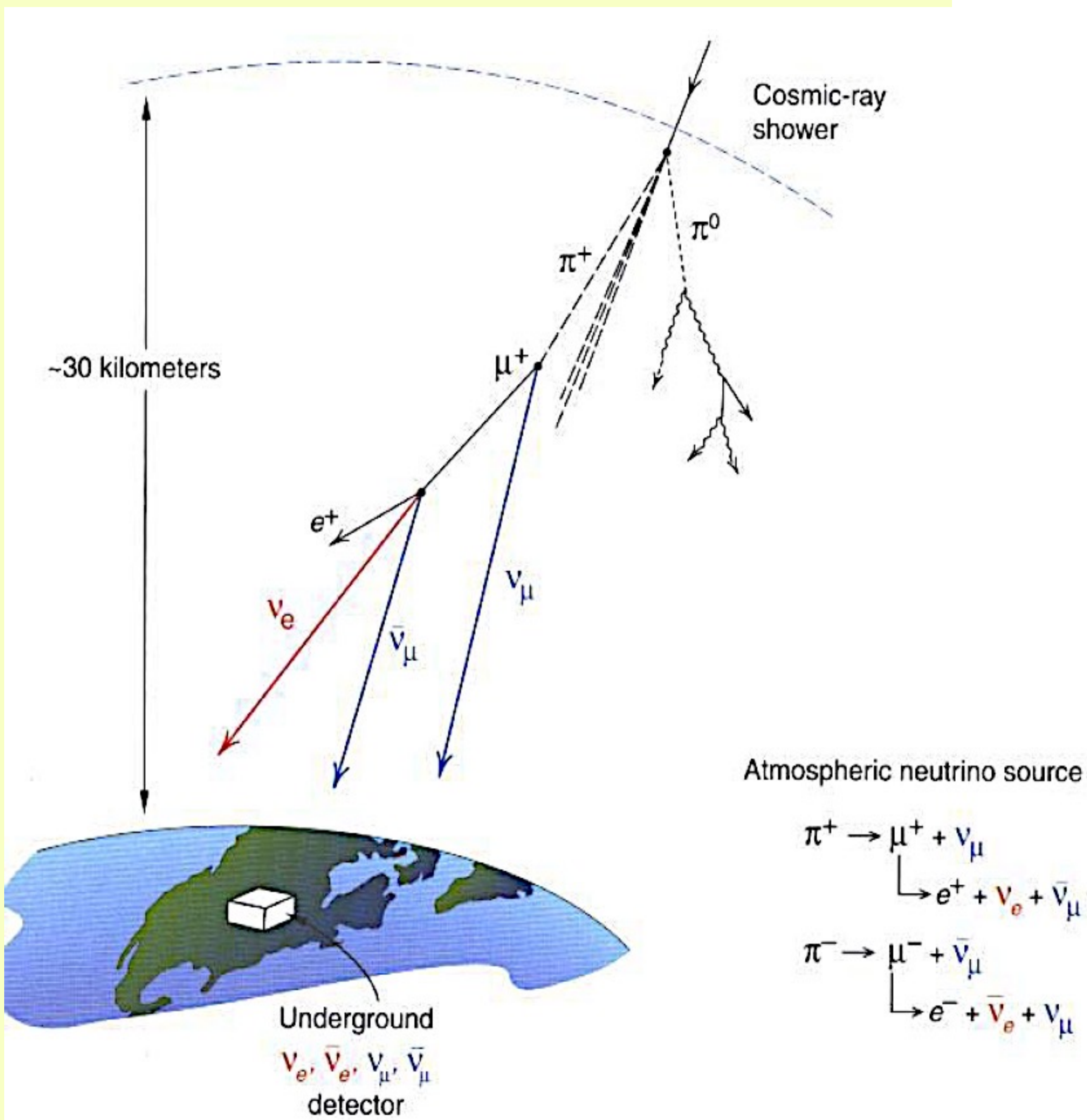

Atmospheric neutrino "deficit" measured

Since 1992 …
Kamiokande (Kamioka Nucleon Decay Experiment), Japan
IMB (Irvine Michigan, Brookhaven), Ohio
Superkamiocande, Japan
MACRO, Italy

upgoing horizontal downgoing

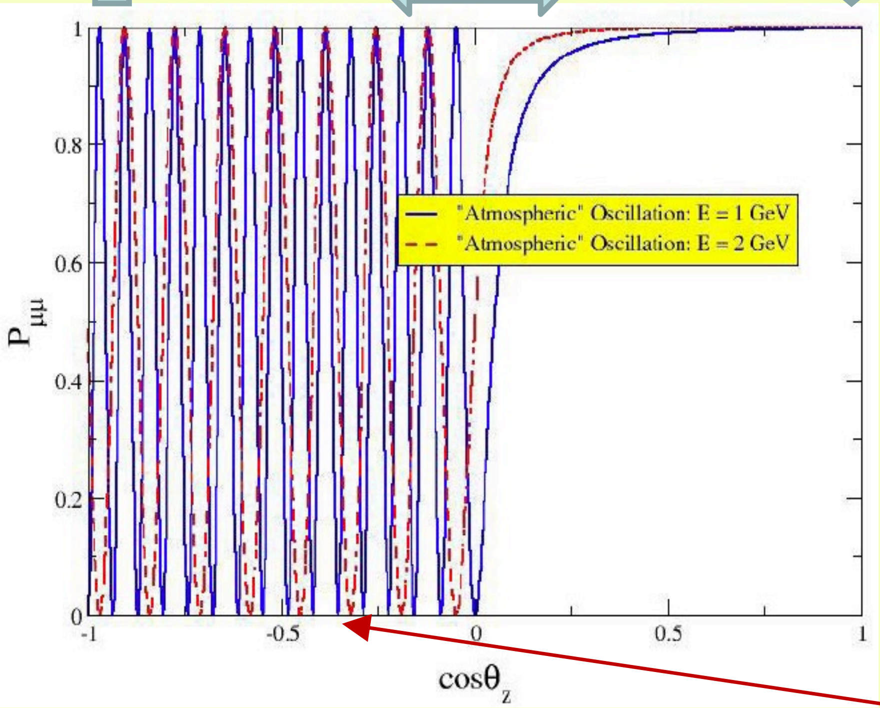

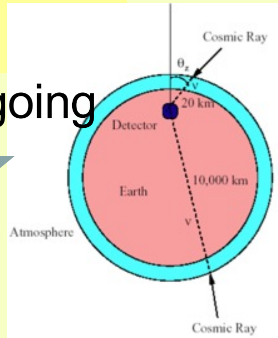

They measure

$\nu_\mu / \nu_e \sim 2$

They reveal all the "down-going" neutrinos expected but only half of those "from below"

In 1998 Superkamiocande officially announces the evidence of "oscillations" of atmospheric neutrinos.

There was still no confirmation of oscillations of "solar" neutrinos. The observed "deficit" could still reflect an error in the calculation of fluxes.

$$P(\nu_\mu \to \nu_\mu) = 1 - sin^2 2\Theta \ sin^2\left(1.27 \frac{\Delta m^2 L}{E}\right)$$

here $2\theta \sim \pi/2$ then the $P_{\mu\mu}$ goes to 0 when $1.27 \frac{\Delta m^2 L}{E} \sim \frac{\pi}{2}$!

ANTARES: atmospheric ν: results

❖ Measurement of atmospheric neutrino oscillations

➢ Two-flavour mixing approximation:

$$P(\nu_\mu \to \nu_\mu) \approx 1 - \sin^2(2\theta_{32})\sin^2\left(\frac{1.27\Delta m^2_{32} L}{E_\nu}\right) = 1 - \sin^2(2\theta_{32})\sin^2\left(\frac{1.27\Delta m^2_{32} D_{Earth}\cos\Theta}{E_\nu}\right)$$

unknown
measurable

world data: first oscillation minimum at $\cos\Theta = 1,\ E_\nu = 24$ GeV (typical μ range ≈ 120 m)

➢ Dedicated low-energy data sample:
2007-2010 (863 active days)
20 GeV < E_ν < 100 GeV
median angular resolution 0.8° (multi-line) → 3° (single-line)

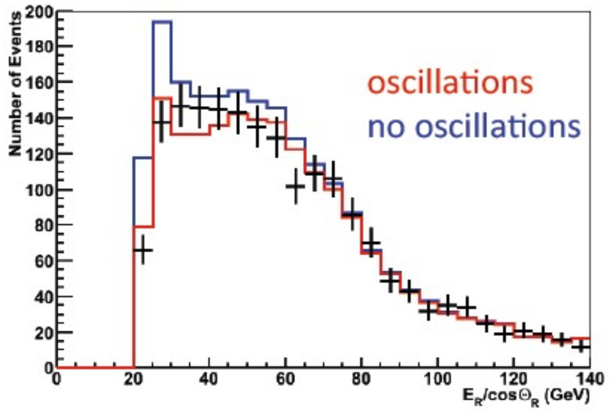

➢ First measurement of neutrino oscillation parameters by neutrino telescope !
(now also measured by IceCube)

➢ Underlines the potential of low-energy extensions of the detector:
→ORCA feasibility study for the measurement of neutrino mass hierarchy (KM3NeT)

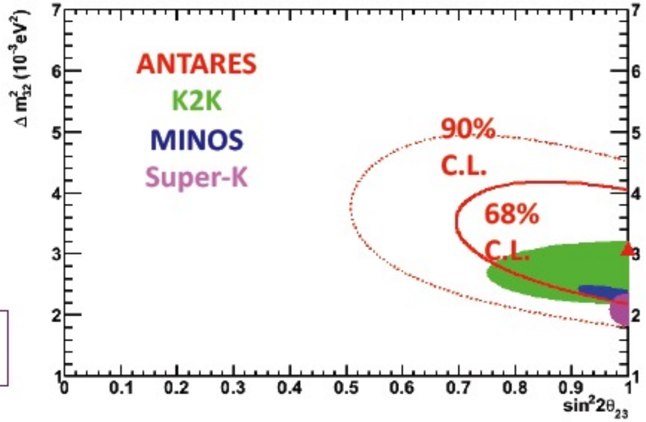

Phys. Lett.B 714 (2012) 224

ν masses and ν oscillations

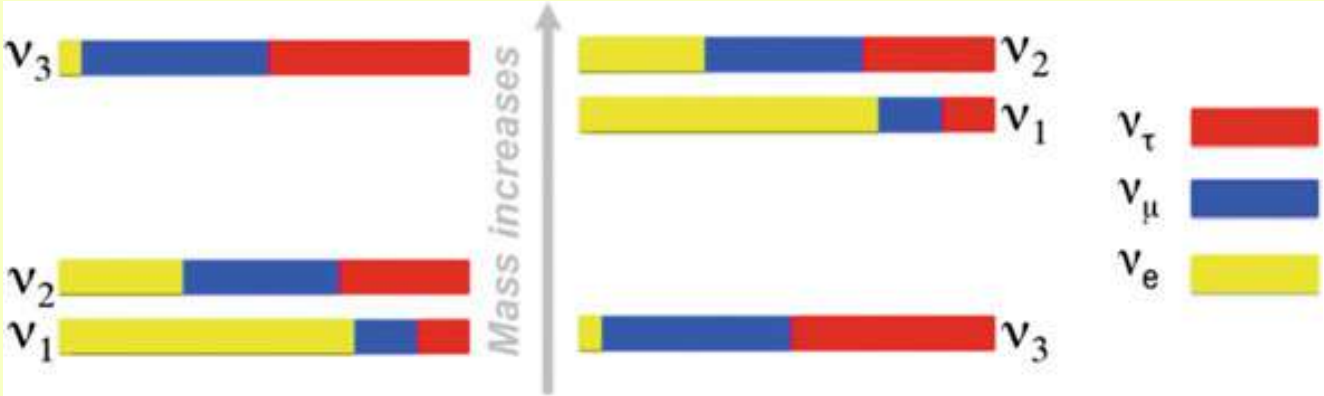

Illustration of the mass spectra compatible with the data from neutrino oscillations; *left* normal hierarchy; *right* inverted hierarchy

	Normal (inverted)	Error (%)	Units
Δm^2	2.50 (2.46)	1.8	10^{-3} eV^2
δm^2	7.37 (7.37)	2.4	10^{-5} eV^2
$\sin^2\theta_{13}$	2.17 (2.19)	4.8	10^{-2}
$\sin^2\theta_{12}$	2.97 (2.97)	6.2	10^{-1}
$\sin^2\theta_{23}$	4.43 (5.75)	16	10^{-1}
δ	1.39 (1.39)	19	π

Results of the global analysis of oscillation data

Indirect search for Dark Matter in the Sun

6 years of ANTARES data: 2007-2012

Distribution of the angular distance between reconstructed the track direction of events and the Sun position for two different track reconstruction algorithms in order to maximize the event reconstruction for single line and multi-lines events.

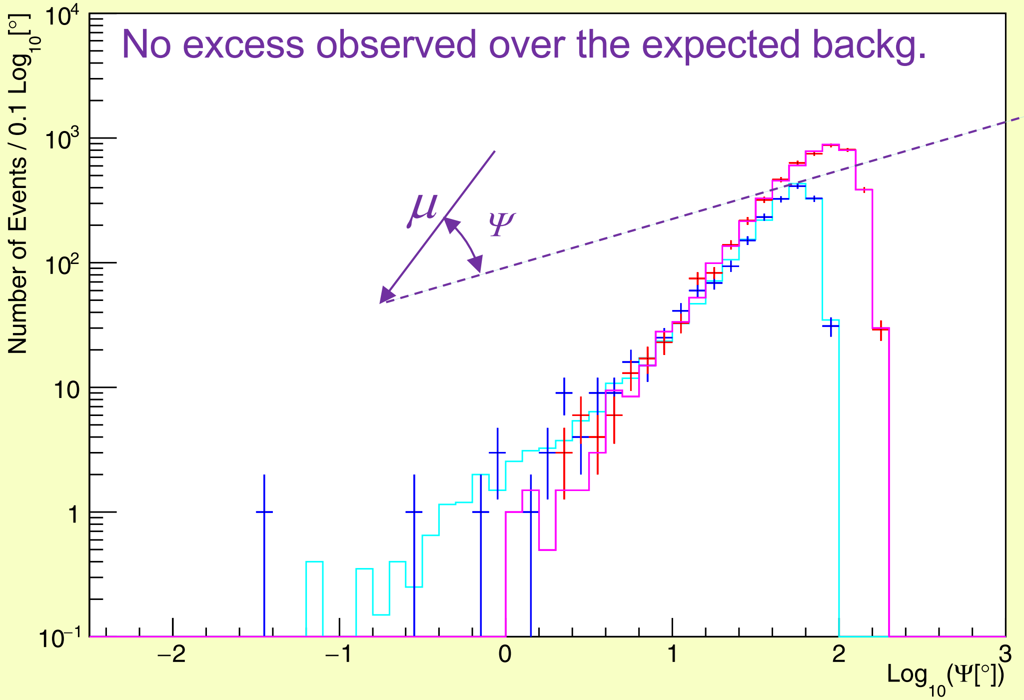

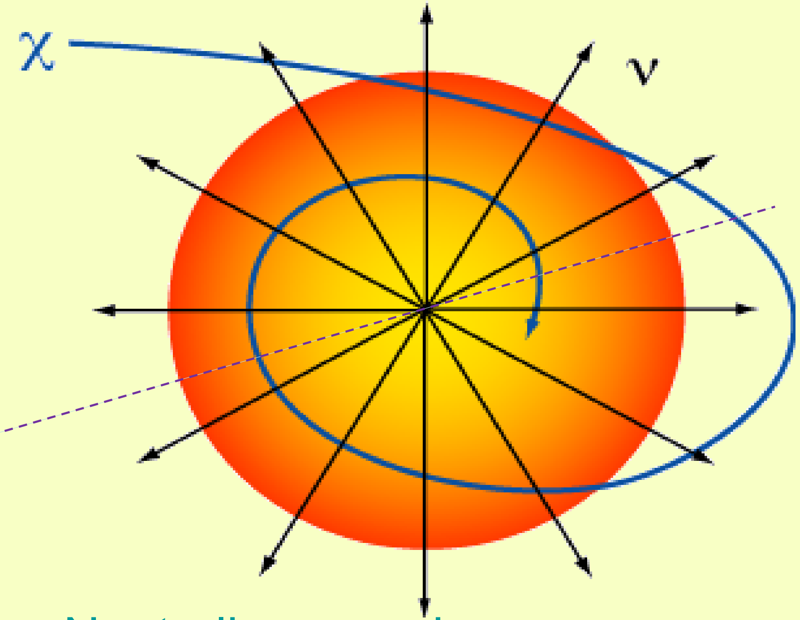

Neutralino search: $\chi\chi \rightarrow \nu + \ldots$

Neutrino spectrum

from WIMPSIM (M. Blennow, J. Edsjö, T. Ohlsson, J. Cosmol. Astropart. Phys. 0801 (2008) 021.)

Background

estimated from time-scrambled data.

Neutrino fluxes from $\boldsymbol{WIMP + WIMP \rightarrow b\bar{b}, W^+W^-, \tau^+\tau^-}$ → $\bar{\nu}\,\nu + \ldots$

evaluated for 50 GeV/c^2 < M_{WIMP} < 5 TeV/c^2

→ limits to ν fluxes and to WIMP-nucleon cross sections

The analysis strategy

Maximization of a likelihood function based on the knowledge of the probability density functions, for the contribution of a background event, *B(Ψ, N_{hit}, β)*, or a signal event, *S(Ψ, N_{hit}, β), to the observed distribution*.

$$\mathcal{L}(n_s) = e^{-(n_s+N_{\rm bg})} \prod_{i=1}^{N_{\rm tot}} \left(n_s S(\psi_i, N_{hit,i}, \beta_i) + N_{\rm bg} B(\psi_i, N_{hit,i}, \beta_i) \right)$$

N_{hit} = number of hit used for the track reconstruction
β = the angular error estimate for the reconstructed track
N_{tot} = tot. Number of reconstructed events
n_s and N_{bg} are the number of signal and background events in the maximization procedure

B(Ψ, N_{hit}, β) obtained by the collected data randomising the right ascension of the event
S(Ψ, N_{hit}, β) obtained from MC simulation using the ν energy spectra given by WIMPSIM

High statistics Pseudo-MC experiments are performed for each combination of M_{WIMP}, annihilation channel:

- *with only background $n_s = 0$ → allow to evaluate $\mathcal{L}(0)$*
- *with a given value of simulated signal-like events $n_s > 0$. For each one of these pseudo-MC experiment a maximum likelihood analysis is performed searching for the value of n_s that maximize the likelihood. We then get $\mathcal{L}(n_{max})$*

We can now evaluate a Test Statistic $\boldsymbol{TS = \log_{10}\frac{\mathcal{L}(0)}{\mathcal{L}(n_{max})}}$ that gives us a measure of the probability to assume a fluctuation of the background as a distribution of events with $n_s \neq 0$.

ANTARES: indirect search for DM, Background estimation

- The background is estimated by scrambling the data in time
- A fast algorithm is used for muon track reconstruction (Astrop. Phys. 34 (2011) 652-662)
- The effect of the visibility of the Sun is taken into account

All upward-going events from 2007-2008 data

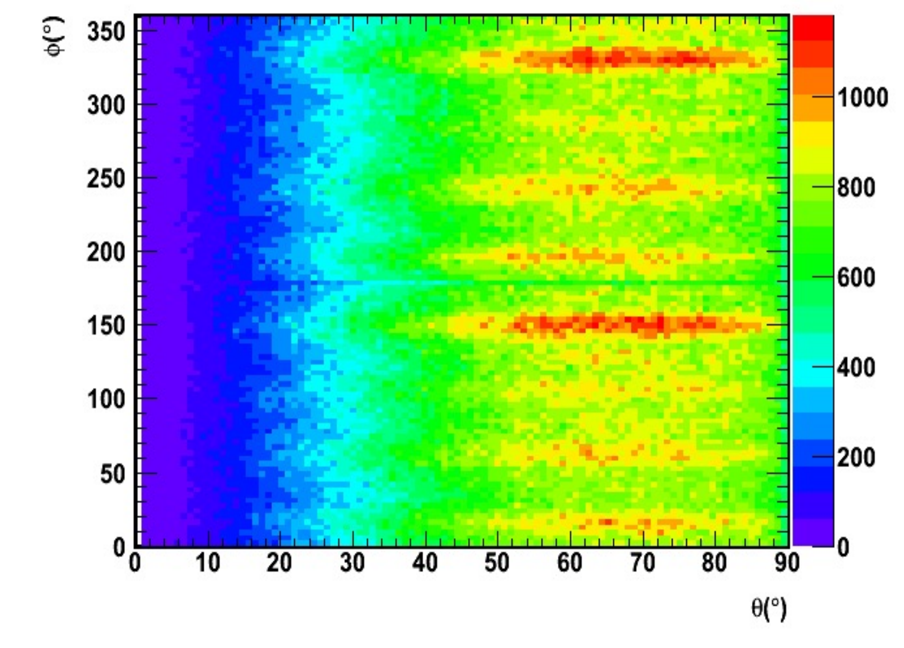

Example of Sun tracking in horizontal coordinates

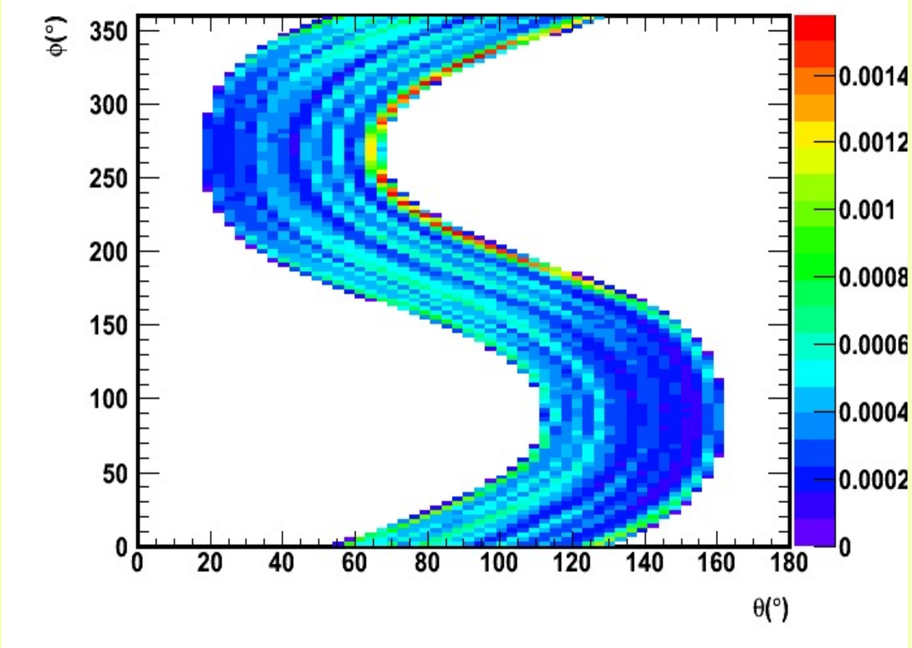

Indirect search for Dark Matter in the Sun

No excess observed over the expected background: evaluate 90% C.L. upper limits for expected signal

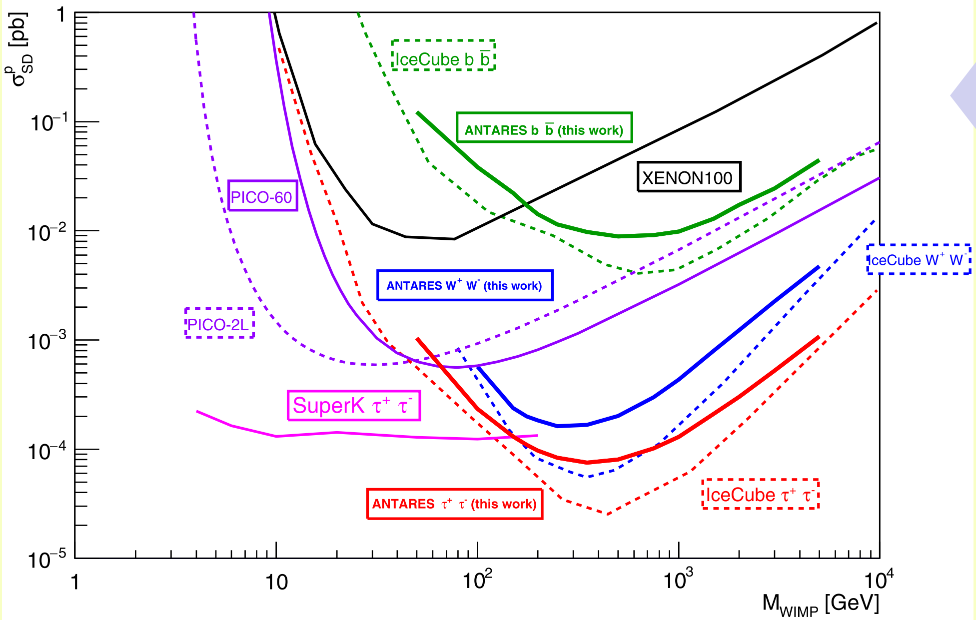

Limits on the spin-dependent WIMP-nucleon scattering cross-section as a function of WIMP mass for the $b\bar{b}$, $\tau^+\tau^-$ and W^+W^- channels.

assumptions:

- capture and annihilations in equilibrium
- local D.M. density =0.4 GeV cm^{-3}
- υ^{DM}_{SUN} according to Maxwell distr. 270 km s^{-1} r,m.s.

Limits on the spin-independent WIMP-nucleon scattering cross-section as a function of WIMP mass for the different channels considered.

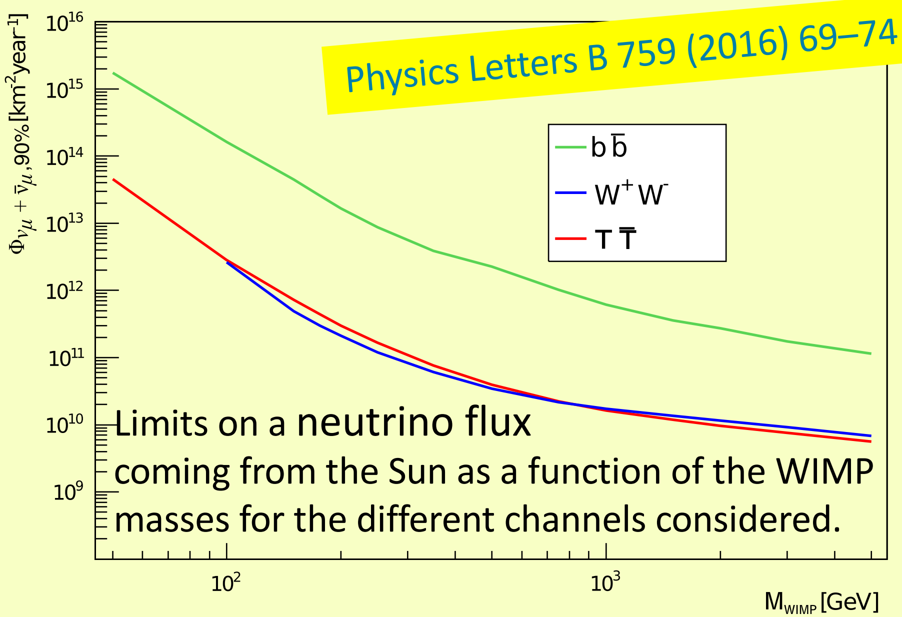

Physics Letters B 759 (2016) 69–74

Limits on a neutrino flux coming from the Sun as a function of the WIMP masses for the different channels considered.

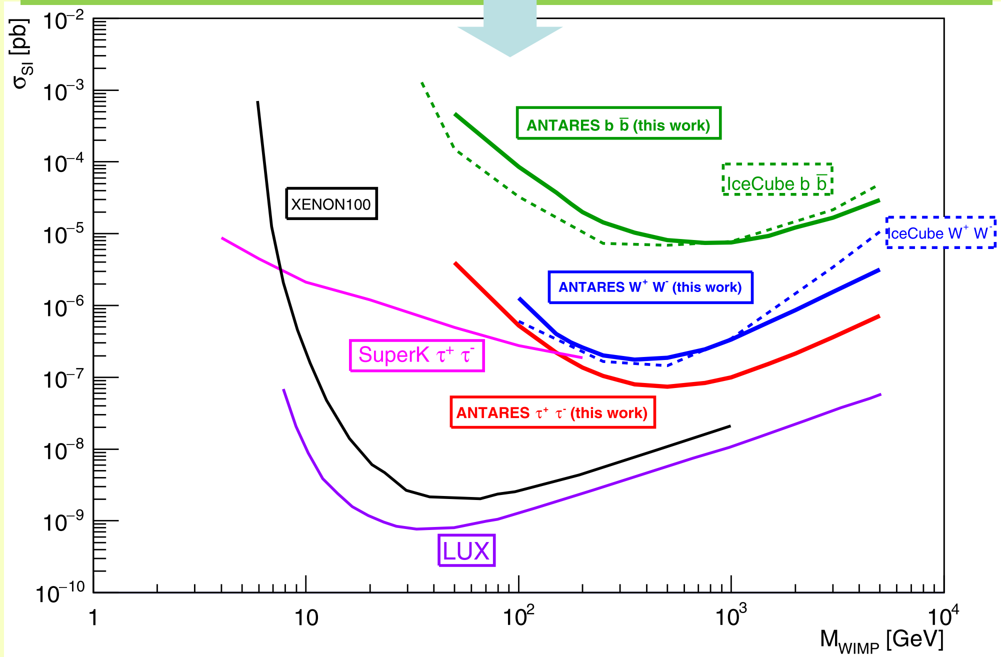

Indirect search for Dark Matter in the Galactic Centre

9 years of ANTARES data: 2007-2015 - ANTARES ”observes” the G.C > 66% time

Search performed for:

- 50 GeV/c^2 < M_{WIMP} < 100 TeV/c^2
- $\boldsymbol{WIMP + WIMP \rightarrow b\bar{b}, W^+W^-, \tau^+\tau^-, \mu^+\mu^-, \nu\bar{\nu}}$

$$\frac{d\Phi_{\nu_\mu+\bar{\nu}_\mu}}{dE_{\nu_\mu+\bar{\nu}_\mu}} = \frac{<\sigma v>}{8\pi M^2_{WIMP}} \cdot \frac{dN_{\nu_\mu+\bar{\nu}_\mu}}{dE_{\nu_\mu+\bar{\nu}_\mu}} \cdot J_{int}(\Delta\Omega)$$

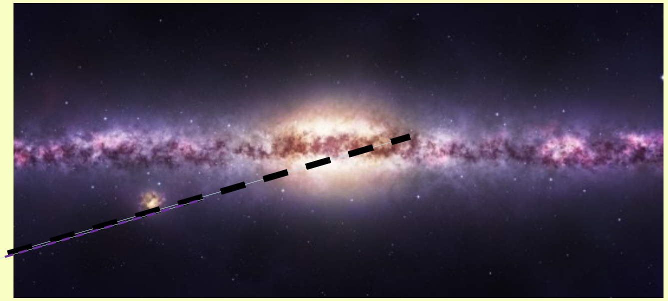

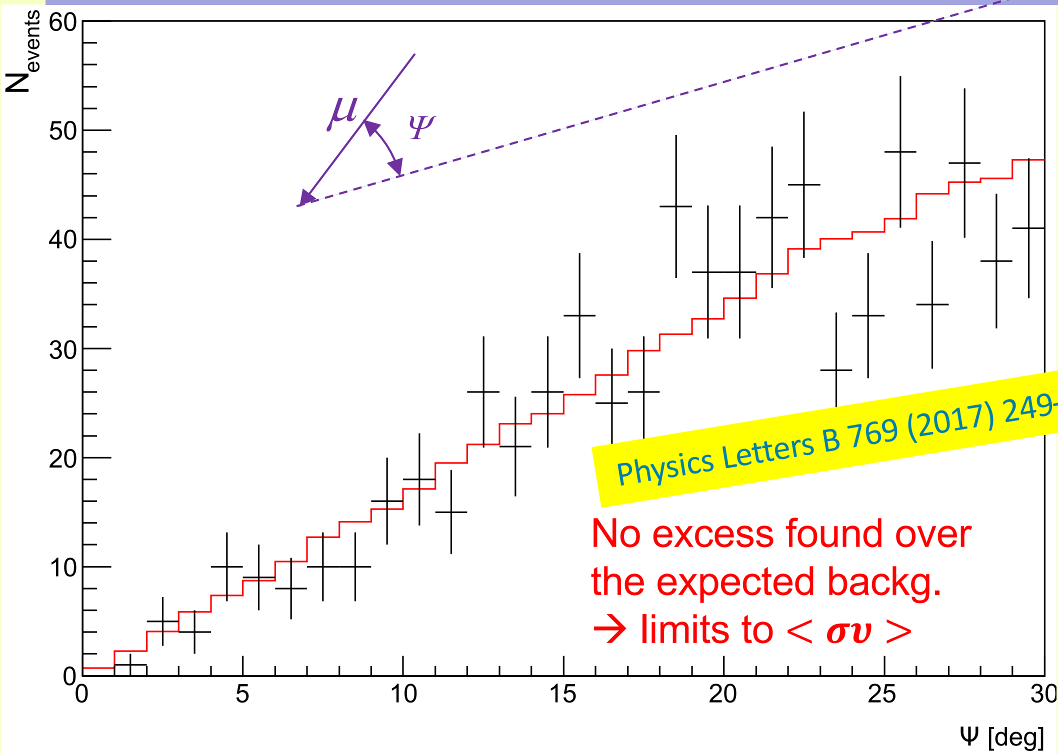

Distribution of measured angles between reconstructed tracks and the Galactic Centre (crosses). The red line describes what is expected from background event.

The expected ν flux depends on the DM distribution around the GC.

3 halo models have been considered

Parameter	NFW	Burkert	McMillan
r_s [kpc]	$16.1^{+17.0}_{-7.8}$	$9.26^{+5.6}_{-4.2}$	17.6 ± 7.5
ρ_{local} [GeV/cm^3]	$0.471^{+0.048}_{-0.061}$	$0.487^{+0.075}_{-0.088}$	0.390 ± 0.034

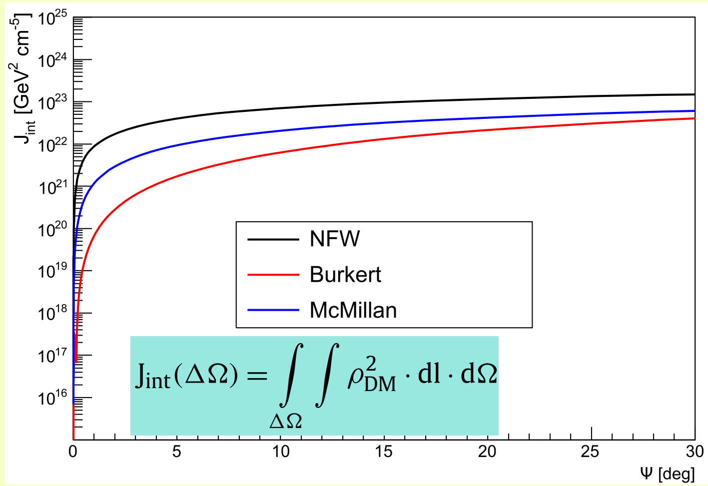

The integrated J-Factor, J_{int} , for a cone-shaped region centred on the G.C. with an opening angle Ψ

Indirect search for Dark Matter in the Galactic Centre

No excess found over the expected background

➟ limits to $<\sigma v>$

$$\frac{d\Phi_{\nu_\mu+\bar{\nu}_\mu}}{dE_{\nu_\mu+\bar{\nu}_\mu}} = \frac{<\sigma v>}{8\pi M^2_{WIMP}} \cdot \frac{dN_{\nu_\mu+\bar{\nu}_\mu}}{dE_{\nu_\mu+\bar{\nu}_\mu}} \cdot J_{int}(\Delta\Omega)$$

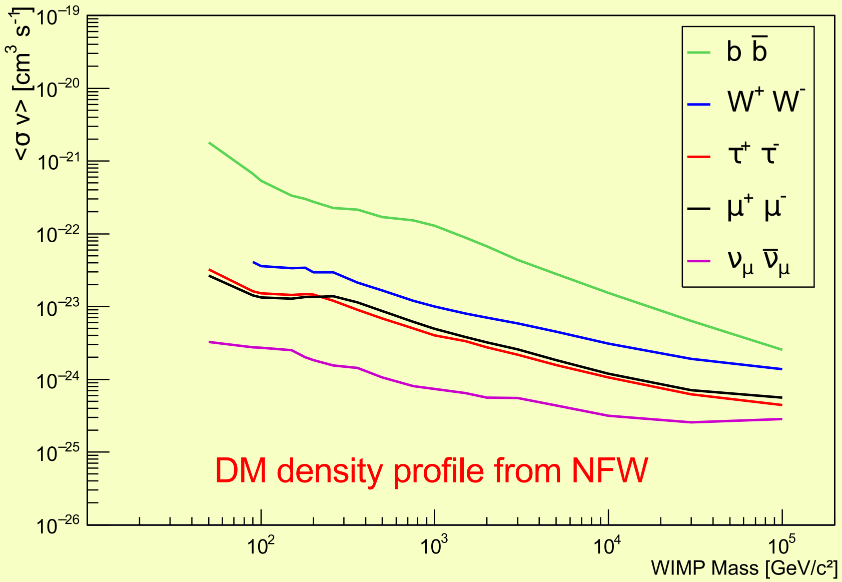

90% C.L. limits on the thermally averaged annihilation cross-section ⟨σv⟩ from WIMP annihil. in the Milky Way

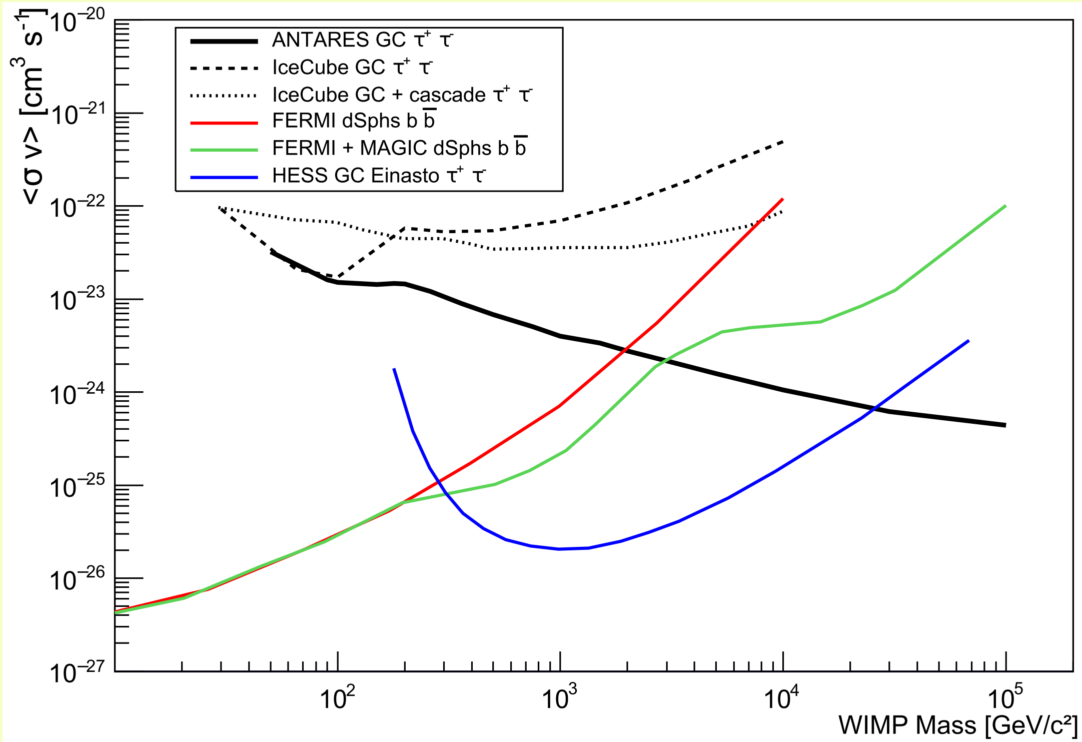

90% C.L. limits on the thermally averaged annihilation cross-section, ⟨σ v⟩, as a function of M_{WIMP}. The results from IceCube and ANTARES were obtained with the NFW profile.

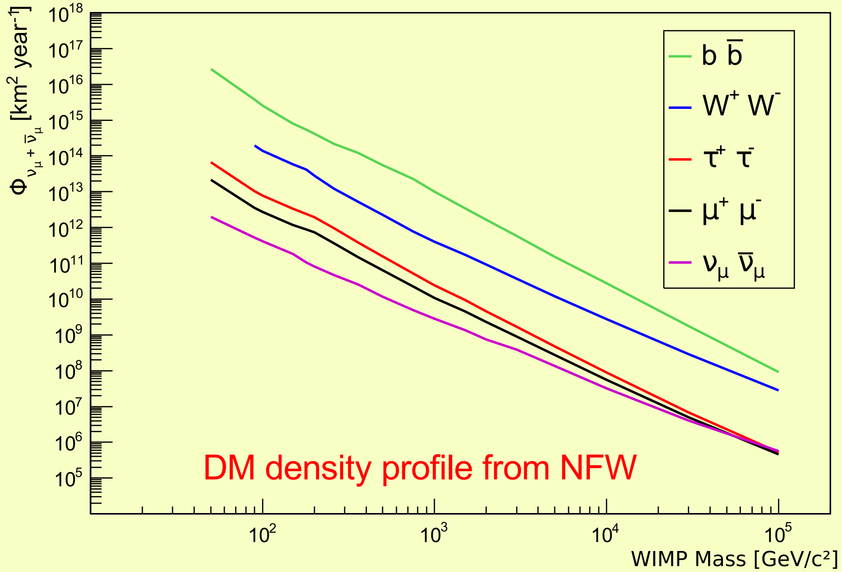

90% C.L. upper limits on the neutrino flux from WIMP annihilations in the Milky Way.

Indirect search for Dark Matter in the Earth

- WIMPS can be gravitationally bound to the Earth if $v_{WIMP} < v_{escape}^{Earth}$
- $v_{escape}^{Earth} \sim 14 \frac{km}{s}$; $v_{WIMP} = \bar{v}_{270}$ following a Maxwell-Boltzmann distr. with r.m.s. velocity 270 km/s → only a small fraction of WIMPS captured on the Earth.
- WIMPS-nucleons collision described by spin-independent cross section σ_p^{SI}.
- Fe and Ni most abundant in the Earth → effective capture for $M_{WIMP} \sim 50\ GeV$.
- In the Earth the capture ($\Gamma_C(t)$) and annihilation ($\Gamma_A(t)$) rates would reach the equilibrium in $\tau \sim 10^{11}$ y >> Earth age ($t_{Earth} = 4.5\ 10^9$ y)
- In these conditions:

$$\Gamma_A(t_{Earth}) \propto \left[\frac{\sigma_p^{SI}\rho_{0.3}^{\chi}}{m_\chi \bar{v}_{270}} \sum_i F_i^*(m_\chi)\right]^2 \frac{\langle\sigma_A v\rangle_{Earth}}{V_{Earth}} \left(\frac{m_\chi}{20\ GeV}\right)^{\frac{3}{2}}$$

Needed to estimate the ν fluxes with WimpSim

C_C^2 capture factor

C_A annih. factor

$\rho_{0.3}^{\chi}$=0.3 GeV/cm³
Local D.M. density

the capture is very effective when $m_{WIMP} \sim m_{target}$

ANTARES, Physics of the Dark Universe 16 (2017) 41–48

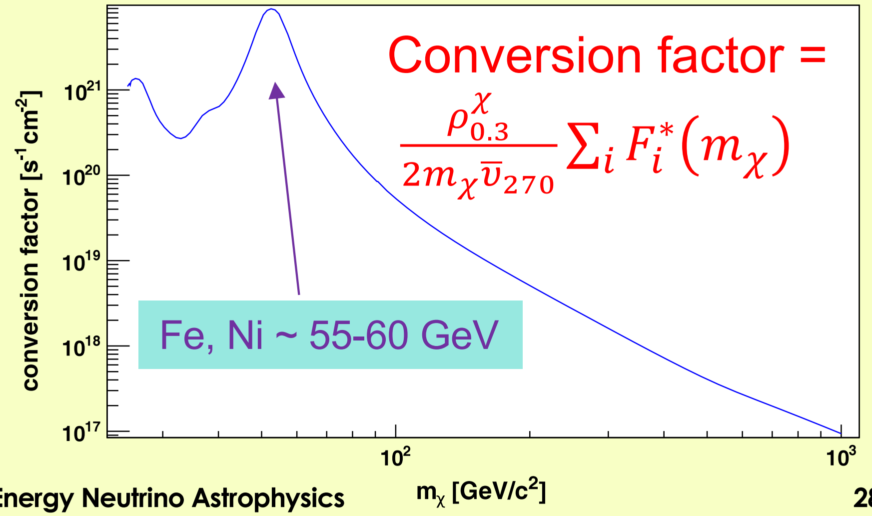

Indirect search for Dark Matter in the Earth

6 years of ANTARES data: 2007-2012

25 GeV/c^2 < M_{WIMP} < 1 TeV/c^2

$$WIMP + WIMP \rightarrow b\bar{b}, W^+W^-, \tau^+\tau^-, \nu\bar{\nu}$$

No excess found over the expected background

Limits on the WIMP-WIMP annihilation rate in the Earth

Limits on the spin independent WIMP-nucleon cross-section

ANTARES, Physics of the Dark Universe 16 (2017) 41–48

Indirect search for Dark Matter in the Earth

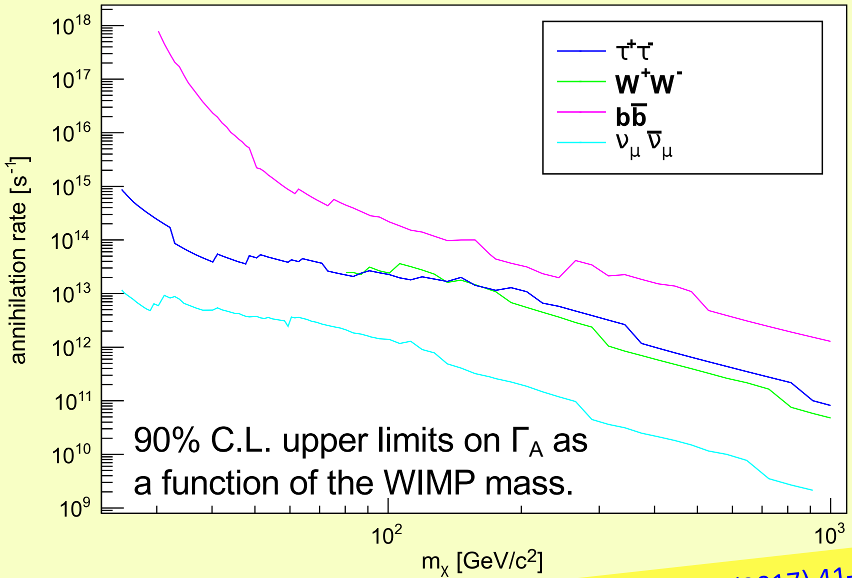

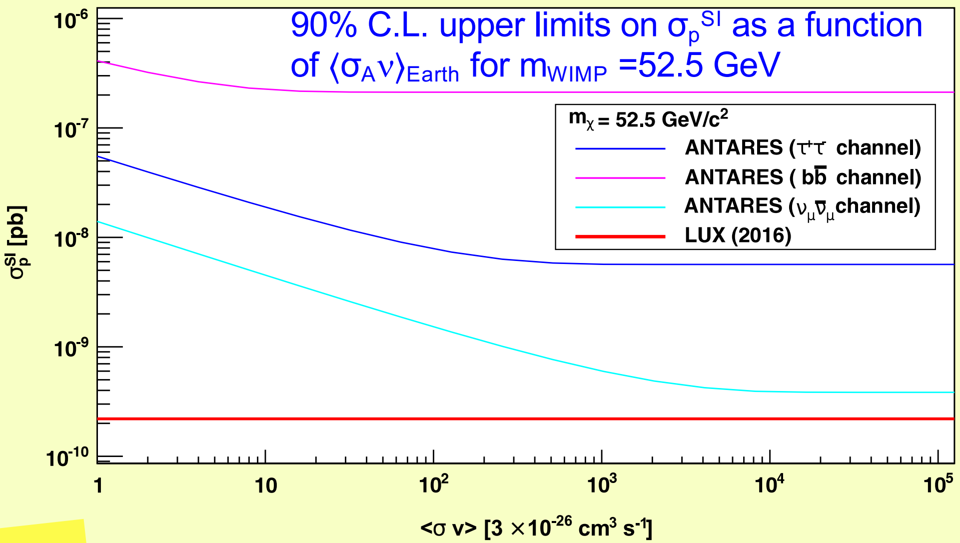

ANTARES, Physics of the Dark Universe 16 (2017) 41–48

90% C.L. upper limits on σ_p^{SI} as a function of the WIMP mass for ANTARES 2007–2012 (Earth) and ANTARES 2007–2012 (Sun), assuming $\langle\sigma_A \boldsymbol{v}\rangle_{Earth} = 3\cdot10^{-26}$ cm^3 s^{-1} and WIMP pair annihilation to 100% into either $\tau^+\tau^-$ (blue), $W^+ W^-$ (green) or $\boldsymbol{b\bar{b}}$ (purple).

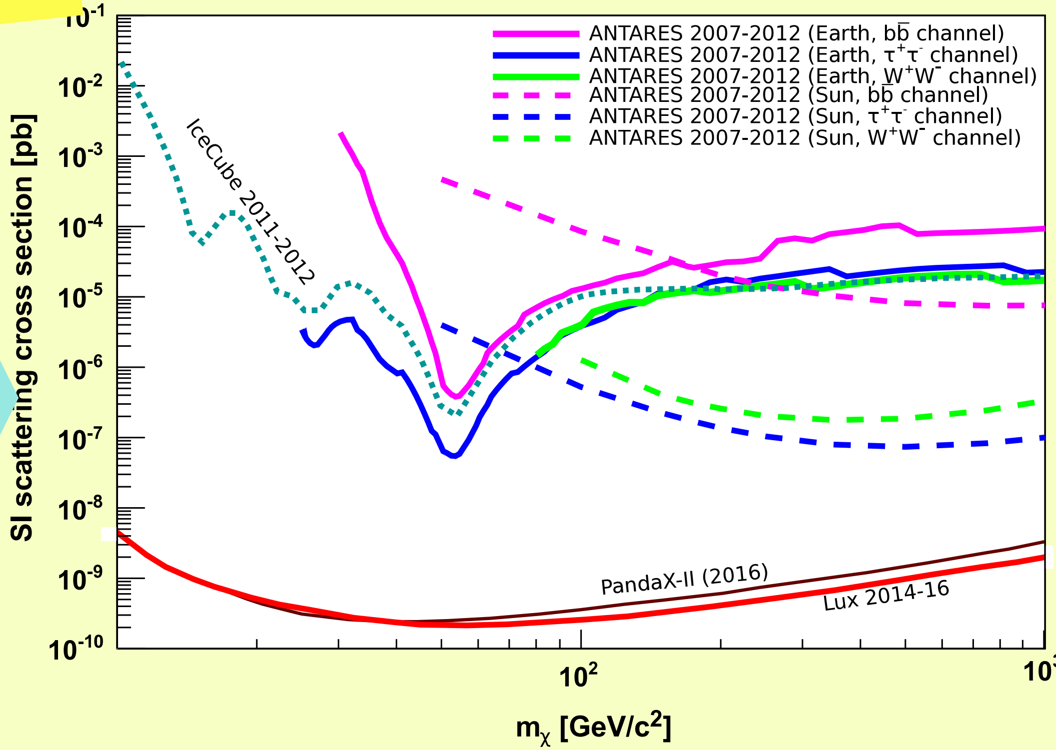

25 Gev/c^2 < M_{WIMP} < 1 Tev/c^2

KM3NeT - Collaboration

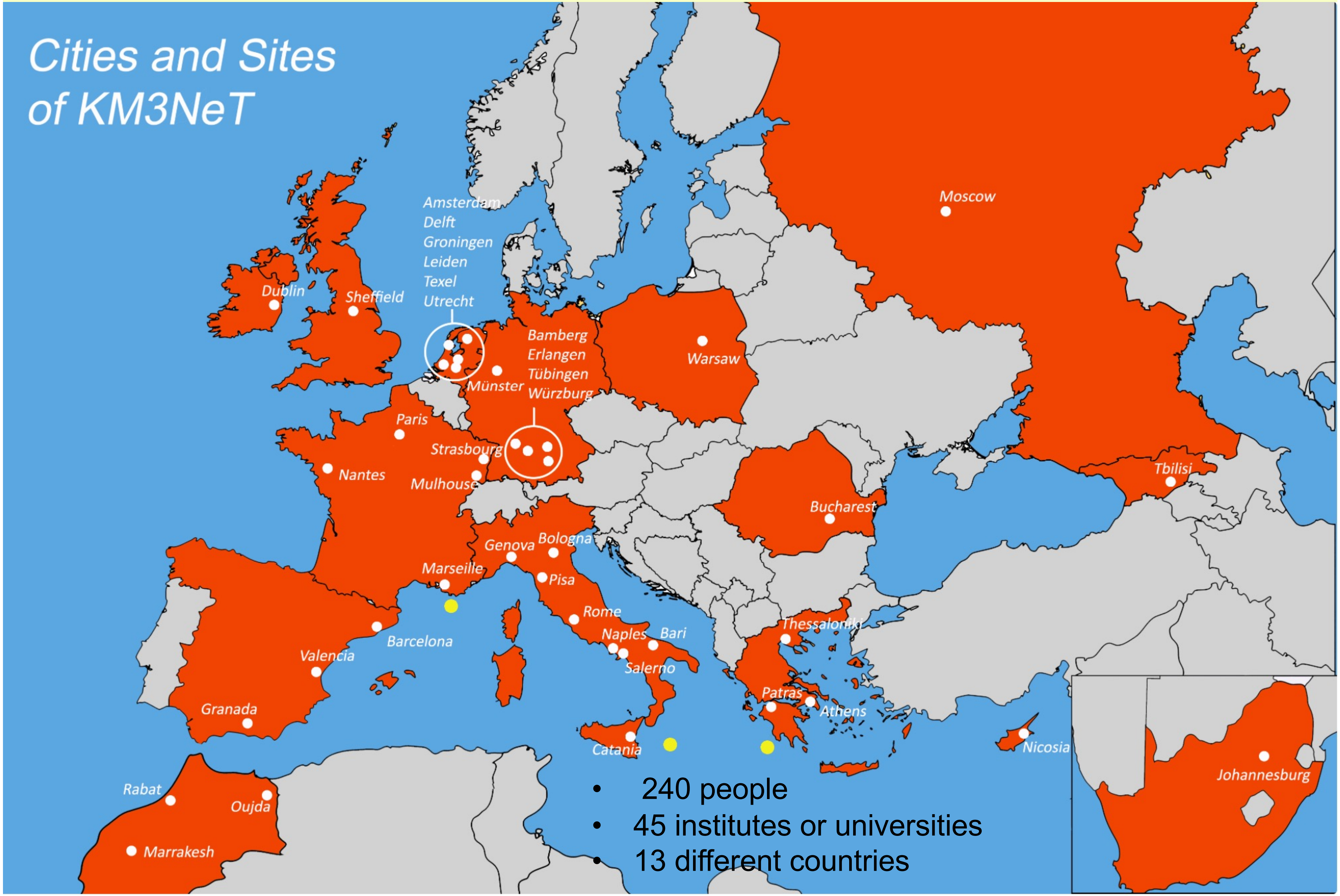

- 240 people
- 45 institutes or universities
- 13 different countries

KM3NeT Neutrino Telescope science scopes

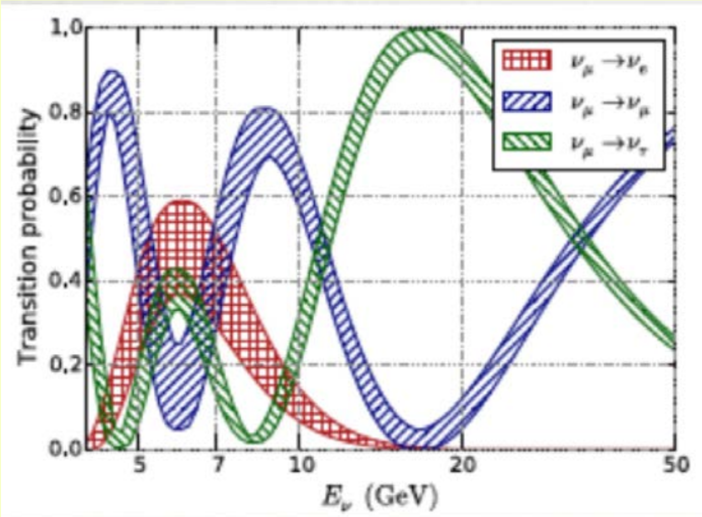

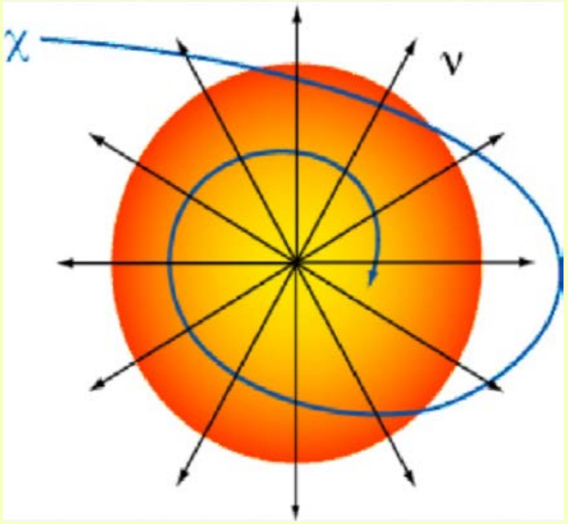

Low Energy	Medium Energy	High Energy
MeV < E_ν < 100 GeV	M eV < E_ν < 100 GeV	E_ν > 1 TeV

- Neutrino Oscillations
- Neut. Mass Hierarchy
- Sterile neutrinos
- **Neut. From** Supernovae

- Dark Matter search
- Monopoles
- Nuclearites

- Neutrinos from extra-terrestrial sources
- Origin and production mechanism of HE CR

KM3NeT-ORCA ANTARES KM3NeT-ARCA

… and synergies with Sea-Sciences: oceanography, biology, seismology, …

KM3NeT Building Blocks

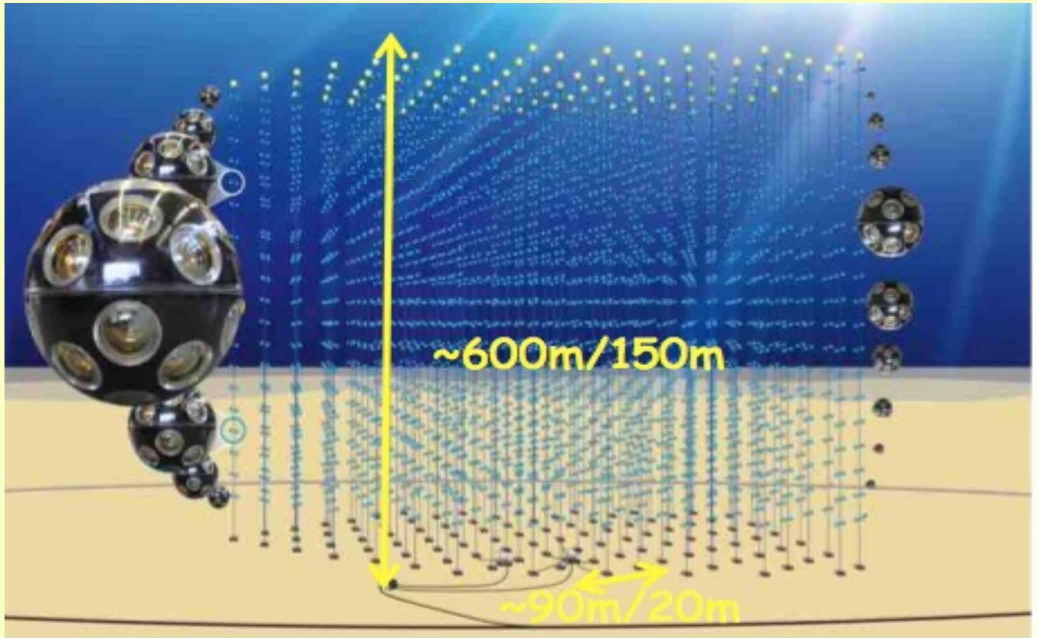

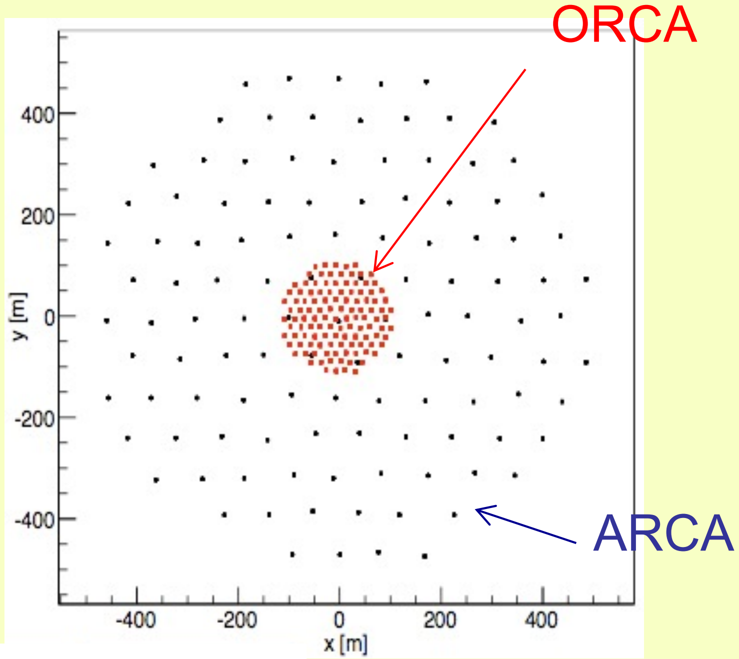

	ARCA	ORCA
Location	Italy – Capo Passero	France - Toulon
Detector Lines distance	90m	20m
DOM spacing	36m	9m
Instrumented mass	500Mton	5,7 Mton

KM3NeT phased implementation

Phase	Building Blocks		Number of DUs		Phisics Goals	
	ARCA	ORCA	ARCA	ORCA	ARCA	ORCA
1	0.2	0.06	24	7	Proof of feasibility and first science results. Joined analysis with ANTARES.	
2.0	2	1	230	115	Study of the IceCube signal.	Determination of neutrino mass hyerarchy.
3	6	1	690	115	All flavour neutrino astronomy.	

L.O.I. KM3NeT ARCA and ORCA:

- J. Phys. G43 (2016) n. 8, 084001
- arXiv: 1601.07459

KM3NeT-ARCA

ARCA detector

- ARCA: 2 blocks
- 115 strings/block
- 90m horizontal spacing
- 18 Optical Modules/strings
- 36m vertical spacing

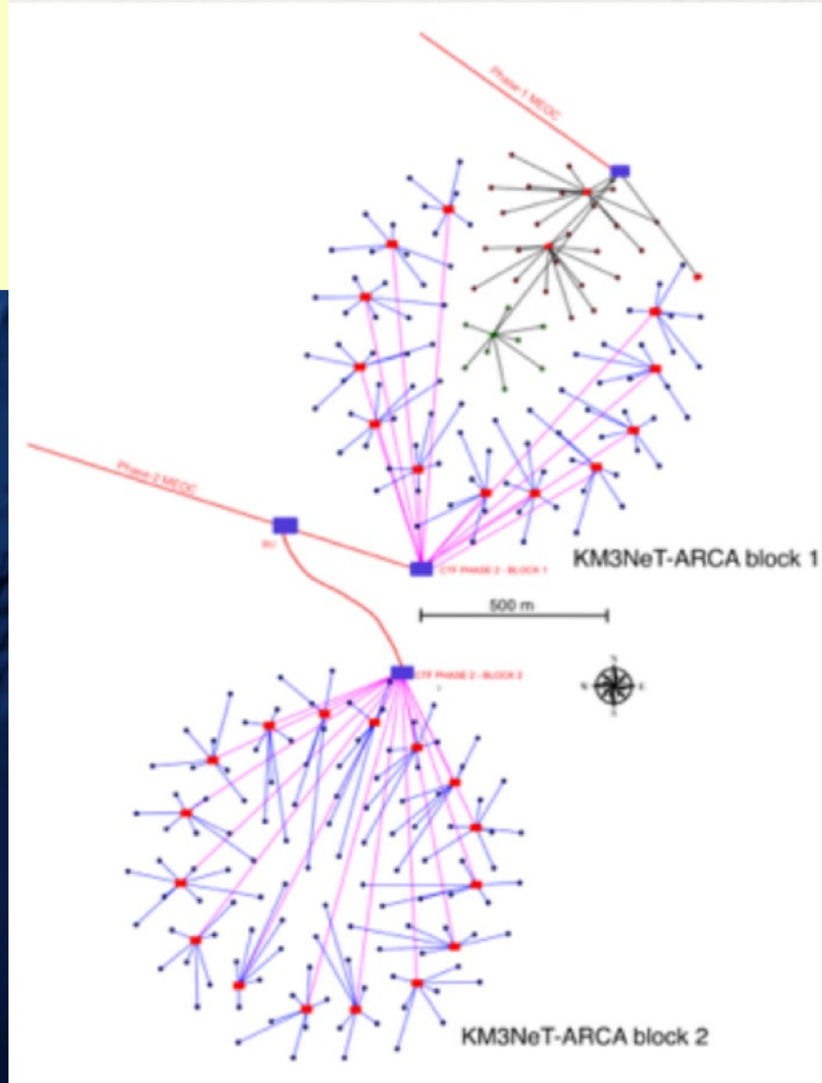

~1km^3

Total Volume 1.2 km^3

ARCA (Phase 2) discovery potential for ν diffuse fluxes

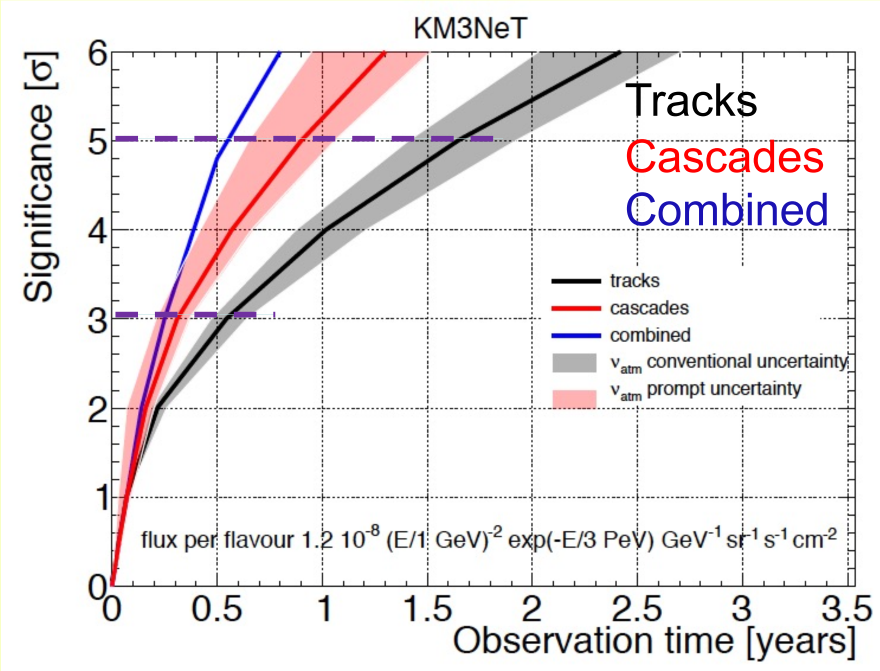

Tracks:

- up-going tracks θ_{zenit} >80°
- analysis based on Maximum Likelihood
- cuts on reconstruction quality parameter **Λ**
- cuts on N_{hits} (→ muon energy)

Cascades:

- Containment cut on reconstructed vertex to remove atmospheric muons

Discovery at 5σ significance (50% probability) in less than one year (combined analysis)

Reconstructed vertex position for atm. muons and for ν_e CC cascades.

MUON VETO

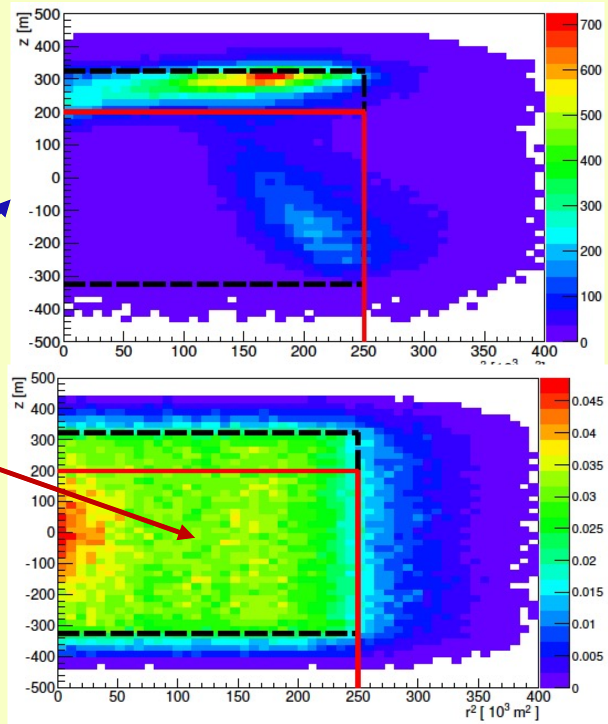

ARCA (Phase 2) search for point-like Galactic sources

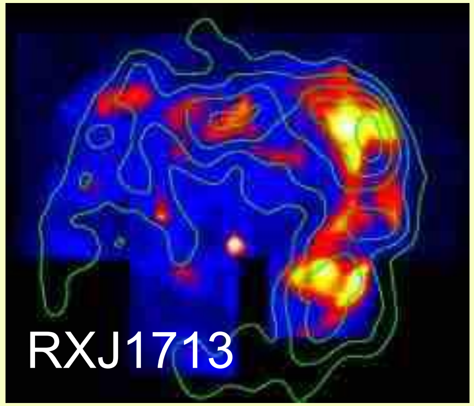

Hypothesis:

- Neutrino fluxes/spectra inferred from gamma-rays data
  .
- S.R. Kelner, et al. PRD 74 (2006) 034018
- F.L. Villante and F. Vissani, PRD 78 (2008) 103007
- 100% hadronic source
- transparent source

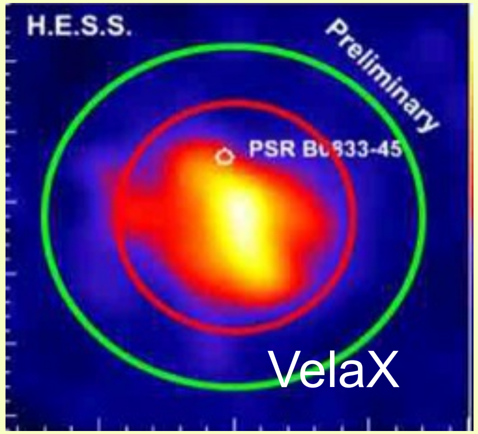

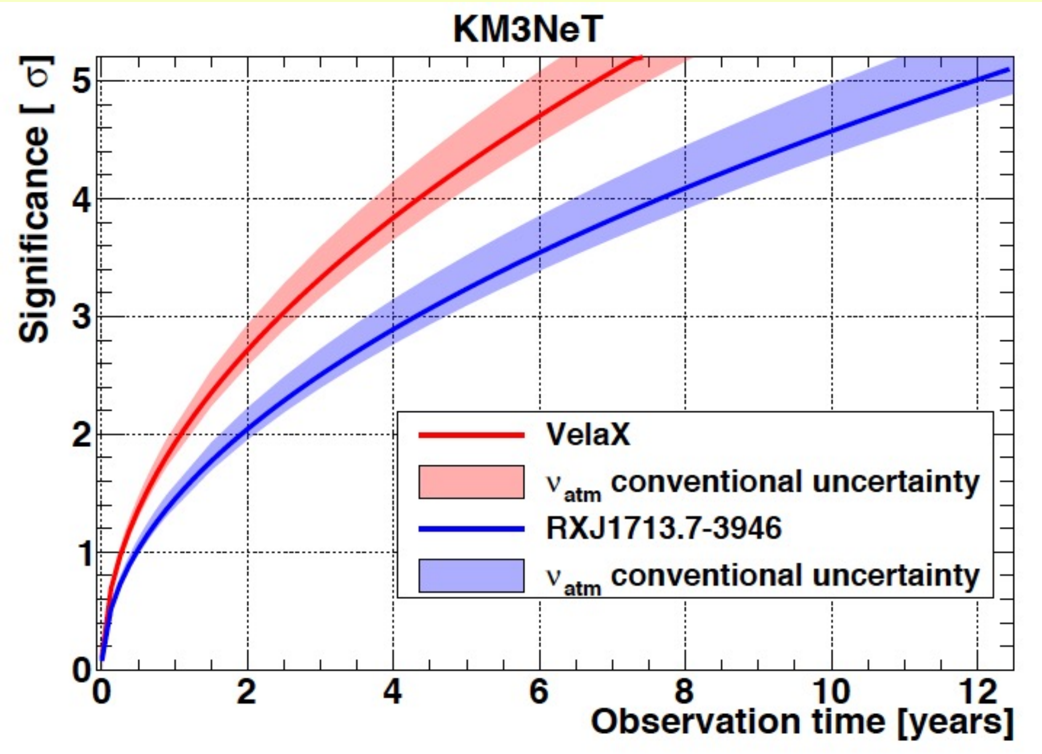

VelaX : 3σ discovery in ~ 2 years
RX1713: 3σ discovery in ~ 4 years

ARCA (Phase 2) discovery potential for point-like sources

- Hypothesis:
- Neutrino spectra ~ E_ν^{-2}.
- 3 years observation time

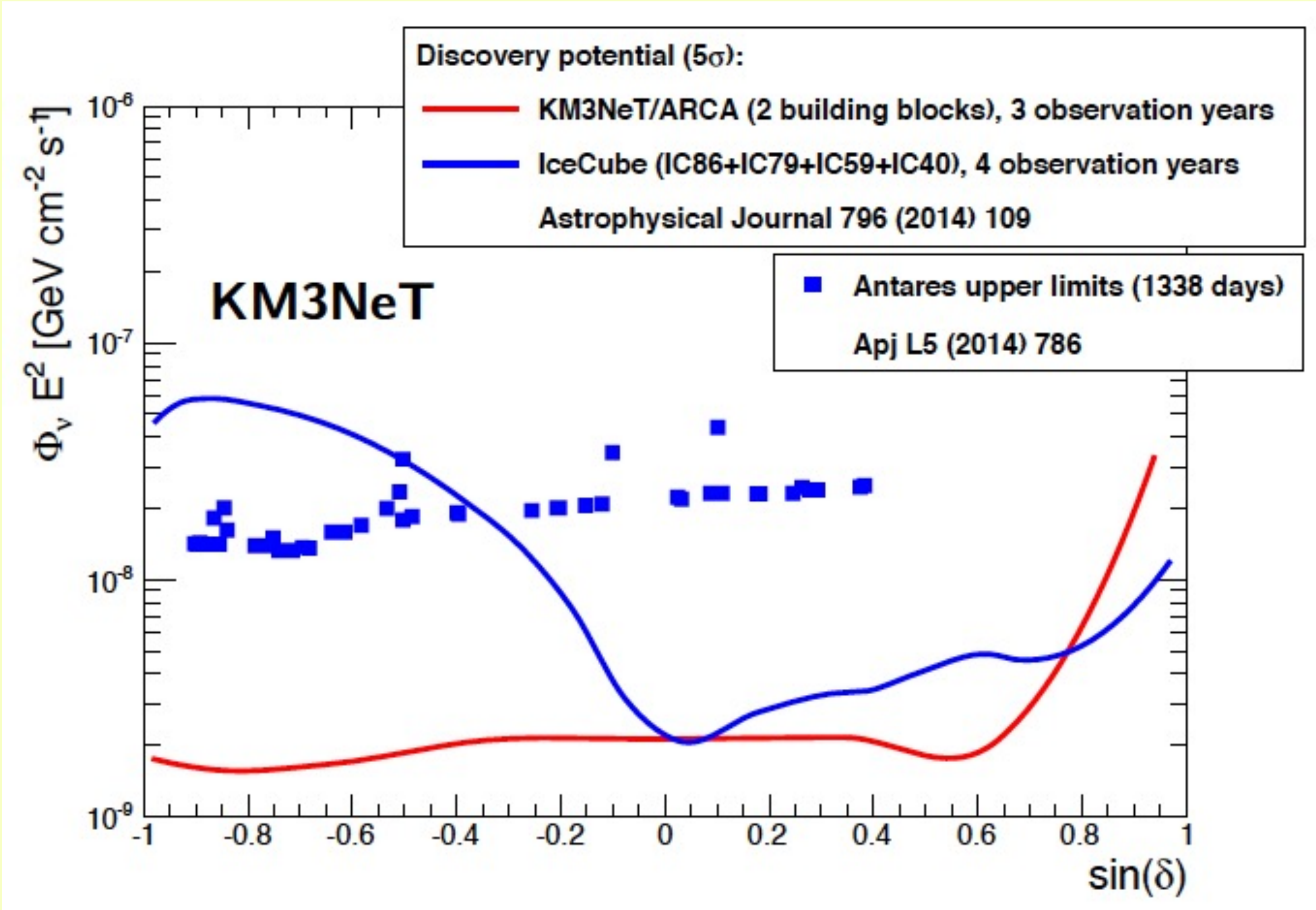

The Detector Unit deployment

Launcher vehicle

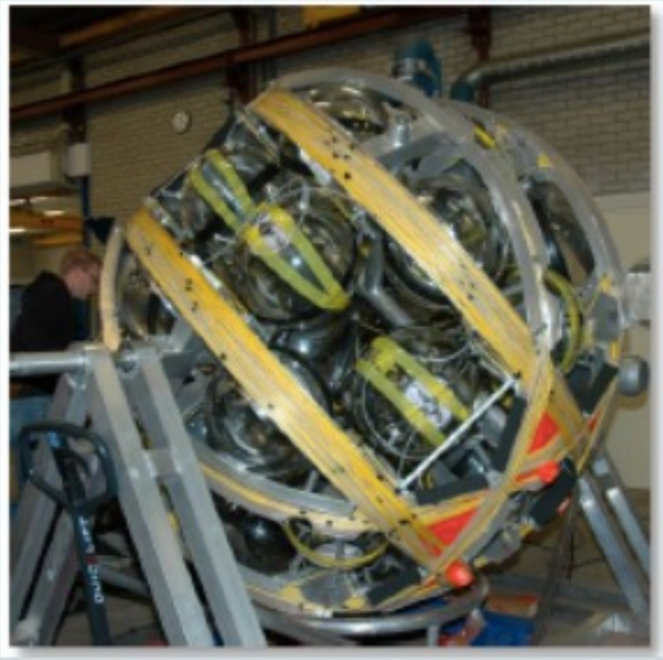

- rapid deployment
- autonomous unfurling
- recoverable

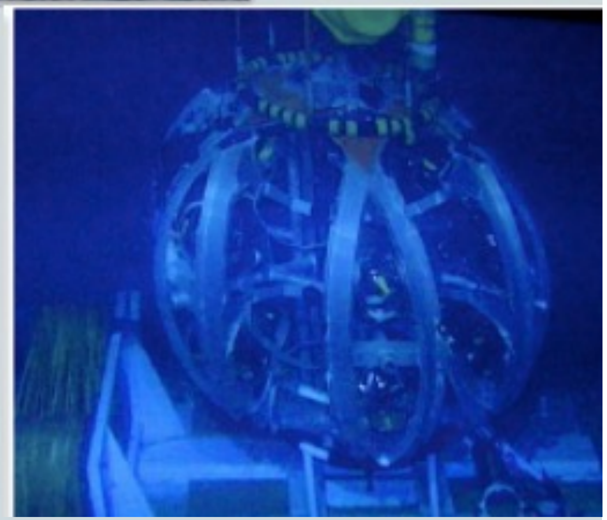

Deployment of the new Junction Box

The Detector Unit deployment

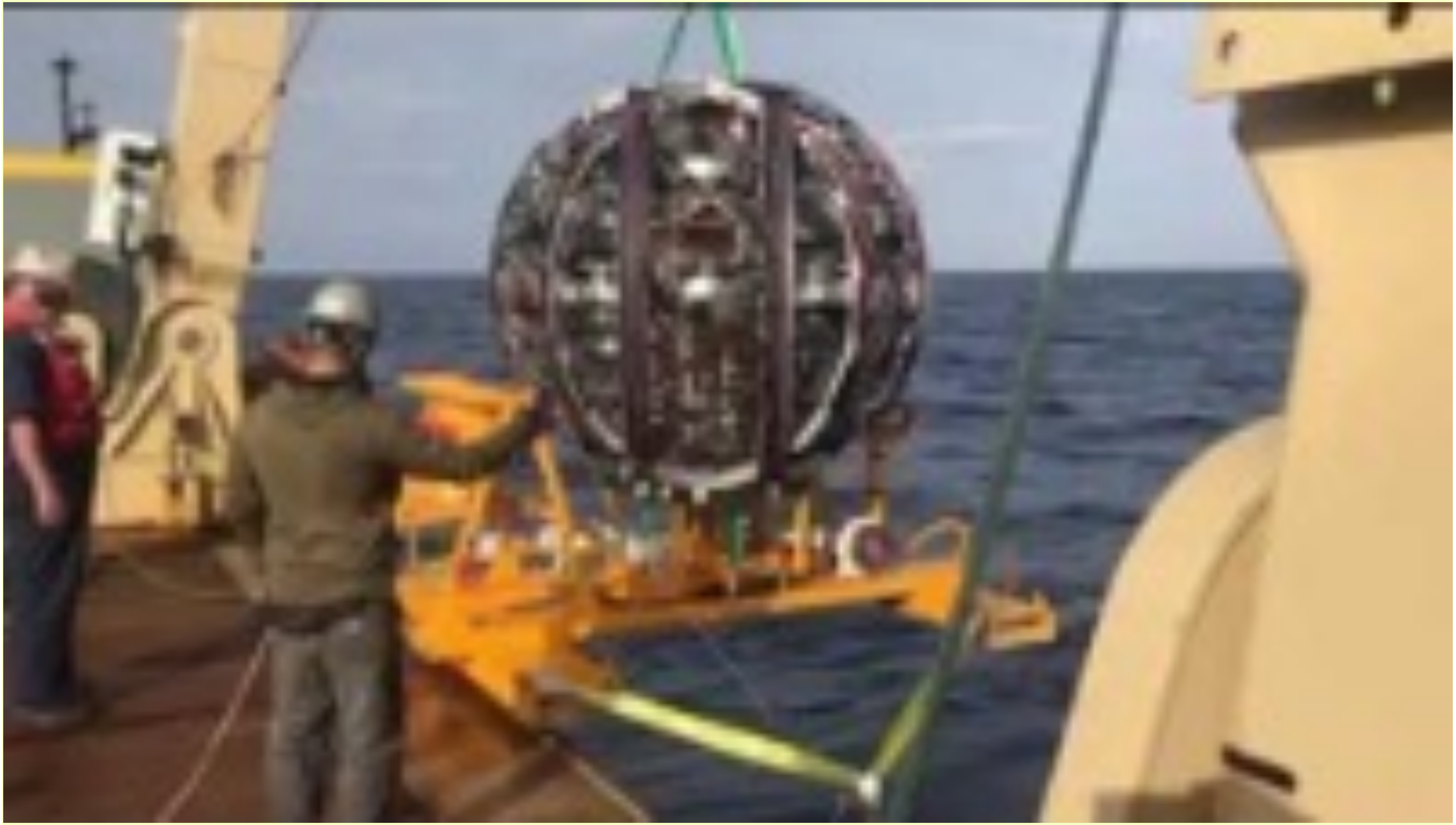

The Detector Unit deployment

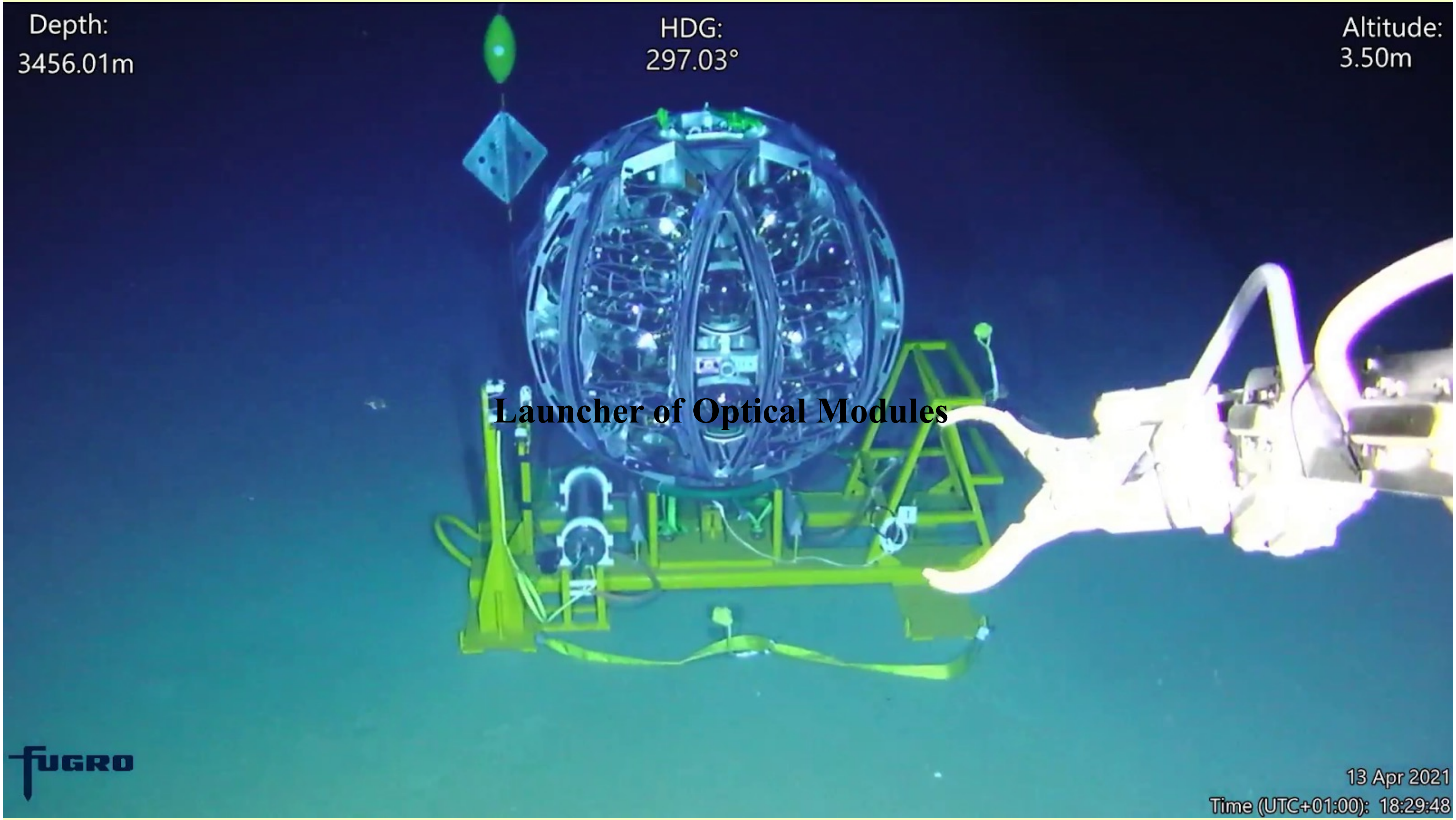

The unfurling mechanism

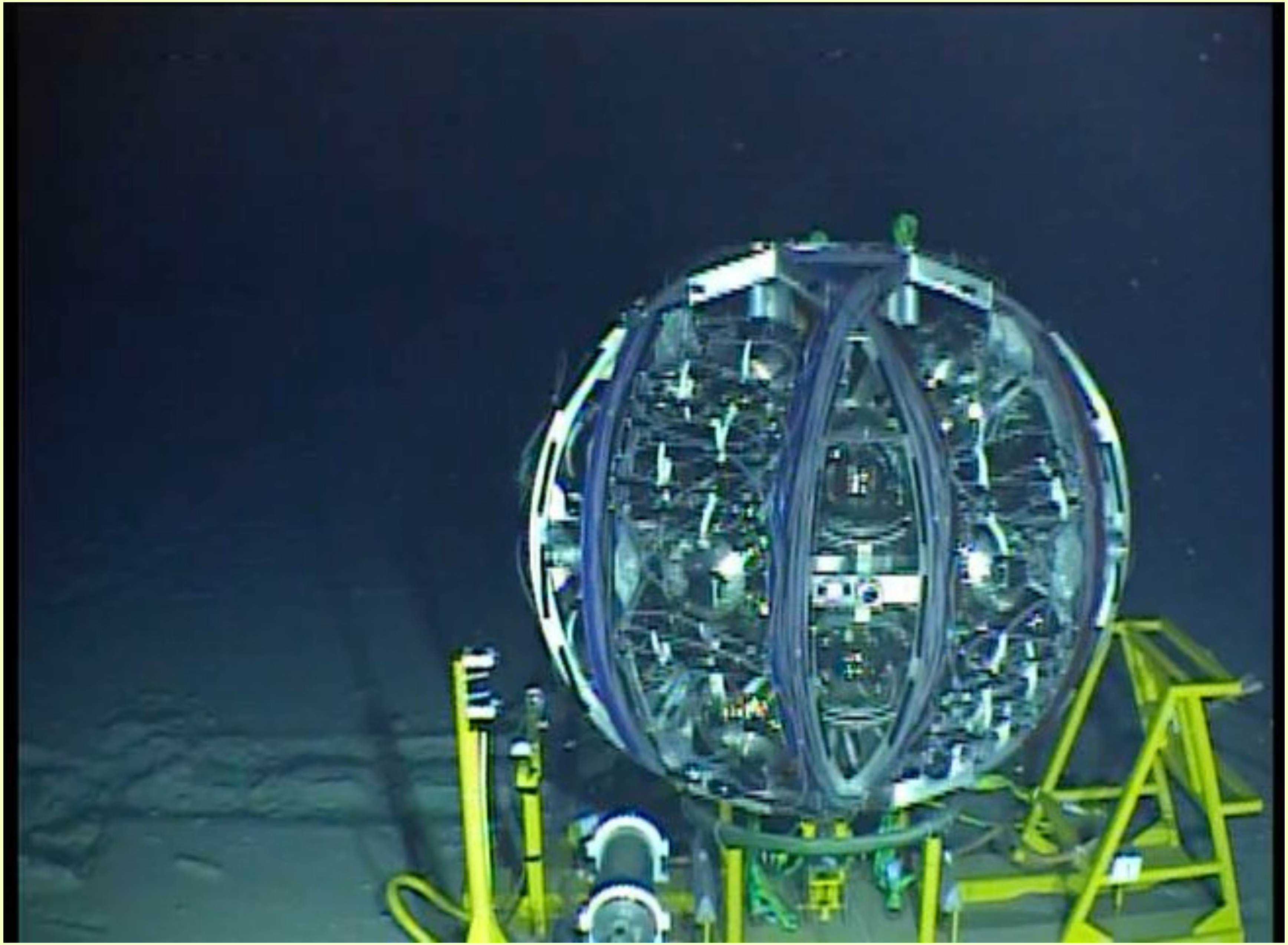

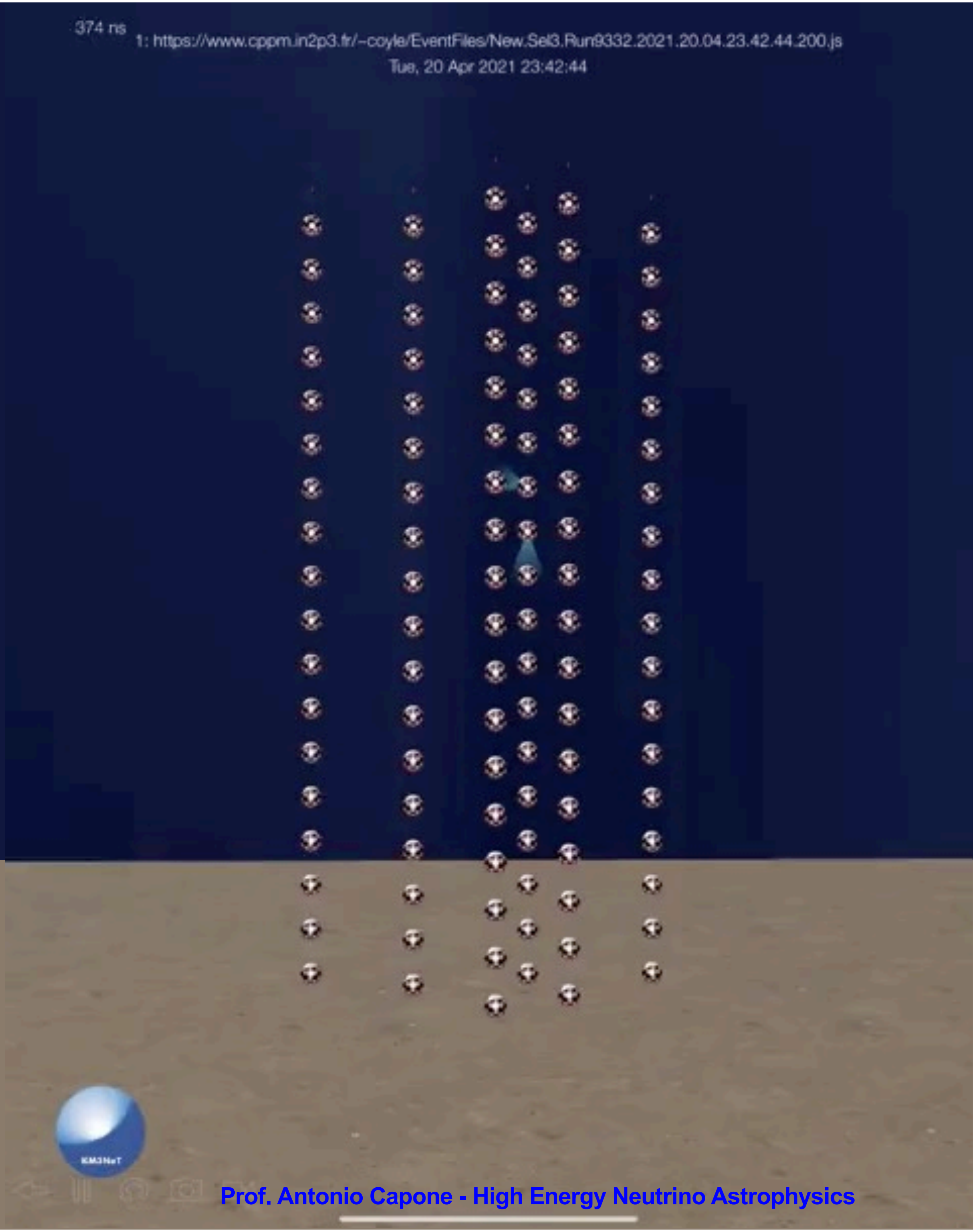
374 ns
1: https://www.cppm.in2p3.fr/~coyle/EventFiles/New.Sel3.Run9332.2021.20.04.23.42.44.200.js
Tue, 20 Apr 2021 23:42:44

The future of Neutrino Astronomy in the Mediterranean Sea

KM3NeT ORCA

ORCA detector:

- 115 lines
- 20 m horizontal spacing
- 9 m vertical DOM spacing
- 18 DOMs / string
- ~6 Mt instrumented volume

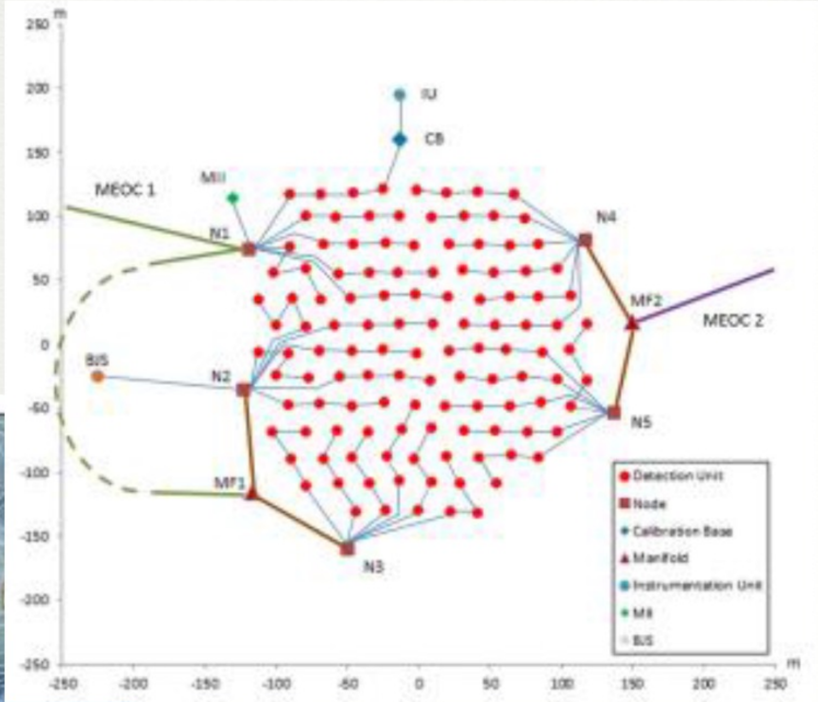

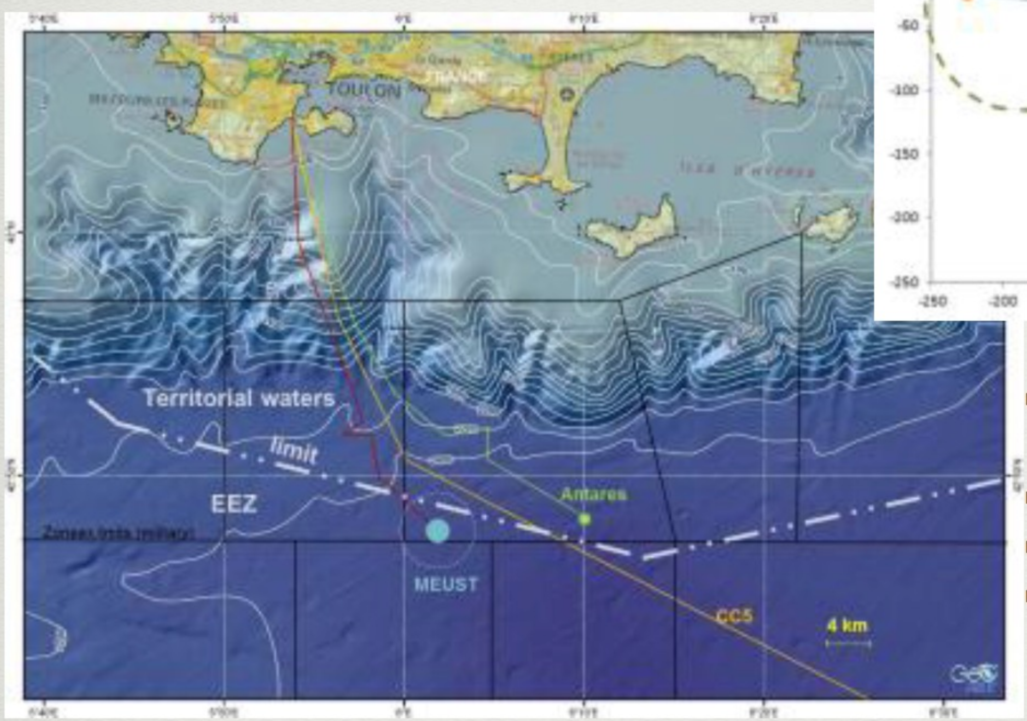

- ➡ Located closed to ANTARES at a depth of ~2475m
- ➡ Shore station La Seyne sur Mer
- ➡ Infrastructure already deployed
- ➡ 2 new ORCA lines will be deployed before summer

Measurement of ν Mass Hierarchy with atmospheric neutrinos

- **Broad range of baselines (50 → 12800 km) and energies (GeV ÷ 100 TeV)**
- **Oscillation signal enhanced, by MSW effect, at resonance energy in matter**

We have seen before: "fast" oscillation due to Δm_{13} has first maximum for L/E~500 km/GeV

→ for atmospheric ν with $\langle E_\nu \rangle$ ~ 20 GeV the maximum at L~10.000 km, the Earth diameter

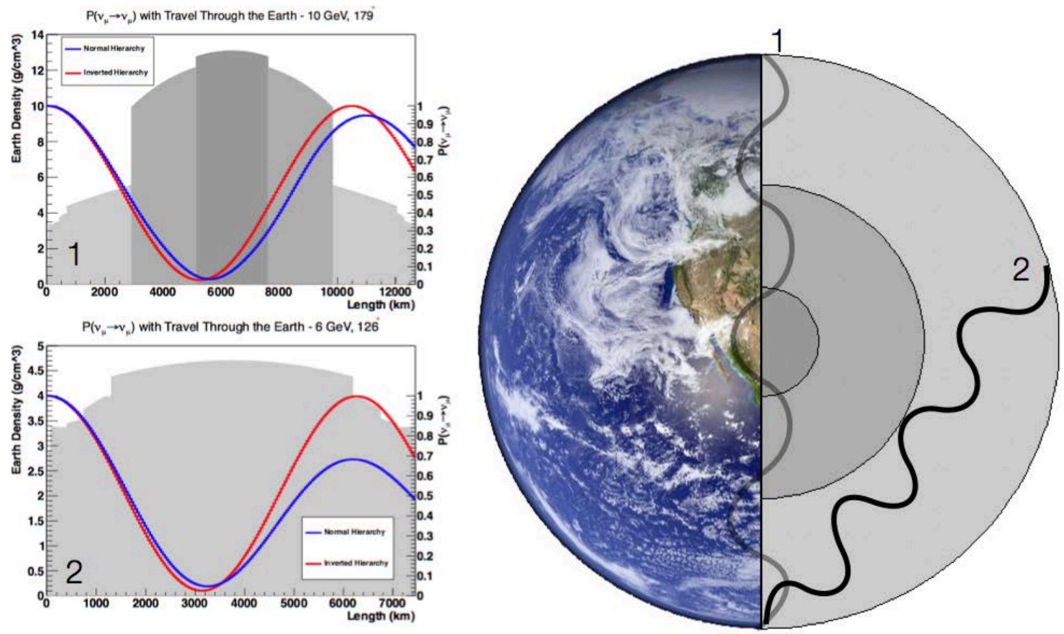

$$P_{e\to\mu} \approx P_{\mu\to e} \approx \sin^2\theta_{23}\sin^2(2\theta_{13}^{\text{eff}})\sin^2\left(\frac{\Delta_{13}^{\text{eff}}L}{2}\right)$$

$$\Delta_{13} = \frac{\Delta m_{13}^2}{2E_\nu} \qquad \sin^2(2\theta_{13}^{\text{eff}}) = \frac{\Delta_{13}^2\sin^2(2\theta_{13})}{\Delta_{13}^{\text{eff}}L}$$

$$\Delta_{13}^{\text{eff}} = \sqrt{[\Delta_{13}\cos(2\theta_{13}) - A]^2 + \Delta_{13}^2\sin^2(2\theta_{13})}$$

$A = \sqrt{2}G_F N_e$ for ν and $A = -\sqrt{2}G_F N_e$ for $\bar{\nu}$

$$E_\nu^{\text{res}} = \pm\frac{\Delta m_{13}^2\cos(2\theta_{13})}{2\sqrt{2}G_F N_e}$$

Method - 1

- **Proposed by Smirnov at Neutrino 2012 Conference** JHEP 02, 082 (2013)

- **Measuring the neutrino Mass Hierarchy with atmospheric neutrinos in a M-ton scale ice(PINGU)/deep sea(ORCA) Cherenkov detector at GeV energy**

- **MSW effect on up-going neutrinos passing through the Earth modify the oscillation pattern allowing to disentangle NMH-IMH**

- **Exploit ν_μ, ν_e oscillation $P_{\mu e} \leftrightarrow P_{e\mu}$ in atmospheric up-going events**

Method – 2

Proposed by A. Yu. Smirnov at Neutrino 2012 Conference JHEP 02, 082 (2013)

Assuming oscillation with 3 neutrinos the $\nu_\mu \to \nu_e$ and $\nu_\mu \to \nu_\mu$ transition probabilities, in vacuum ad assuming L=oscillation baseline, E_ν neutrino energy, can be written as:

$$P_{3\nu}(\nu_\mu \to \nu_e) \approx sin^2\theta_{23}\ sin^2 2\theta_{13} sin^2\left(\frac{\Delta m^2_{31} L}{4E_\nu}\right)$$

$$P_{3\nu}(\nu_\mu \to \nu_\mu) \approx 1 - 4cos^2\theta_{13}\ sin^2\theta_{23}(1 - cos^2\theta_{13}\ sin^2\theta_{23})\ sin^2\left(\frac{\Delta m^2_{31} L}{4E_\nu}\right)$$

These transitions are functions of θ_{13} and Δm^2_{31} but are **not affected by the sign of Δm^2_{31}** .
If we take into account matter effect (MSW) then the sign of Δm^2_{31} plays a role. We know that the **ν_e can interact, via CC elastic scattering** interactions with the electrons in matter and consequently **acquire an effective potential $V_e = \pm\sqrt{2}G_F N_e$** where the **+(−) sign is for ν_e ($\bar{\nu}_e$)**.

$$P^m_{3\nu}(\nu_\mu \to \nu_\mu) \approx 1 - sin^2 2\theta_{23}\ cos^2\theta^m_{13} sin^2\left(\frac{(\Delta m^2_{31} + \Delta^m m^2)L}{8E_\nu} + \frac{V_e L}{4}\right)$$
$$-sin^2 2\theta_{23}\ sin^2\theta^m_{13} sin^2\left(\frac{(\Delta m^2_{31} - \Delta^m m^2)L}{8E_\nu} + \frac{V_e L}{4}\right) - sin^4\theta_{23}\ sin^2 2\theta^m_{13} sin^2\left(\frac{\Delta^m m^2 L}{4E_\nu}\right)$$

In the formula above appear the "effective neutrino mixing parameters in matter":

$$sin^2\theta^m_{13} \equiv sin^2 2\theta_{13}\left(\frac{\Delta m^2_{31}}{\Delta^m m^2}\right)^2 \text{ and } \Delta^m m^2 \equiv \sqrt{(\Delta m^2_{31} cos2\theta_{13} - 2E_\nu V_e)^2 + (\Delta m^2_{31} sin2\theta_{13})^2}$$

Method - 3

$$sin^2\theta_{13}^m \equiv sin^2 2\theta_{13}\left(\frac{\Delta m_{31}^2}{\Delta^m m^2}\right)^2 \; ; \; \Delta^m m^2 \equiv \sqrt{(\Delta m_{31}^2 cos2\theta_{13} - 2E_\nu V_e)^2 + (\Delta m_{31}^2 sin2\theta_{13})^2}$$

In this formula V_e is positive for neutrinos and negative for antineutrinos. A resonance condition is met when the effective mixing is maximal, i.e $\Delta^m m^2$ is minimal.

This happens for the case of the NH (IH) in the neutrino (antineutrino) channel at the energy:

$$E_{res} \equiv \frac{\Delta m_{31}^2 cos2\theta_{13}}{2\sqrt{2}G_F N_e} \sim 7GeV\left(\frac{4.5g\ cm^{-3}}{\rho}\right)\left(\frac{\Delta m_{31}^2}{2.4\cdot 10^{-3} eV^2}\right) cos2\theta_{13}$$

For neutrinos passing trough the Earth mantle → resonance at 7 GeV

For neutrinos passing trough the Earth core → resonance at 3 GeV

→ ATMOSPHERIC NEUTRINOS WITH LONG-BASELINE EXPERIMENT ARE SENSIBLE TO ν MASS HIERARCHY

Density profile of neutrino path through the Earth

Experimentally will be determined by the zenith angle θ_ν

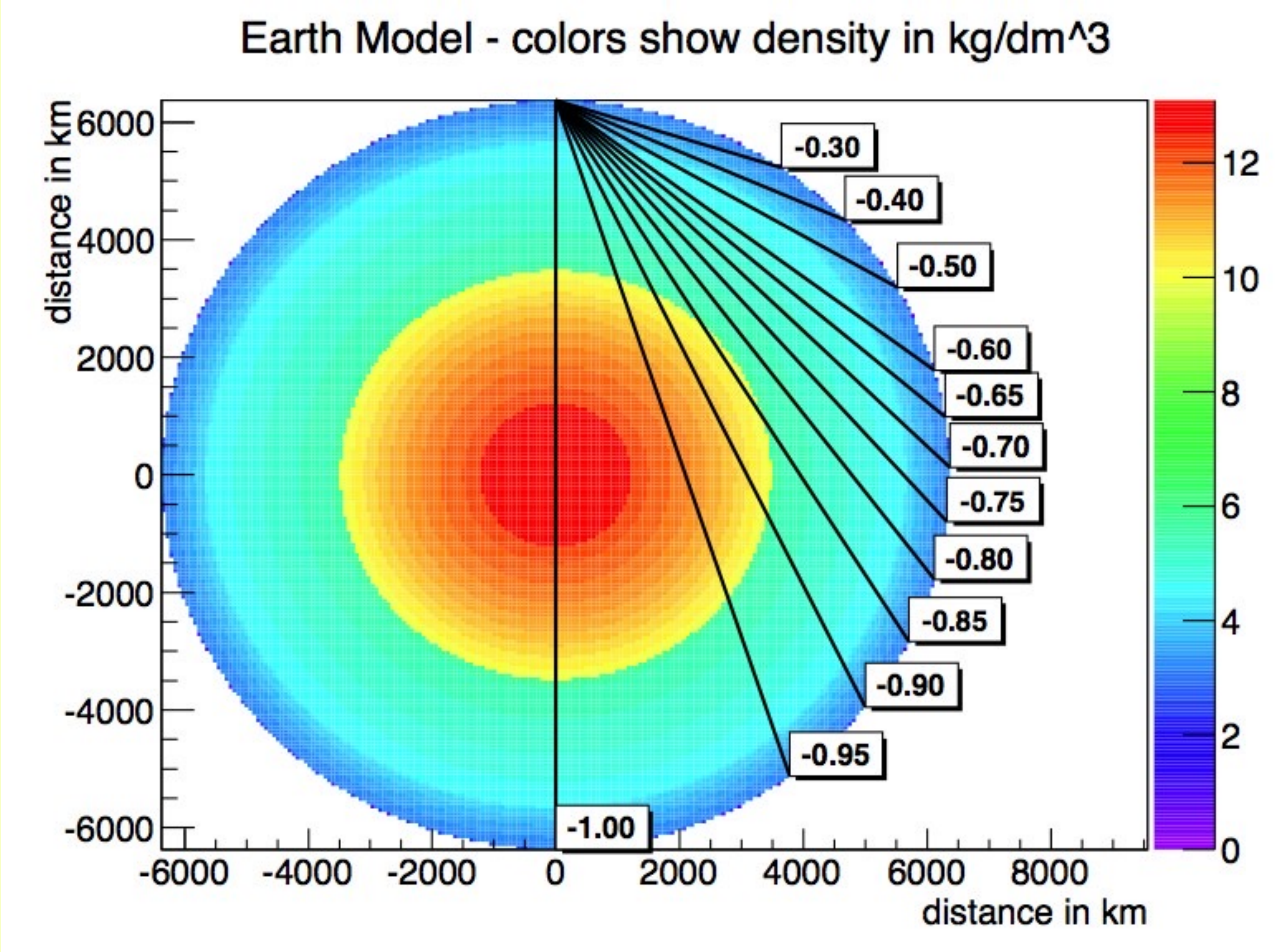

Method – 4 (the oscillogram)

The differences due to NH or IH are visible only for E_ν < 15 GeV, this make the experiment very difficult in a Cherenkov neutrino detector

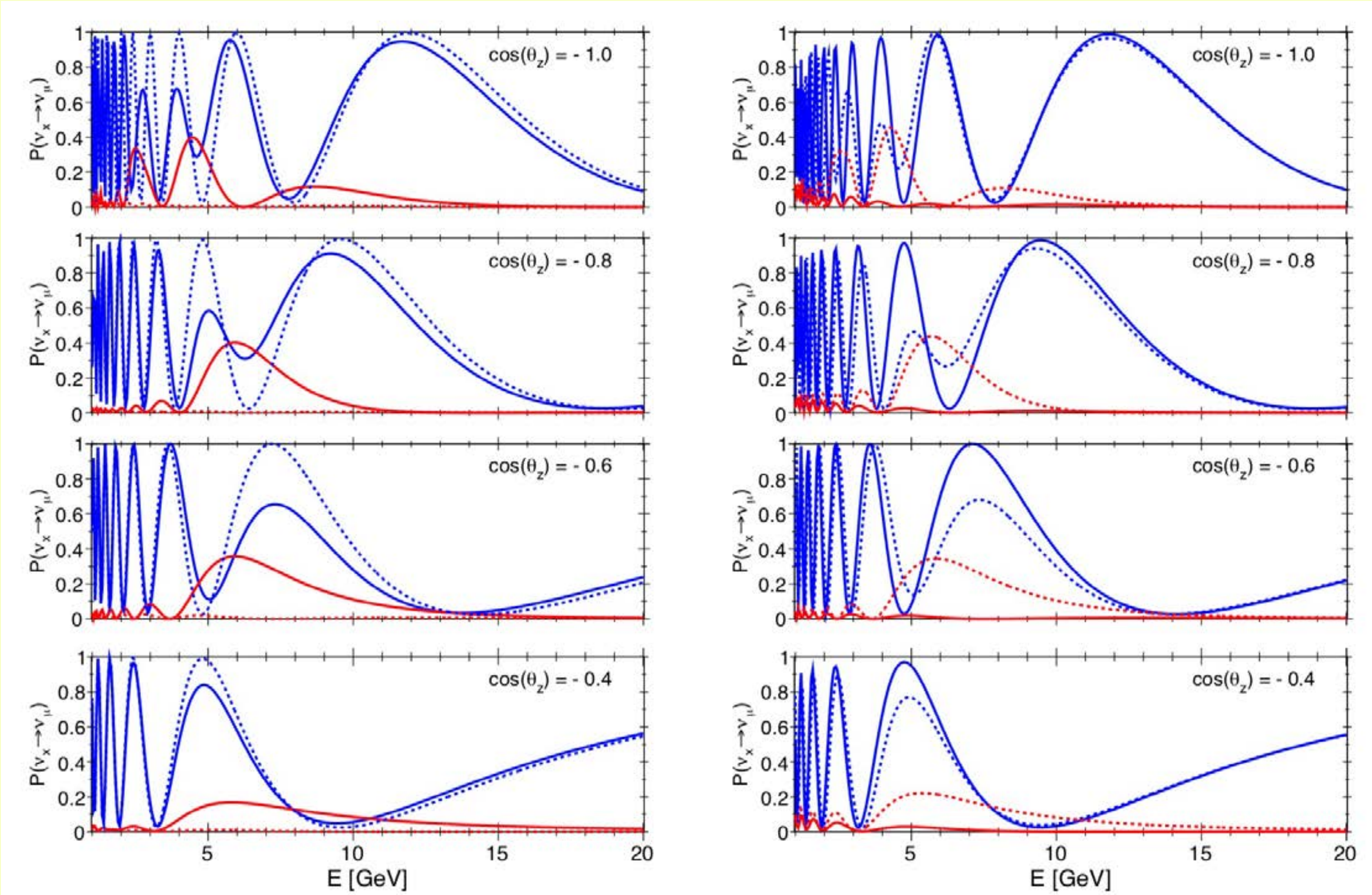

Oscillation probabilities $\nu_\mu \rightarrow \nu_\mu$ (blue lines) and **$\nu_e \rightarrow \nu_\mu$ (red lines)** as a function of the E_ν for several values of the zenith angle (corresponding to different baselines). The solid (dashed) lines are for NH (IH). For neutrinos (left) and for antineutrinos (right).

Can a Cherenkov detector perform this measurement ?

What really matter is the capability to detect, and measure, low energy neutrino interactions: this is function of the "detector granularity"

Detection threshold decreases with increasing photocathode area density

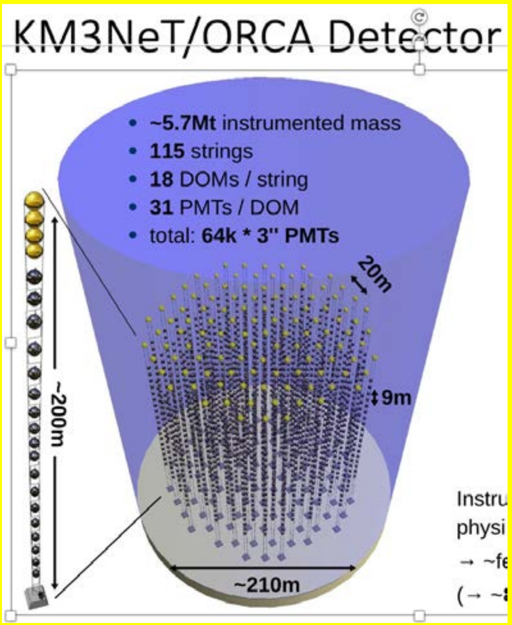

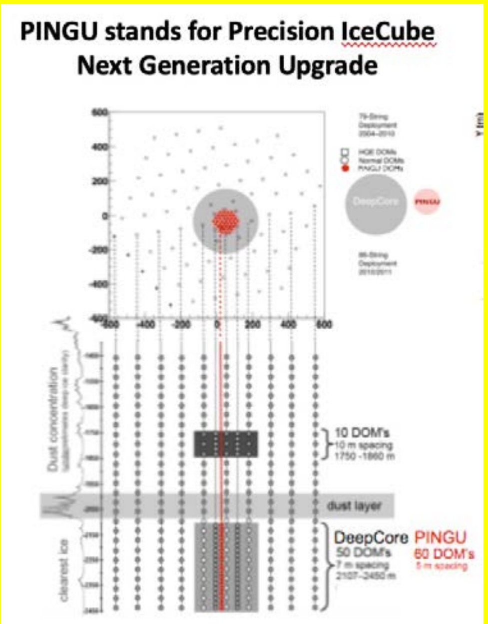

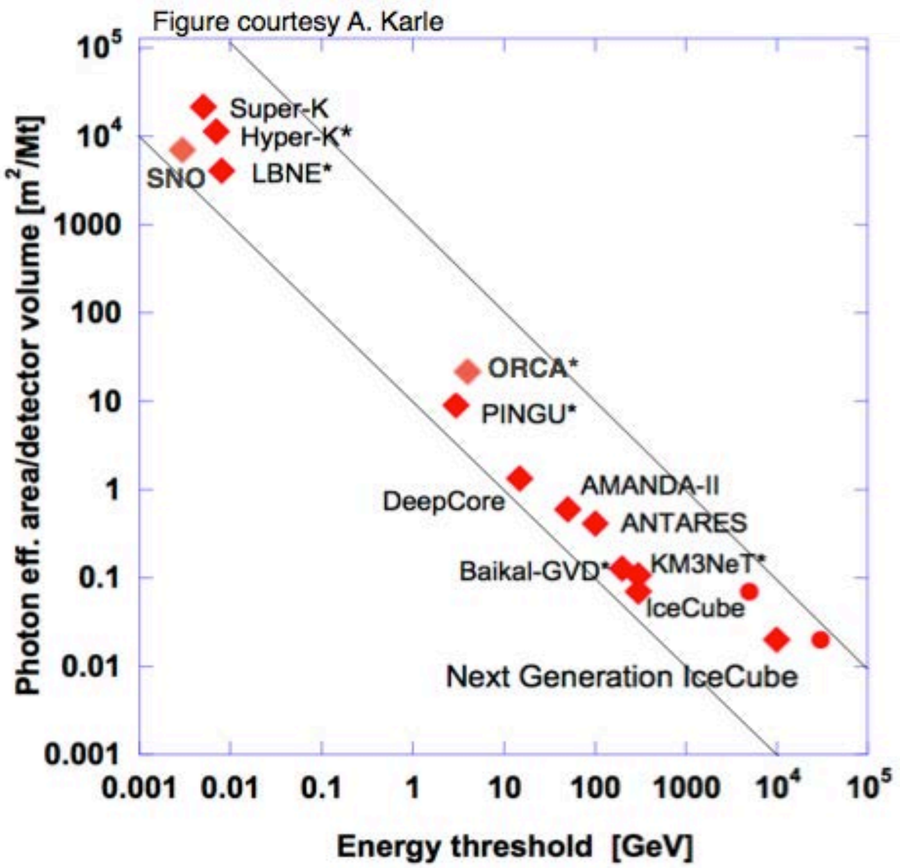

Measurement of ν Mass Hierarchy with atmospheric neutrinos

Cherenkov detectors like PINGU-ORCA have no magnetic field, no way to distinguish neutrino-antineutrino CC interactions.
Neutrinos and antineutrinos are affected differently by the MSW effect but, since what is visible is the sum of μ^+ and μ^-, the effect risks to vanish …

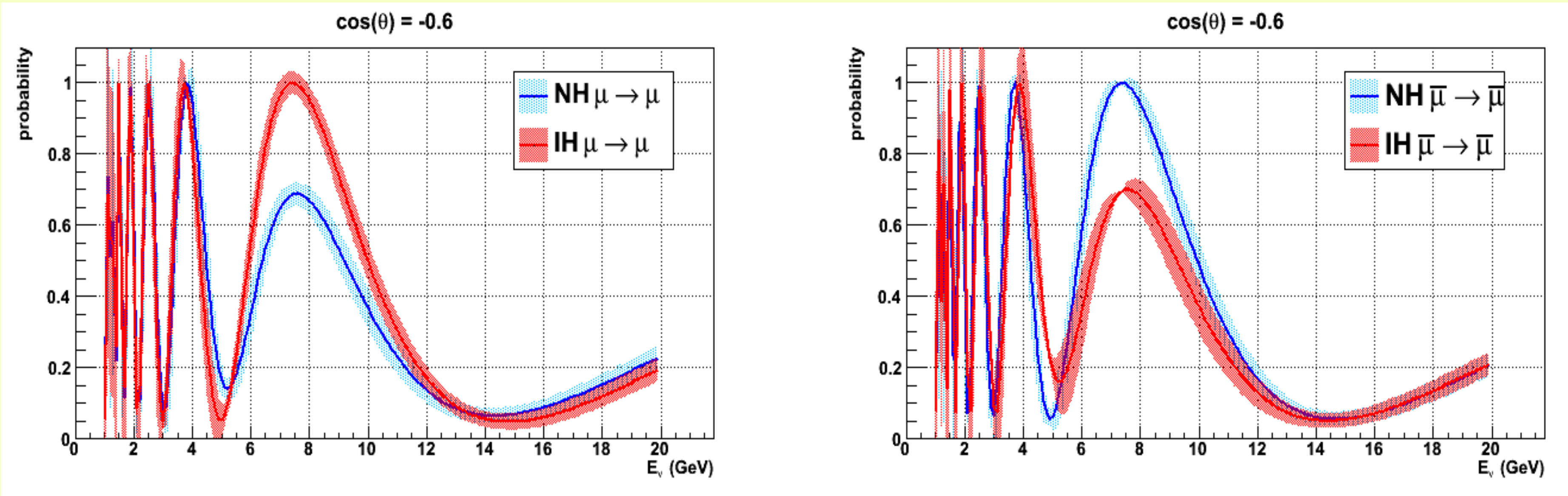

Measurement of ν Mass Hierarchy with atmospheric neutrinos

Fortunately ν_{atm} and $\vec{\nu}_{atm}$ fluxes are different and the CC interaction cross sections for ν and $\vec{\nu}$ are also different: some effect of the passage into the Earth remains.

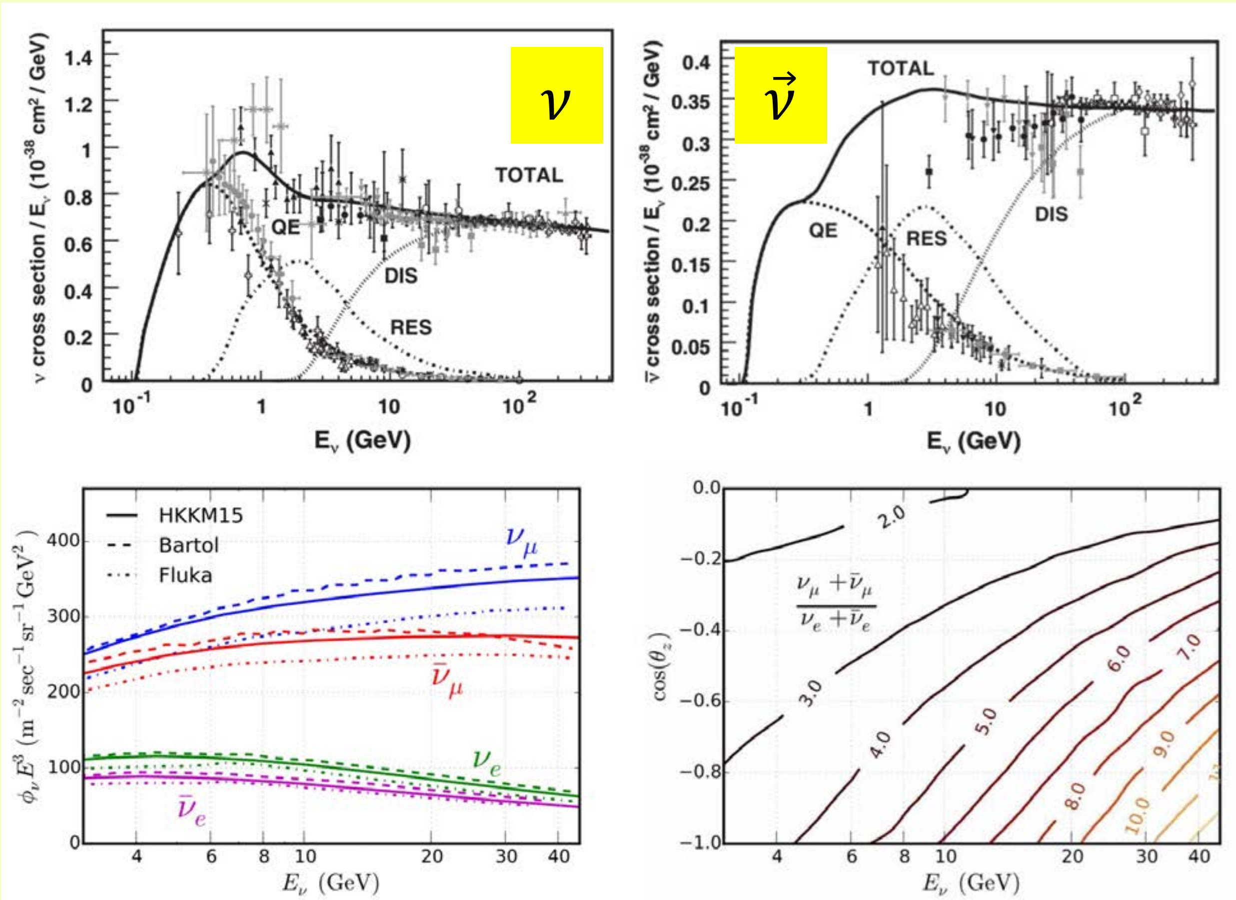

What can be measured

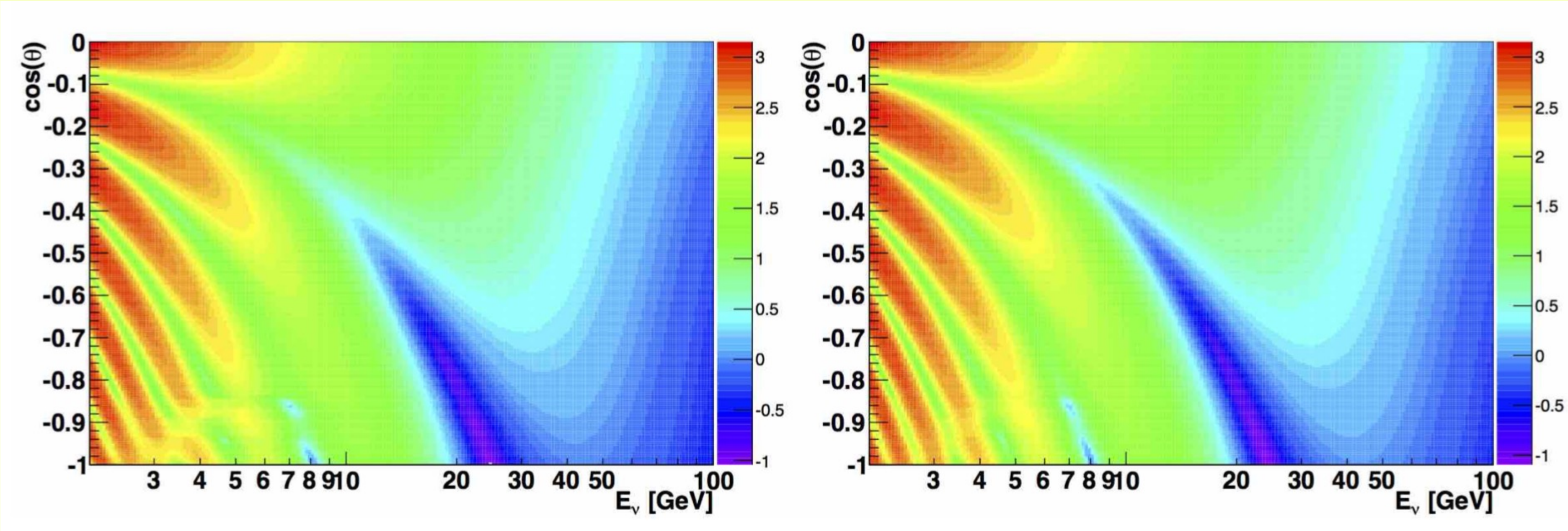

Neutrino “oscillograms”: the colour code gives the $\nu_\mu + \bar{\nu}_\mu$ event rate (in units of $GeV^{-1} \cdot y^{-1} \cdot sr^{-1}$ in log scale) as a function of the neutrino energy and cosine of the zenith angle, for a 1 Mton target volume. The left (right) plot shows the distribution for the normal (inverted) mass hierarchy.

To extract the information about "which hierarchy" corresponds to reality the asymmetry variable can be defined as: $\mathcal{A} = \frac{N_{IH} - N_{NH}}{N_{NH}}$. But these "oscillograms" are built with MC variables. What is the effect of experimental resolutions ??

The effect of detector resolutions

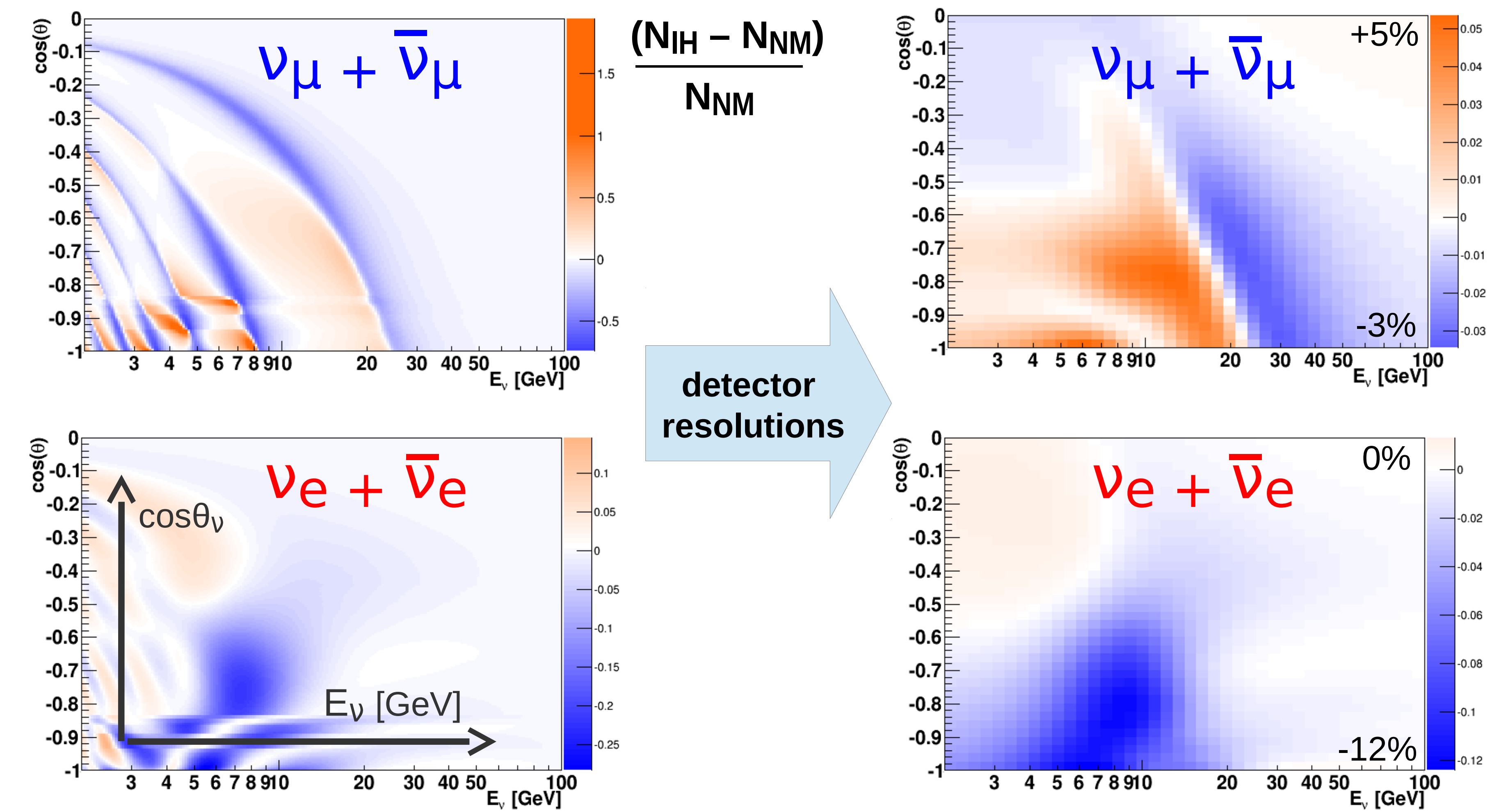

- Both muon & electron channel contribute to MH asymmetry
- Electron channel more robust against resolution effects

What probably will be seen

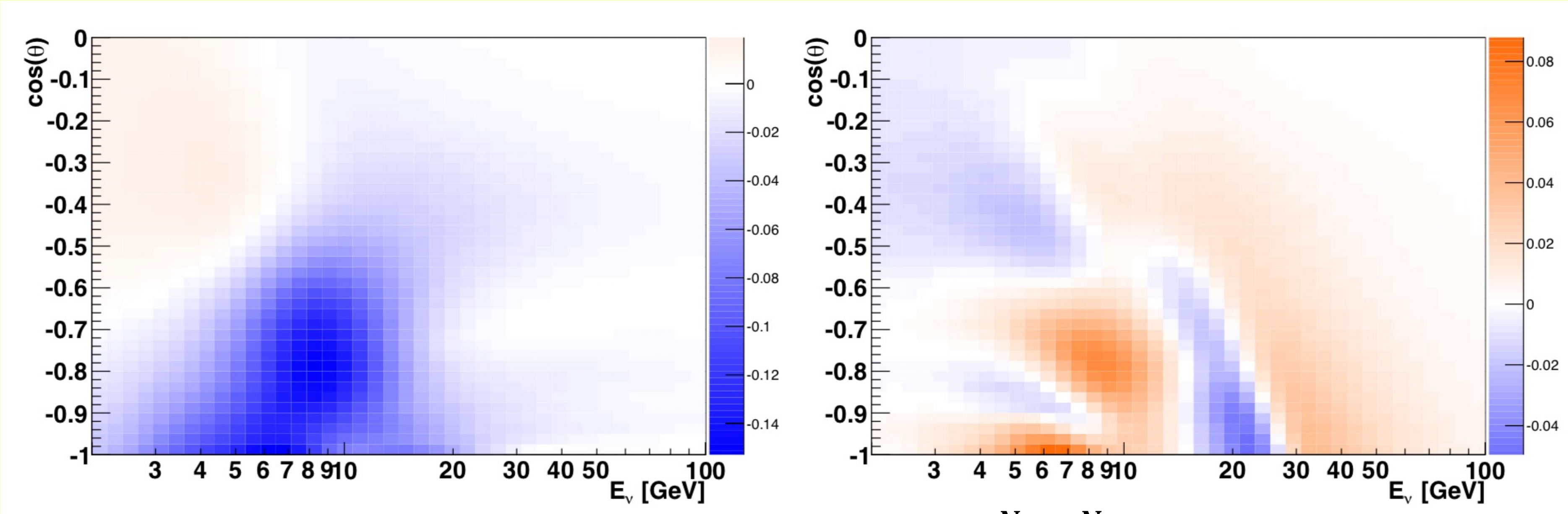

In each bin the color code gives the asymmetry, $\mathcal{A} = \frac{N_{IH} - N_{NH}}{N_{NH}}$, between the number of $\nu_\mu + \bar{\nu}_\mu$ CC interactions expected in case of NH and IH, expressed as a function of the energy and the cosine of the zenith angle. The right (left) plot applies to muon (electron) neutrinos. To account for detector resolutions a smearing of 25% is applied on the energy. On the angle, a smearing $\sigma_\theta = \sqrt{\frac{m_p}{E_\nu}}$ is applied, where m_p denotes the nucleon mass and E_ν the neutrino energy in GeV.
Maximum sensitivity for $(5 < E_\nu < 12)$ GeV

KM3NeT/ORCA Detector

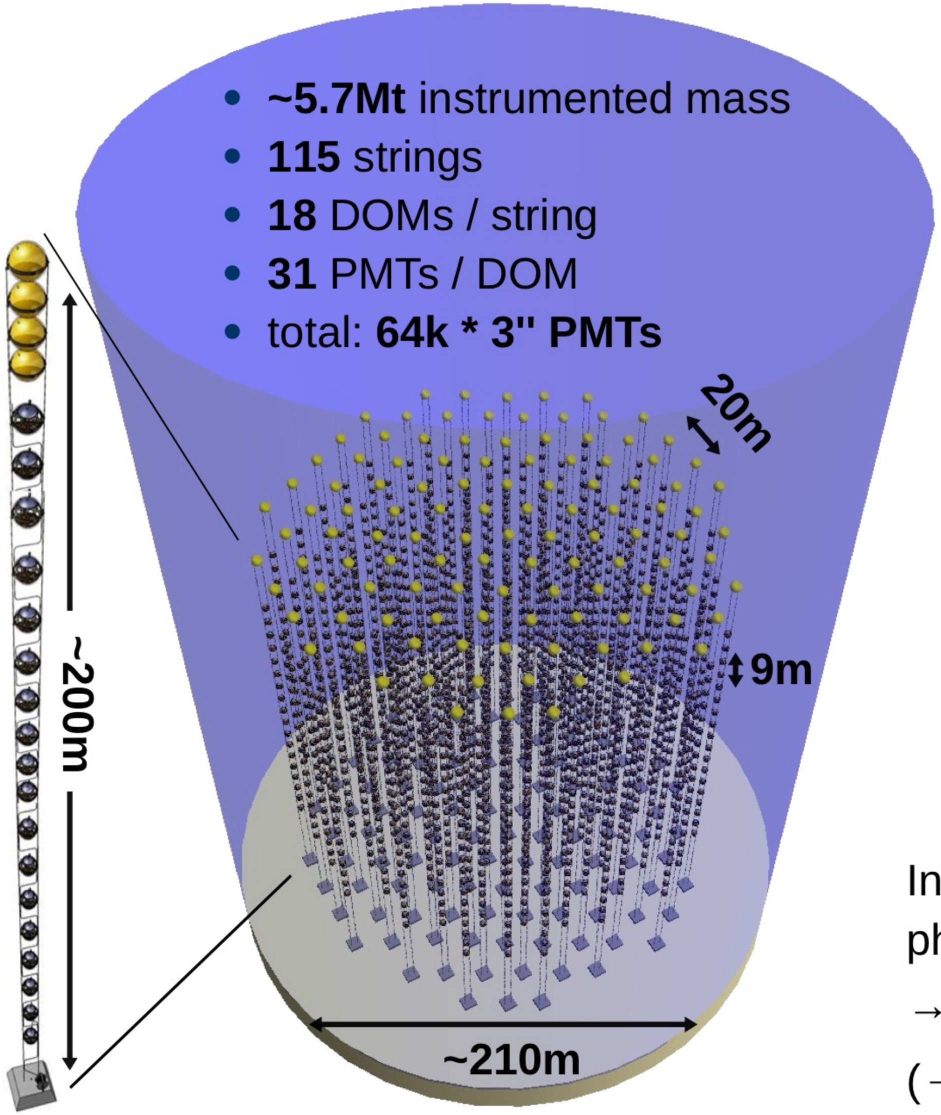

Digital Optical Module (DOM)

- 31 x 3'' PMTs (19 ↓, 12 ↑)
- Uniform angular coverage
- Directional information
- Single photon counting

Instrumentation density driven by main physics goal: neutrino mass hierarchy

→ ~few GeV neutrinos

(→ ~80x denser than ARCA)

ORCA detector

ORCA is part of the KM3NeT research infrastructure

- A different detector with same technology, but Mton instead of Gton scale
- Few GeV signal => more compact detector (75 times denser!)

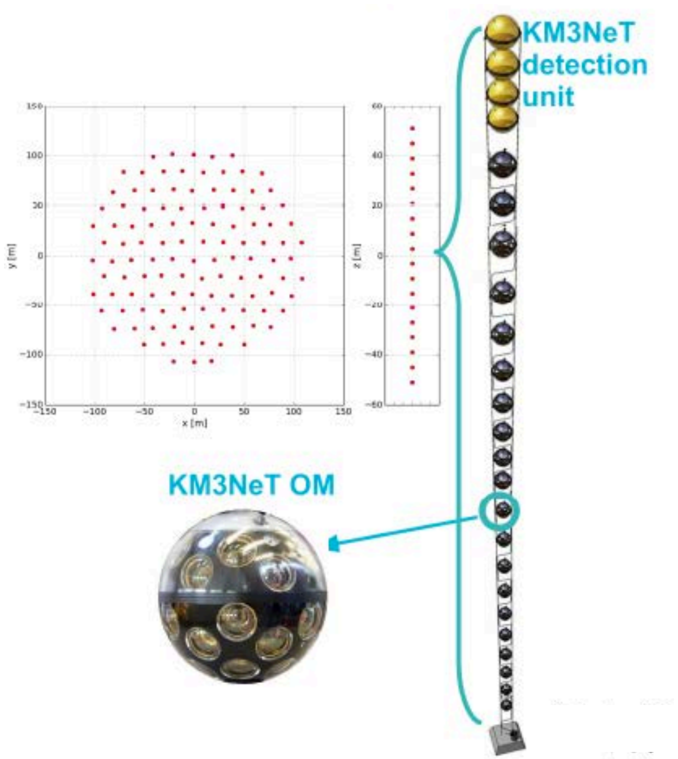

- 115 detection units, 20m spacing
- 18 Optical Modules (DOMs) per detection unit
- 6m vertical distance between DOMs
- 31 3” PMTs/DOM
- Instrumented volume 3.75 Mtons
- Estimated cost   40 M€ (conservative)
- Geometry optimisation study ongoing

Motivations for a future Neutrino Acoustic and Radio Detector: detection techniques

- Predicted neutrino fluxes are very **LOW**
- → Cubic kilometer scale Cherenkov Detectors required for $10^{12}<E_\nu<10^{17}$ eV
  - **NATURAL TARGET (ice, water, rock …), light attenuation (60m)**
  - **It will be very difficult to exceed V_{eff} > 10 km^3**
- Remember $N_\nu \approx N_0\, E^{-2}$, increasing the energy by a decade, the neutrino flux decreases by a factor ≈ 100 !!!

- The detection of neutrinos with $E_\nu>10^{17}$ eV will be possible with signal propagating in water/ice with attenuation lengths of scale O(1km)

Acoustic & Radio signals detection: a possible candidate

High Energy Neutrino Detection

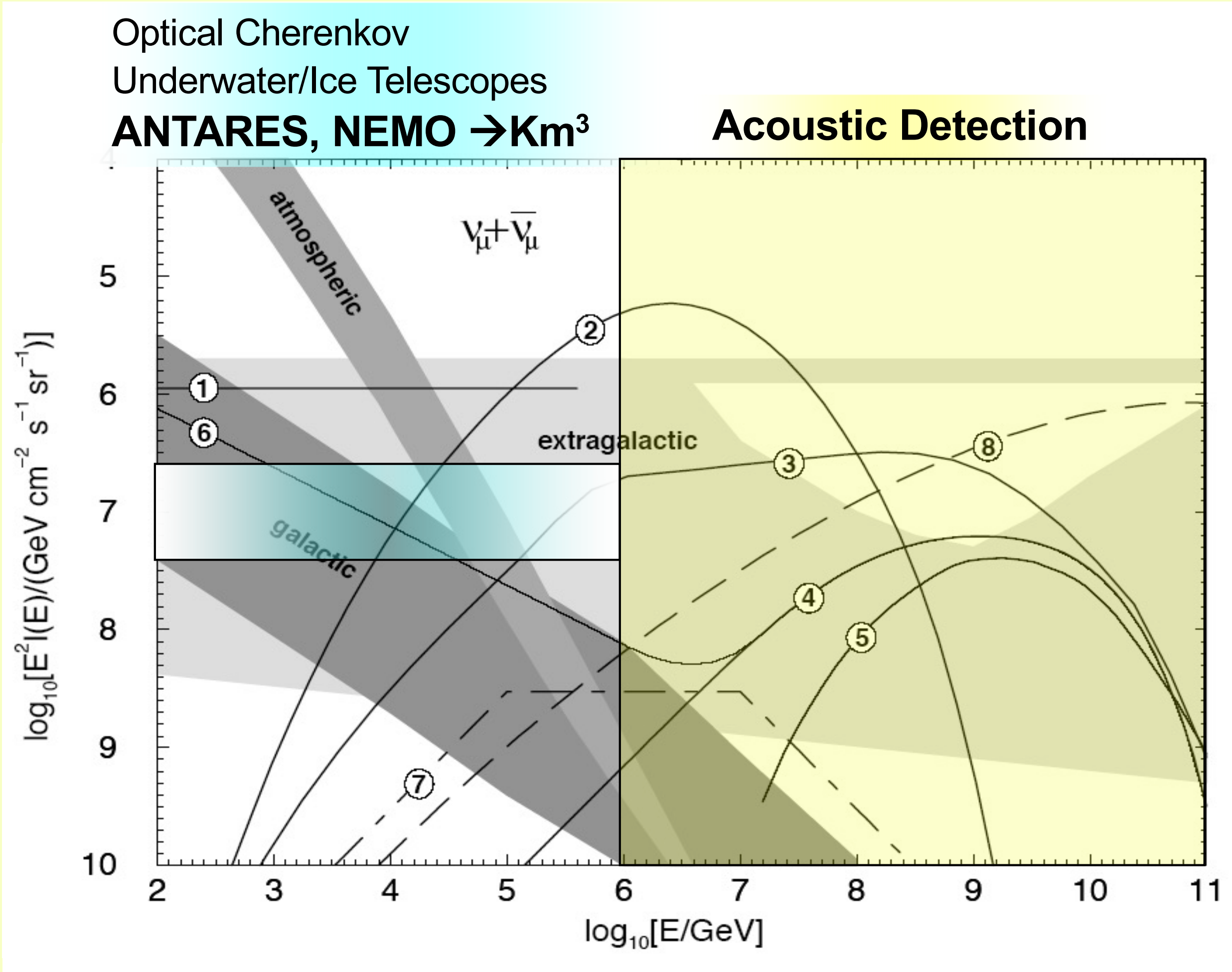

(1-4 and 6) AGN models; *(5)* GZK; *(7)* GRB; *(8)* topological defects
[adapted from Learned and Mannheim, *Annu. Rev. Nucl. Part. Sci.* 50 (2000)]

Acoustic detection principle/features

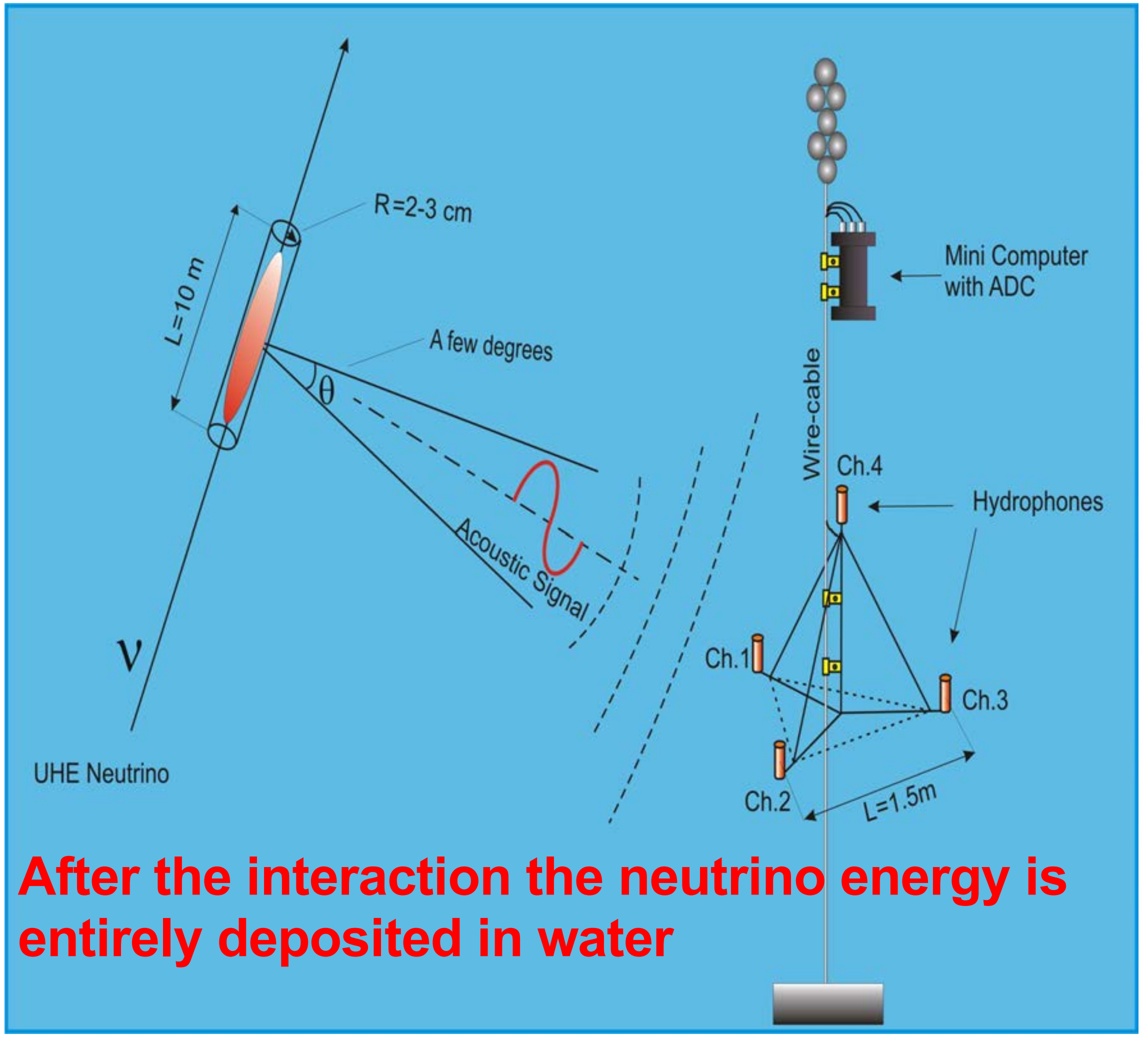

After the interaction the neutrino energy is entirely deposited in water

- Typical cylindrical volume over which the hadronic energy is deposited is ~10m long by a few centimetres wide
- *The energy deposition is instantaneous with respect to the signal propagation*
- Hence the acoustic signal propagates in a narrow "pancake" perpendicular to the shower direction in analogy with light diffraction through a slit

Basics of thermo-acoustic mechanism

A pressure wave is generated instantaneous following a sudden deposition of energy in the medium (neglecting absorption: O(10 km) at 10 kHz)

Istantaneous deposition of heat through ionization

$$t_{deposition} \approx D/c \approx 10^{-7} : 10^{-8} \ sec$$

Thermo-acoustic process:
increase of temperature (specific heat capacity C_p), expansion (expansion coeff β)

$$t_{expansion} \approx 10^{-5} \ sec \gg t_{deposition}$$

$$\nabla^2 \mathbf{p} - \frac{1}{c_s^2}\ddot{\mathbf{p}} = -\frac{\beta}{c_p} \cdot \frac{\partial \varepsilon(\mathbf{r},\mathbf{t})}{\partial \mathbf{t}}$$

For a point like source (micropulse):

$$\mathbf{p}(\mathbf{r},\mathbf{t}) \propto \frac{E_0 \beta}{4\pi c_p} \frac{\partial}{\partial t} \frac{\delta\left(t - \frac{r}{c_s}\right)}{r}$$

Bipolar pulse
spherical expansion

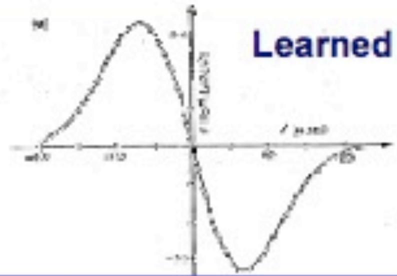

Learned

For a shower heating a volume of matter (macropulse):

$$\mathbf{p}(\mathbf{r},\mathbf{t}) \propto \frac{\beta}{4\pi c_p} \frac{\partial}{\partial t} \int \frac{1}{r} \varepsilon \, dV$$

Sum of pointlike sources: wavefront and signal shape depend on the energy density distribution

Acoustic pulse amplitude in Salt, Water and Ice

Conversion of ionization energy into acoustic energy

	Med Sea	S.P. ice	NaCl
T [°C]	14°	-51°	30°
c_s [m s^{-1}]	1545	3920	4560
β [K^{-1}]	25.5x10^{-5}	12.5x10^{-5}	11.6x10^{-5}
C_P [J kg^{-1} K^{-1}]	3900	1720	839
$\gamma = c_s^2 \frac{\beta}{C_p}$ Gruneisen coefficient	0.12:0.13	1.12	2.87

$$\mathbf{p}_{max} \approx \mathbf{E}_\nu \times \frac{1}{4} \times \gamma \approx 6 \cdot 10^{-21} \mathbf{E}_\nu \left[\frac{\mathbf{Pa}}{\mathbf{eV}} \right]$$

The acoustic detection principle

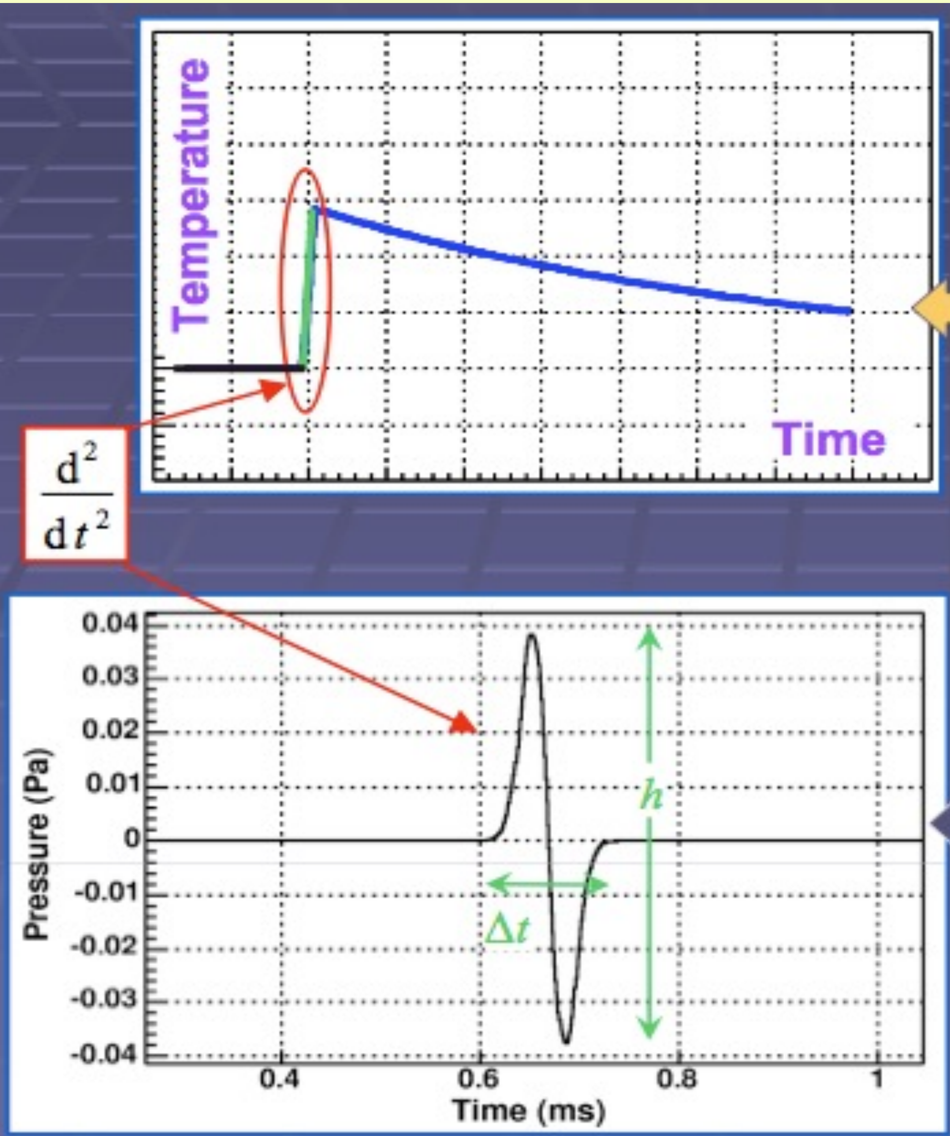

- ***Fast thermal energy deposition*** *(followed by* ***slow heat diffusion****)*
- ***Results in a near-instantaneous temperature increase and material expansion giving rise to an "acoustic shock" sound pulse***

- This pressure pulse is related to the double derivative of the Heaviside step function of the temperature rise and leads to a characteristic expected bipolar pulse shape
- *h* is defined by the properties of the medium:
  - $h \propto \beta / C_p$ where β is the co-efficient of thermal expansivity and C_p is the specific heat capacity
- Δt is defined by the transverse spread of the shower

Acoustic Signal Detection

Particles Interaction in Water - the Acoustic Signal

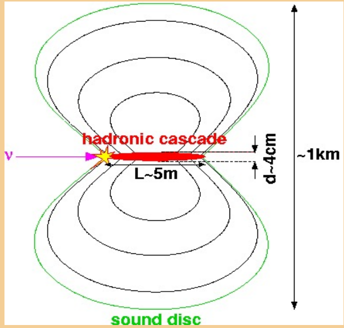

(Askaryan)

" instantaneous "
& localized
energy deposition

↓

local heating of
the medium

↓

Local density variation

↓

PRESSURE WAVE

Thermo-Acoustic (Hydrodynamic) Mechanism of Energy Dissipation

Wave Equation

$$\nabla^2 p(\vec{r},t) - \frac{1}{c_s^2}\frac{\partial^2 p(\vec{r},t)}{\partial t^2} = -\frac{\beta}{C_p}\frac{\partial^2 q(\vec{r},t)}{\partial t^2}$$

- $p(r, t)$ pressure
- $q(r, t)$ energy deposition density
- c_s speed of sound
- β volume expansion coeff.
- C_p heat capacity

Solution (Kirchoff Integral)

$$p(\vec{r},t) = \frac{\beta}{4\cdot\pi\cdot C_p}\int\frac{dV'}{\left|\vec{r}-\vec{r}\right|}\cdot\frac{\partial^2}{\partial t^2}q\left(\vec{r},t-\frac{\vec{r}-\vec{r}}{c_s}\right)$$

Acoustic Signal Detection

$$p(\vec{r},t) = \frac{\beta}{4\cdot\pi\cdot C_p}\int\frac{dV'}{\left|\vec{r}-\vec{r}'\right|}\cdot\frac{\partial^2}{\partial t^2}q\left(\vec{r},t-\frac{\left|\vec{r}-\vec{r}'\right|}{c_s}\right)$$

β , the volume expansion coefficient, depends on temperature **(data in water)**

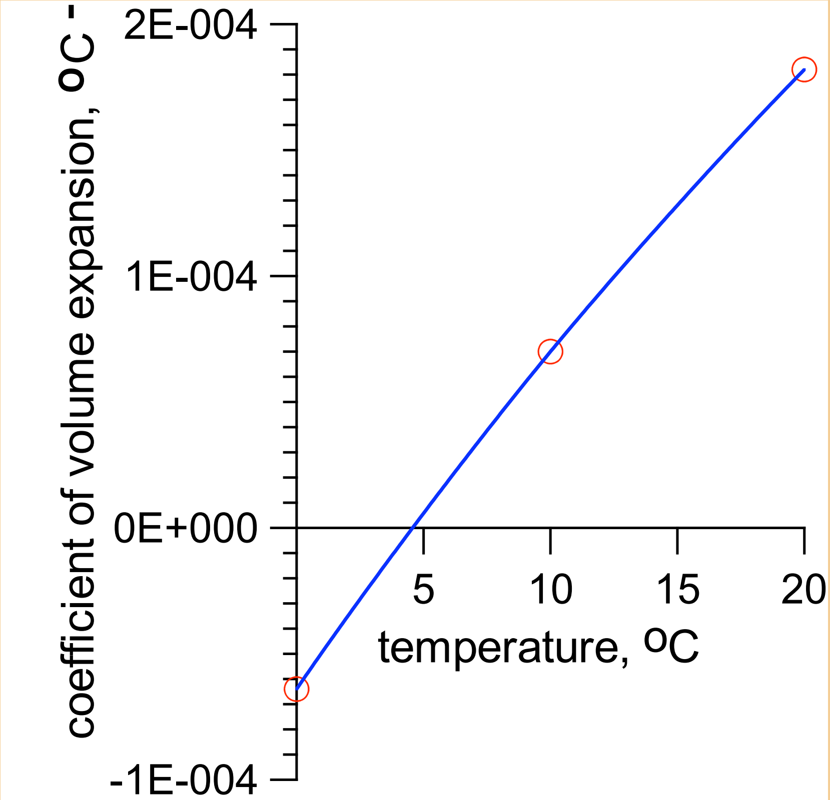

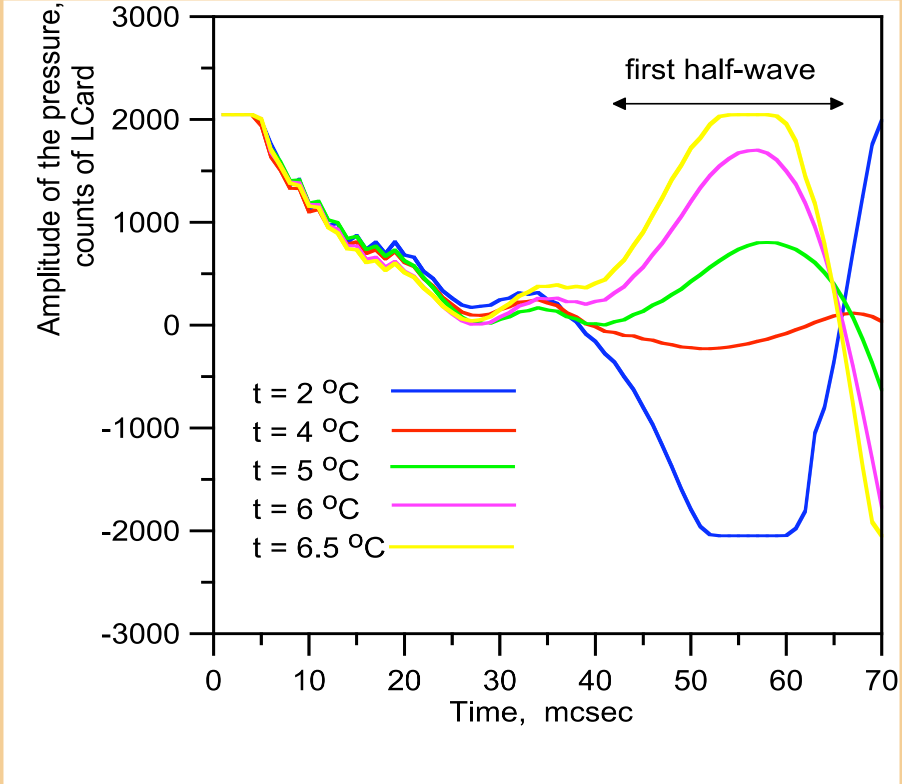

The acoustic signals change polarity close to t ~ 4 °C

Largest Signal in Mediterranean (~14 ° C)

Acoustic Signal from Neutrinos

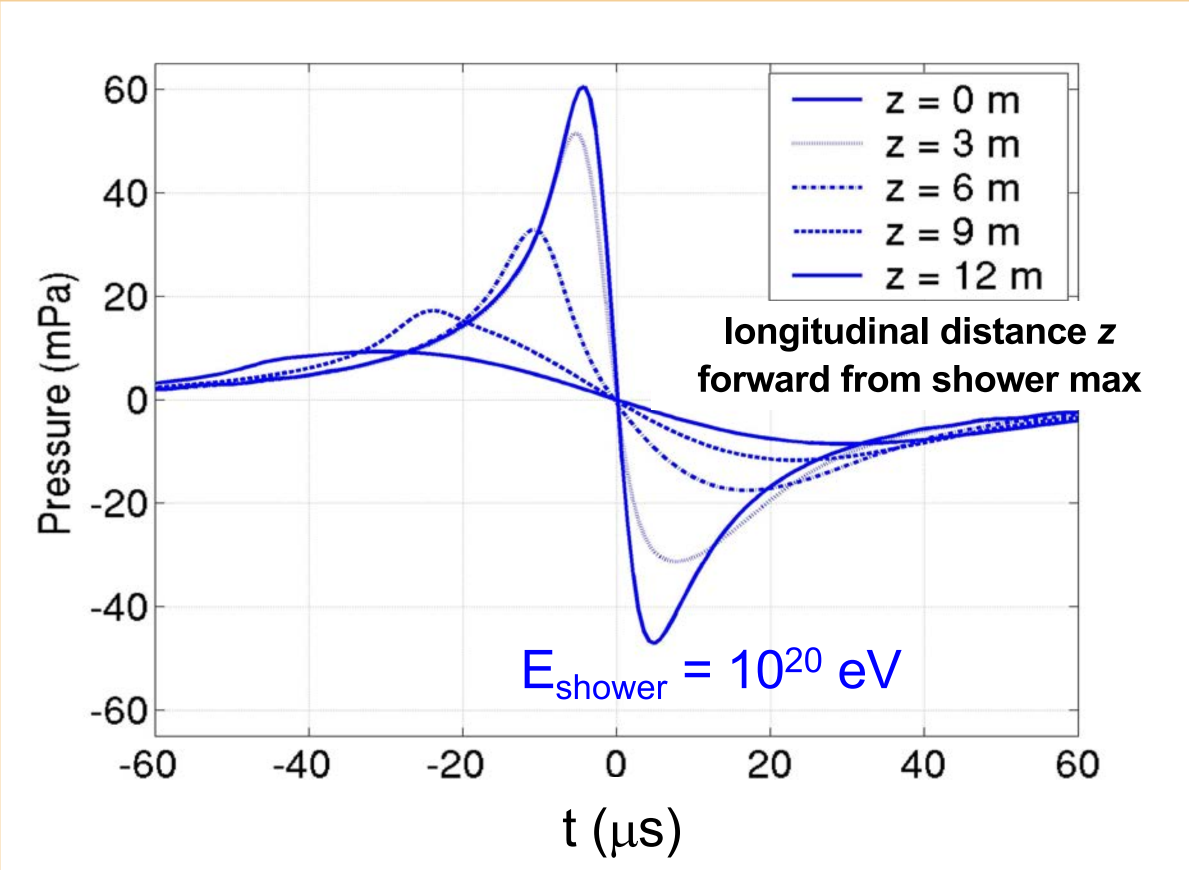

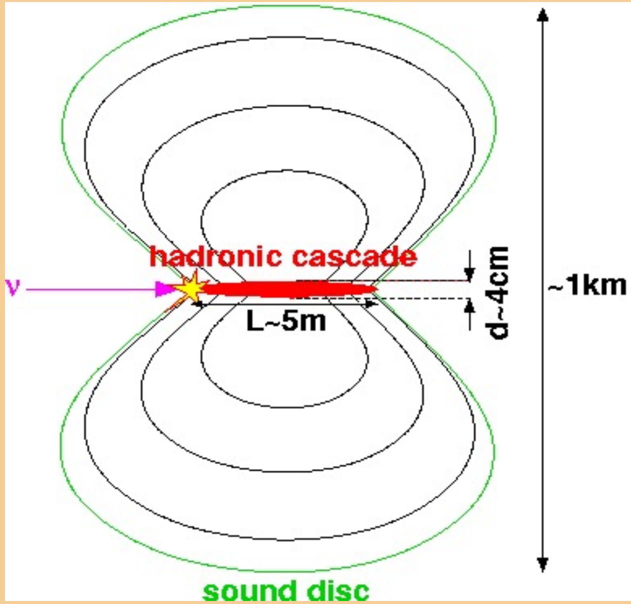

Simulated Neutrino Pulse

1050 m transverse distance from shower

Underwater Noise

other marine sources of sound:
wind, waves, ships, animals

Signal and Noise Spectrum in the Sea

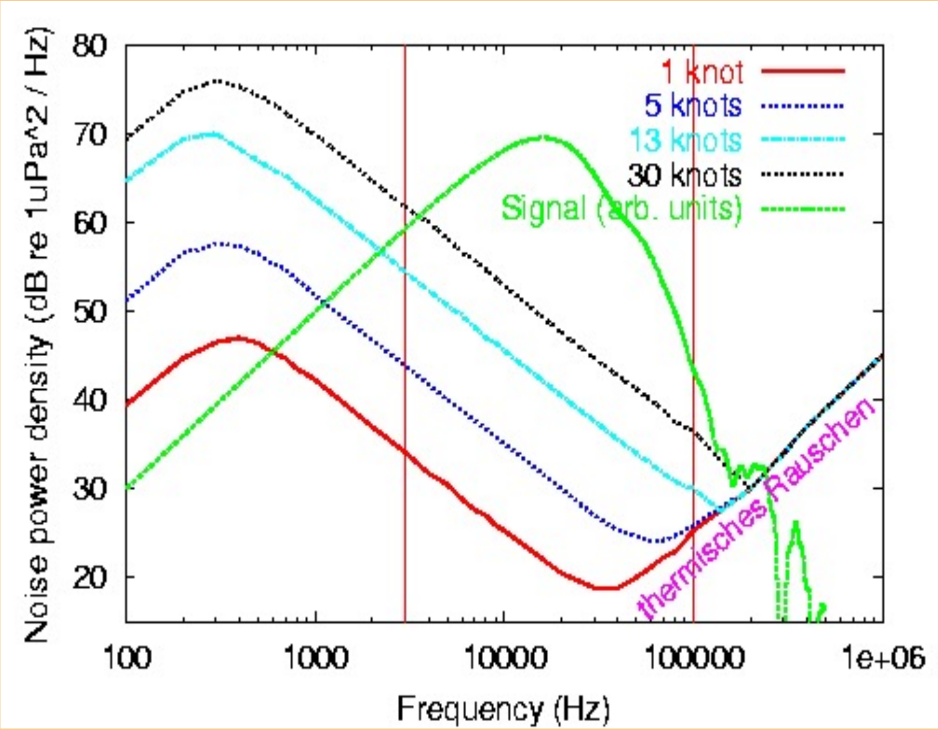

- noise depends on wind speed
- at *high frequencies* dominated by *thermal noise*
- Expected signal maximum between 10 and 50kHz, where noise is minimal (at sea state zero)

⇒ **look for signal in frequency band ~10 to ~50kHz**

Acoustic Signal Detection

Acoustic Sensors Development

The Piezoelectric Effect

Piezoelectric effect consists on voltage produced between surfaces of a solid dielectric (non - conducting substance) when a mechanical stress is applied to it

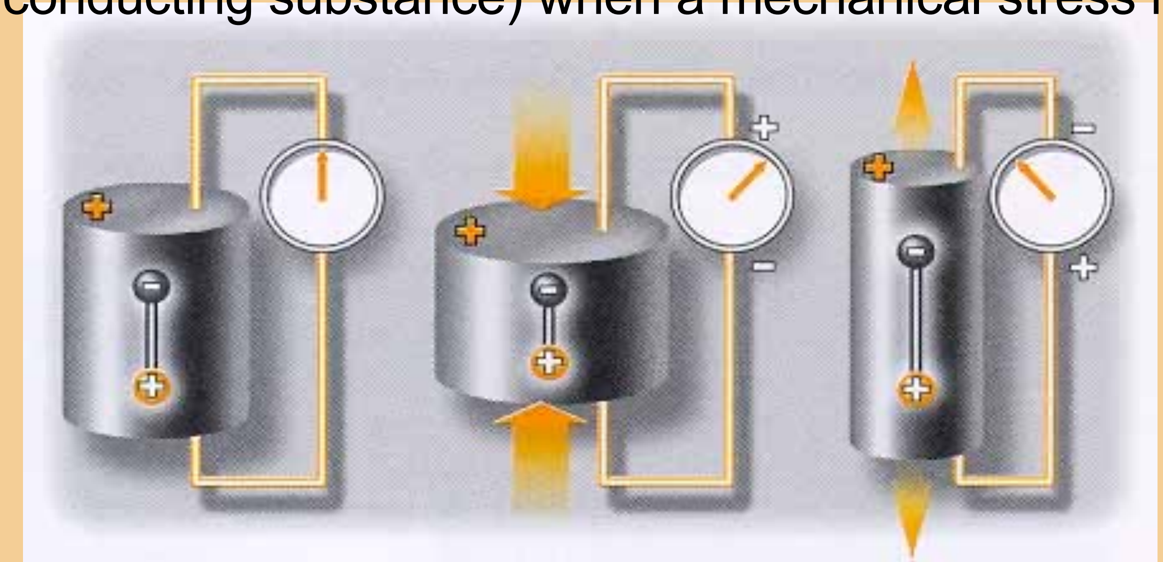

Acoustic Sensors Development

Hydrophones
- Commercial hydrophones
- Self-made hydrophones

Requirements

Hydrophones to be used in an underwater neutrino telescope must be:

- *pressure resistant* (very deep ocean sites)
- *very sensitive* (expected pressure signals from neutrino events ~10mPa peak-to-peak for 10^{18} eV in 400m distance)
- *low cost* (large number of sensors)

Acoustic Sensors Calibration

Electric bulbs

Calibration Sources

Sensitivity Response
Energy Calibration

Proton beam: the Bragg Peak

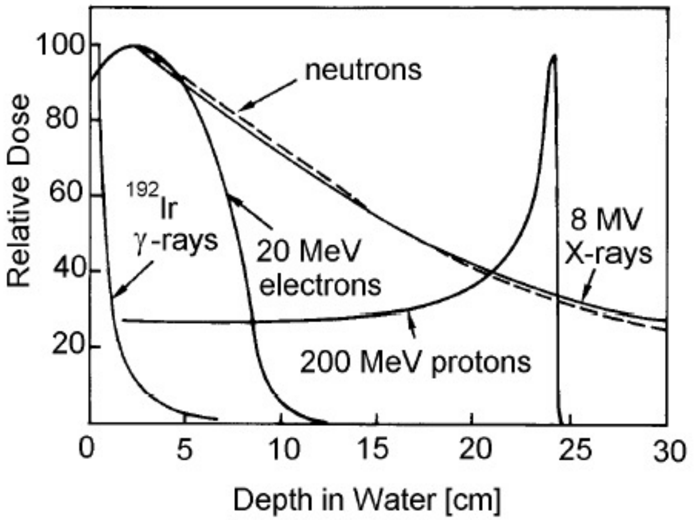

If the proton energy is in the range 100-200 MeV, most of the primary proton energy is deposited at the Bragg Peak.

Heated wires

Laser beam

Piezos

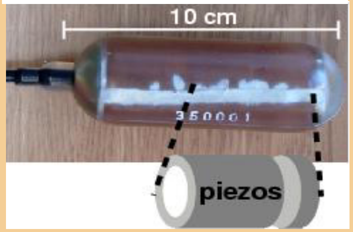

Sparker

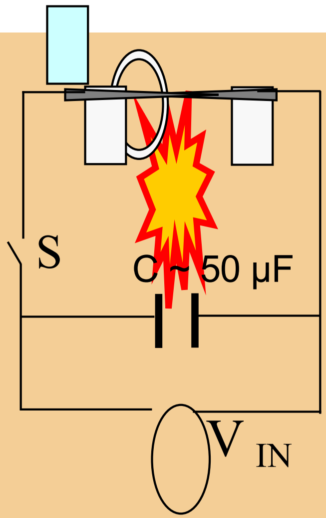

Test at ITEP (Moscow) Proton Beam

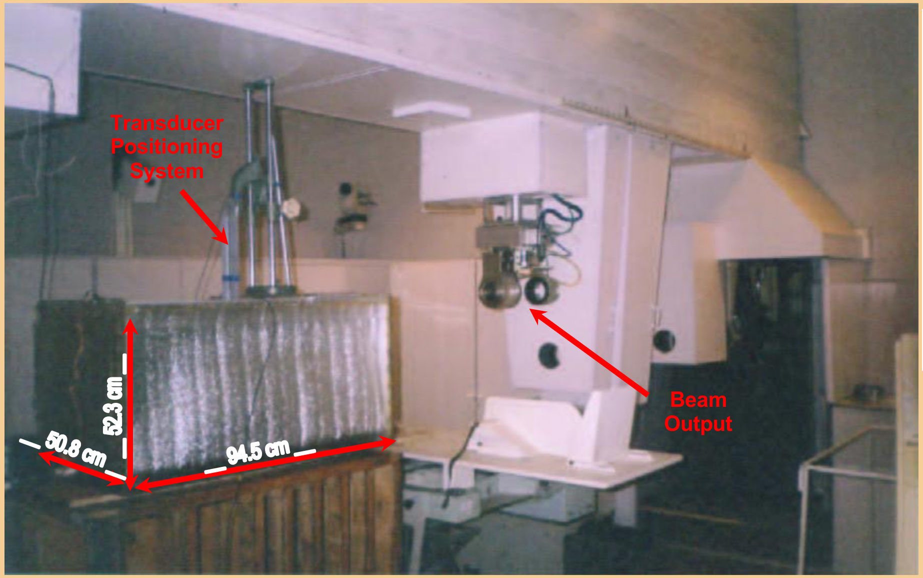

Dimensions
50.8 cm × 52.3 cm × 94.5 cm

The 90% of the basin's volume is filled with fresh water.
NO control on temperature.

Piezo-Electric Hydrophones previously calibrated at the IDAC O.M. Corbino facilities

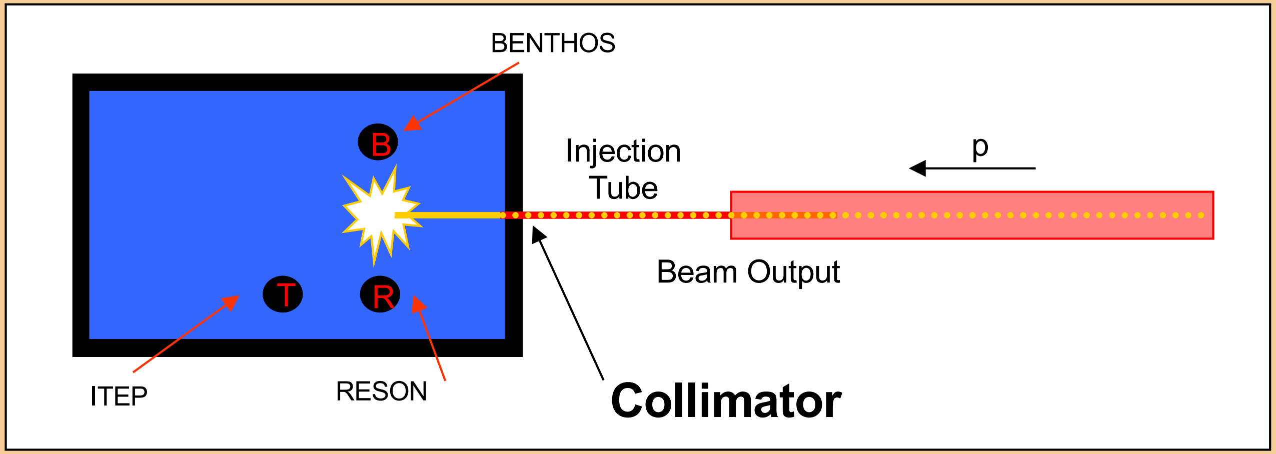

$N_{protons}$/spill ~ 10^{10}
$E_{protons}$ = 100 MeV, 200 MeV

up to 10^{18} eV deposited per spill

Test at ITEP (Moscow) Proton Beam

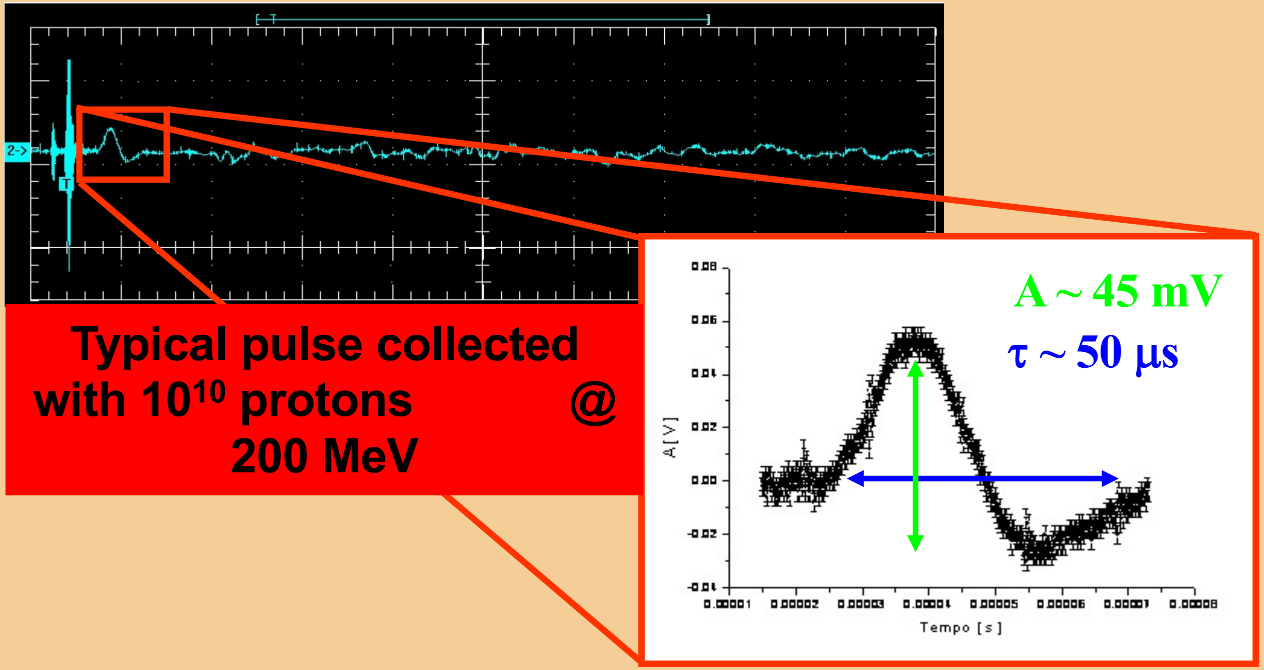

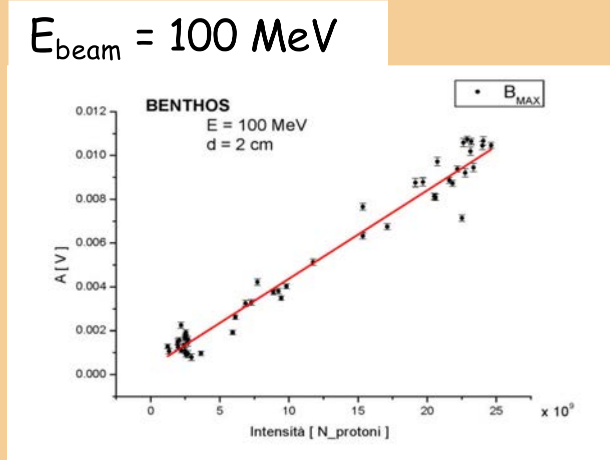

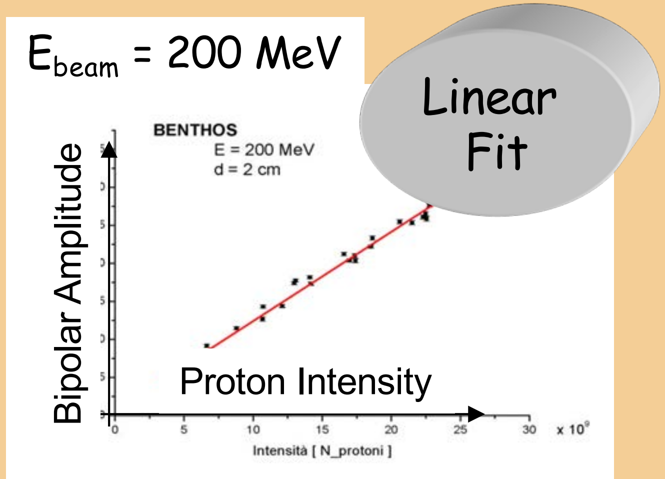

Calibration with Proton and Laser Beams

Signal is Acoustic

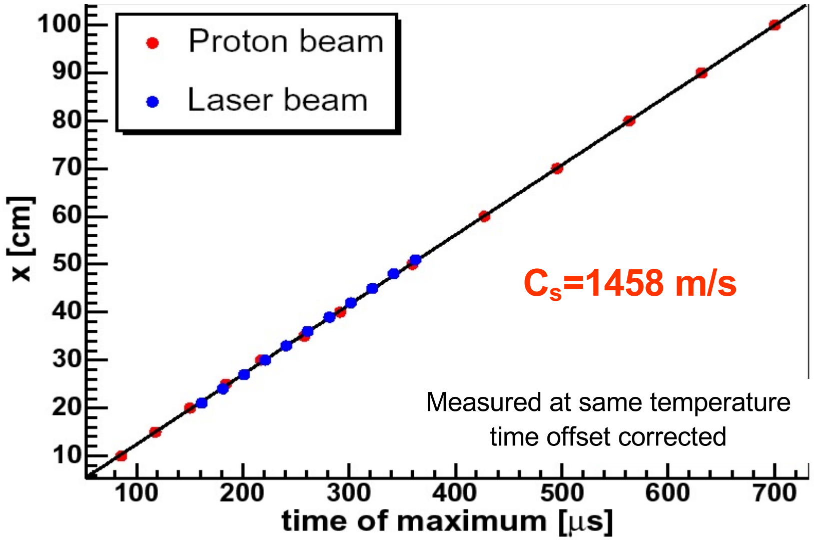

[K. Graf]

Temperature Dependance

Proton Beam | **Laser Beam**

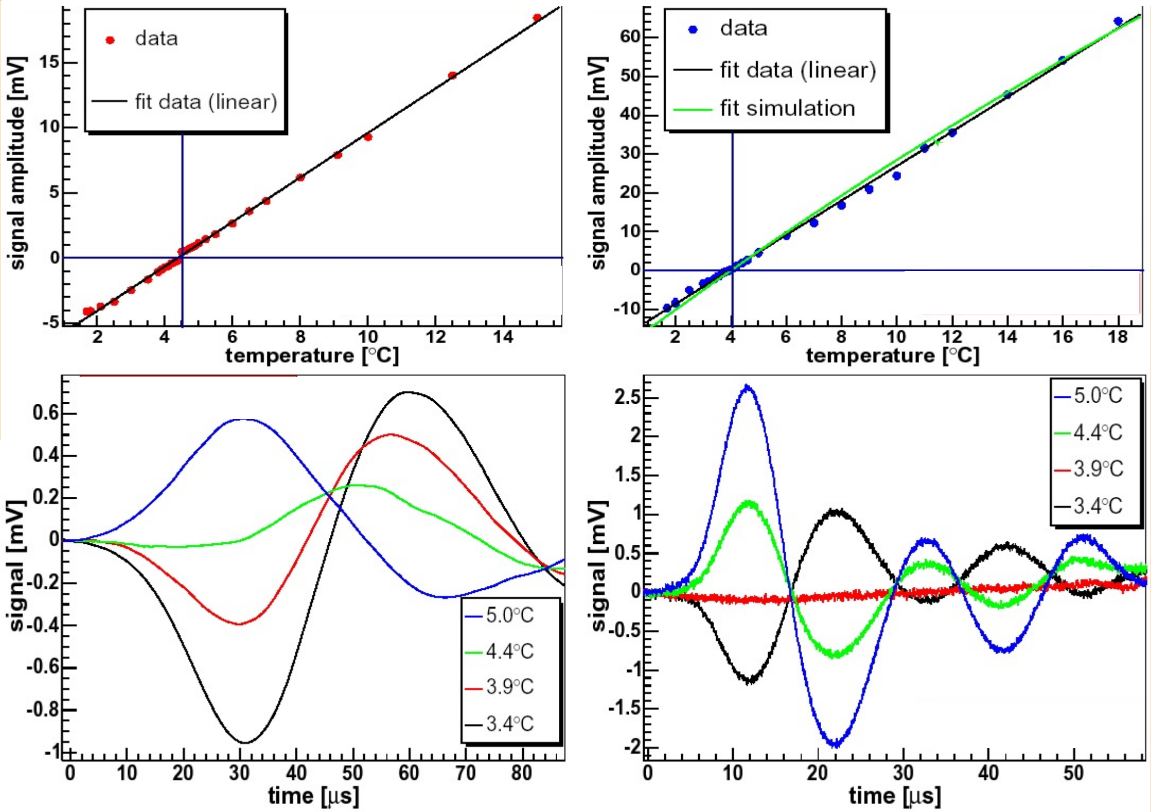

Proton & laser beam experiments confirm thermo – acoustic sound generation is primary effect

- Simulation and model predictions in good agreement with measured signals
- Some minor effect (around 4 ° C) need to be clarified

Existing acoustic detection sites: Lake Baikal

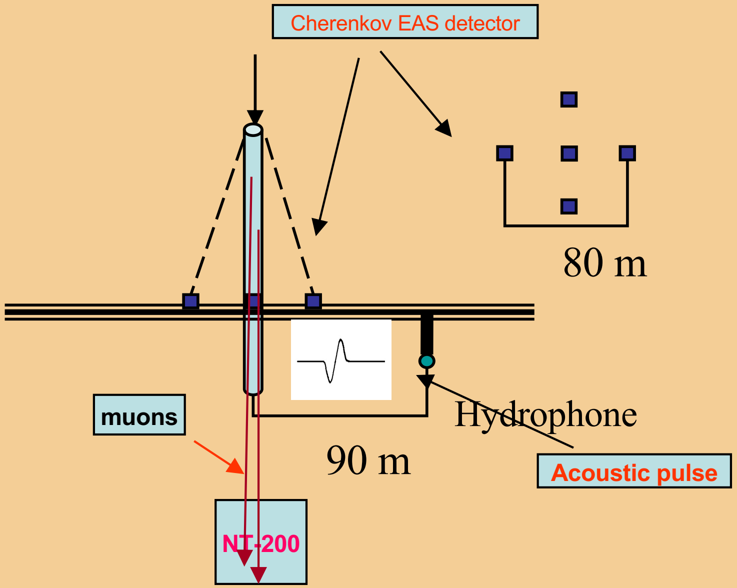

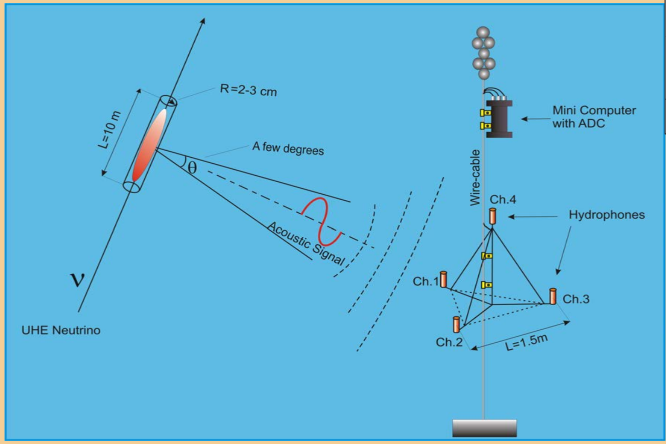

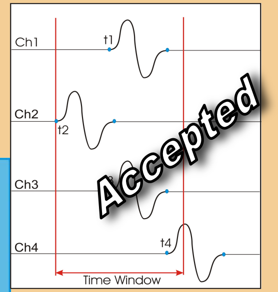

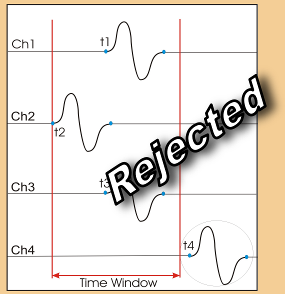

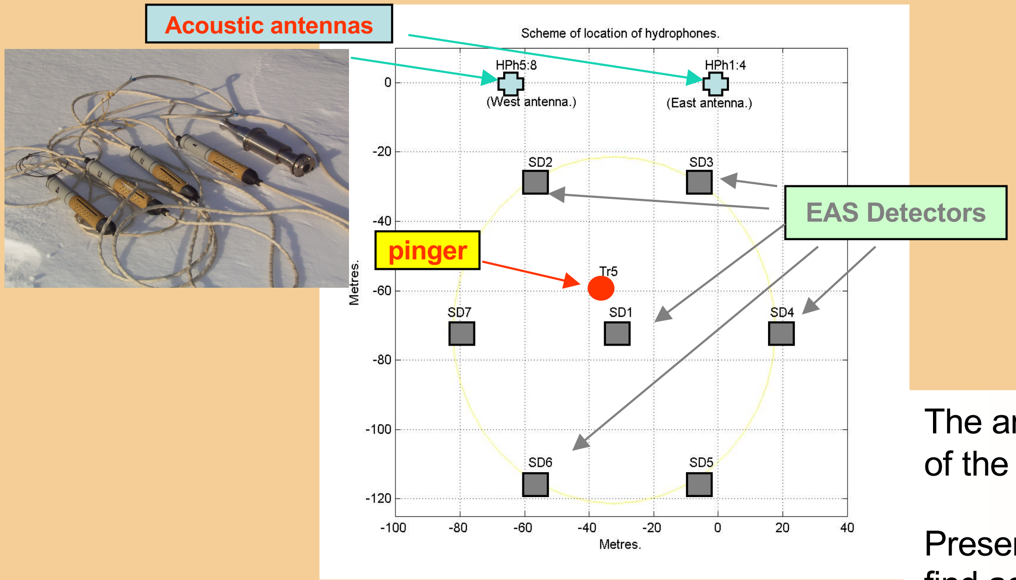

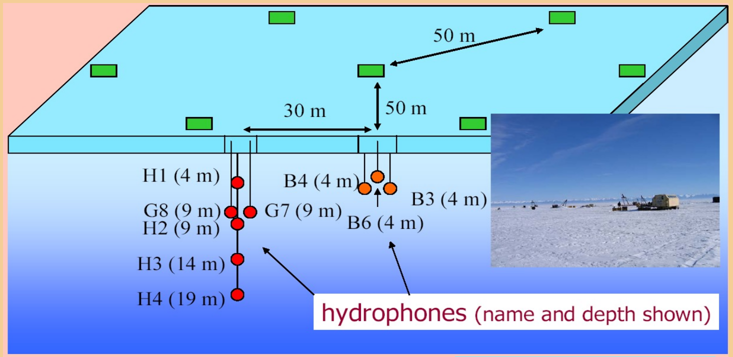

The analysis reveals many interesting features of the under-ice acoustic noise.

Present straightforward method does not allow to find acoustic signal from EAS.

Energy up to ~ 10^{17} eV

Existing acoustic detection sites: SAUND

- The SAUND experiment
- *Stanford based venture using the AUTEC array, naval hydrophones in the Bahamas*
- First limit paper published based on 195 days reading out 7 hydrophones
- *See astro-ph/0406105*

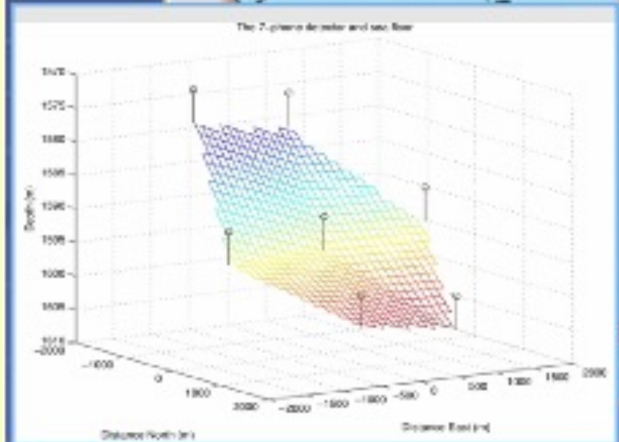

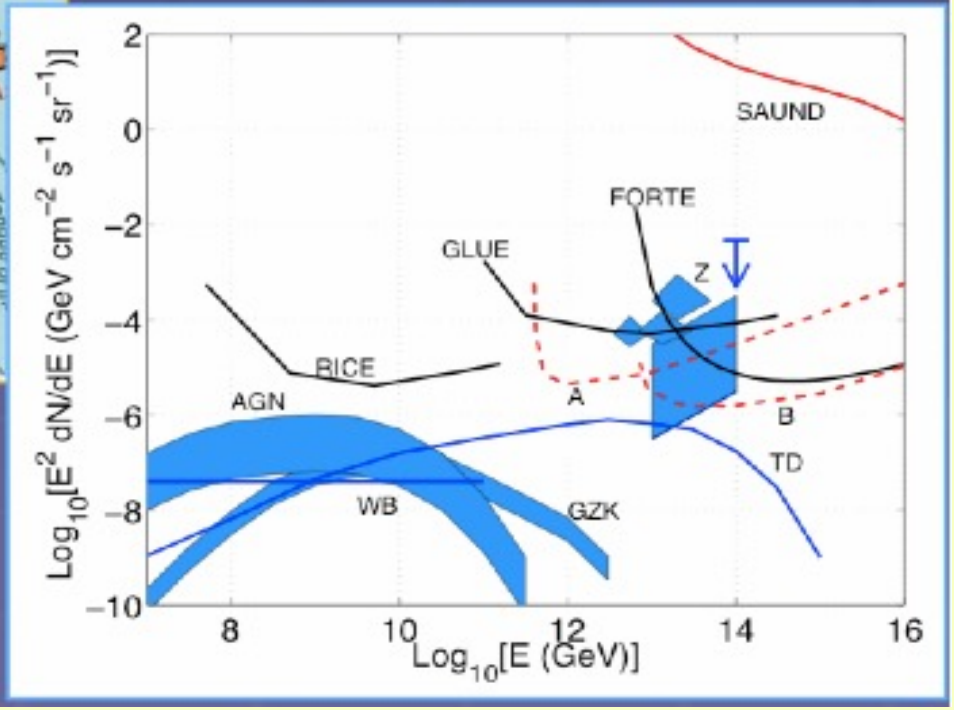

- SAUND II funding approved
- *Move from 7 to ~56 hydrophones*
- Area to be read out is ~1000 km²
- *Mean sensor spacing is 4km*
- Data taking started in June

SAUND

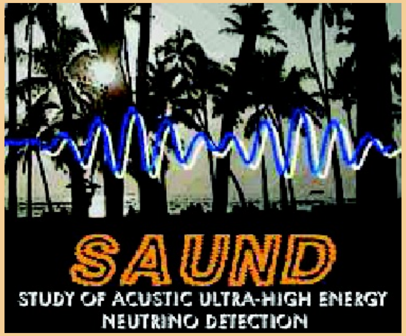

Study of Acoustic Ultra-high-energy Neutrino Detection

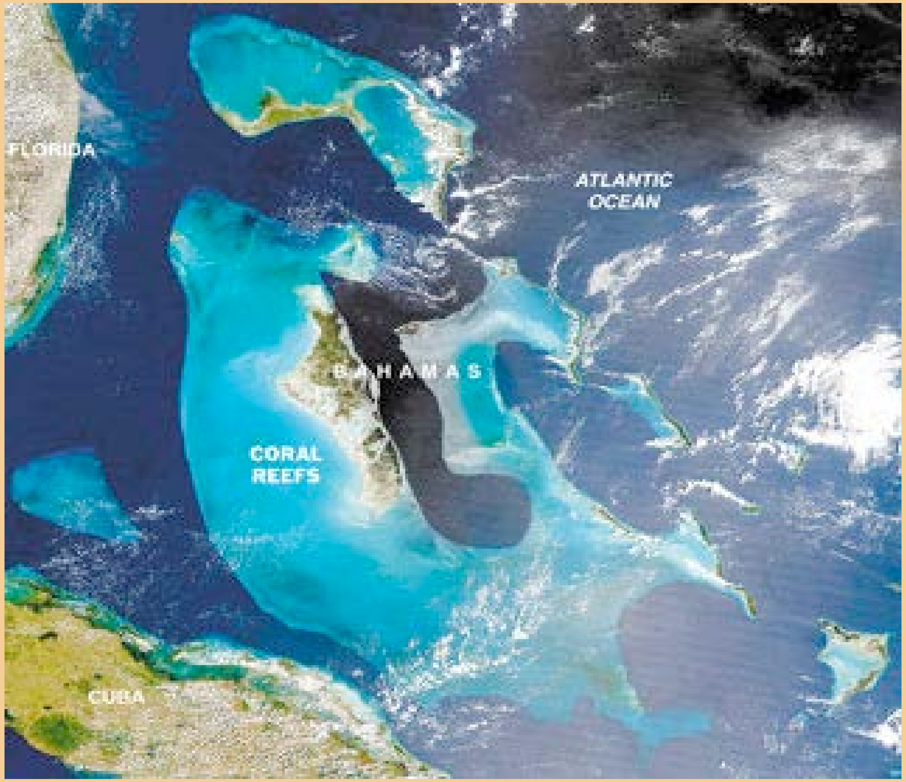

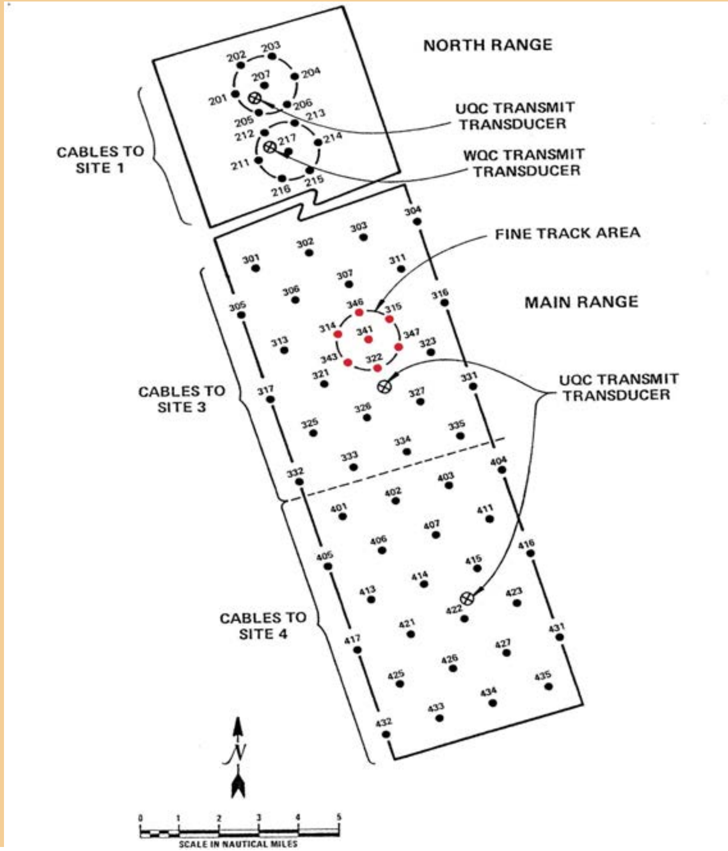

The Atlantic Undersea Test and Evaluation Center (AUTEC) hydrophones

SAUND – 1

7 km^2

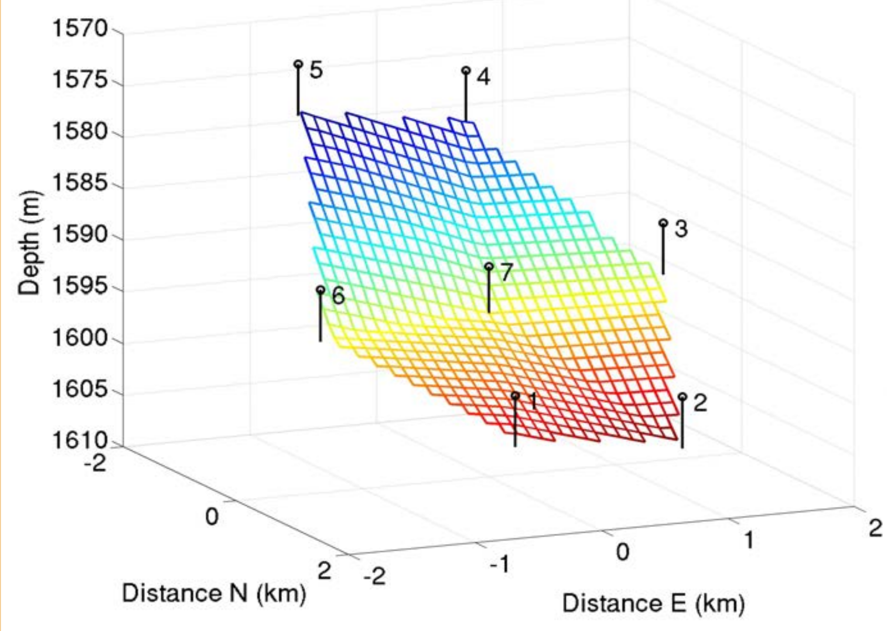

7 hydrophones on sea floor, spacing ~1.5 km

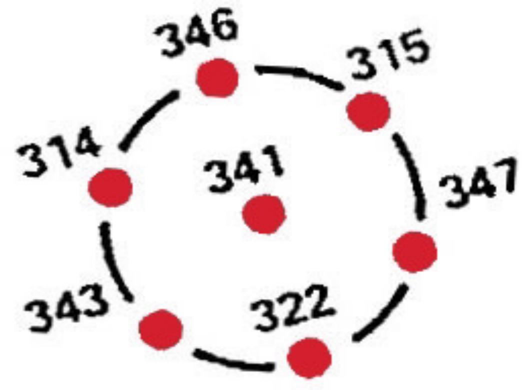

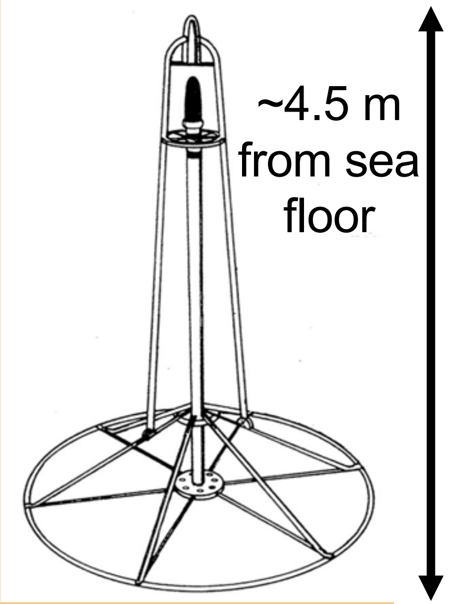

→SAUND – 2 AUTEC array improvment

increased BW, gain, stability

SAUND - Flux Limits

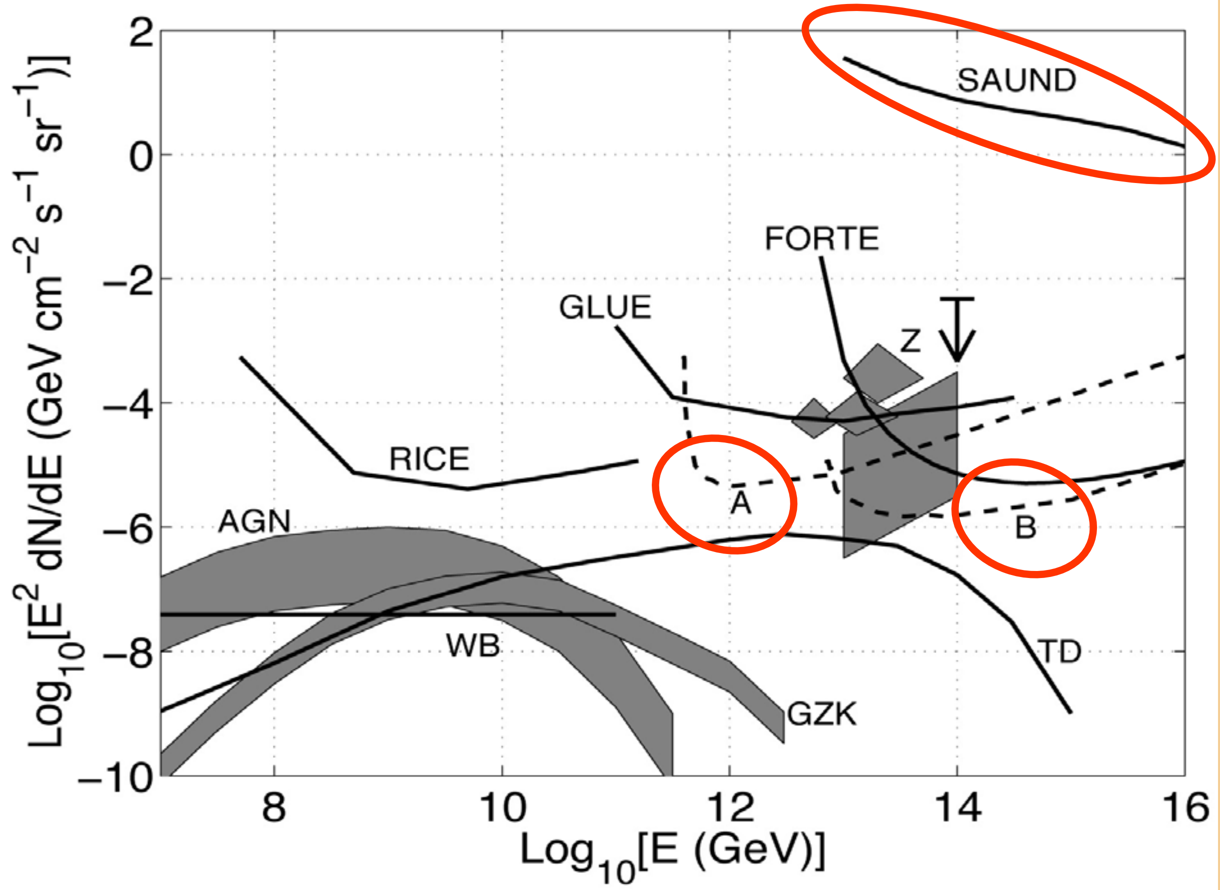

A/B represent 1-year limits from hypothetical large arrays (367 1.5-km strings, spaced 0.5/5 km apart)

Acoustic detection sites: RONA

RONA: a military array used by physicists

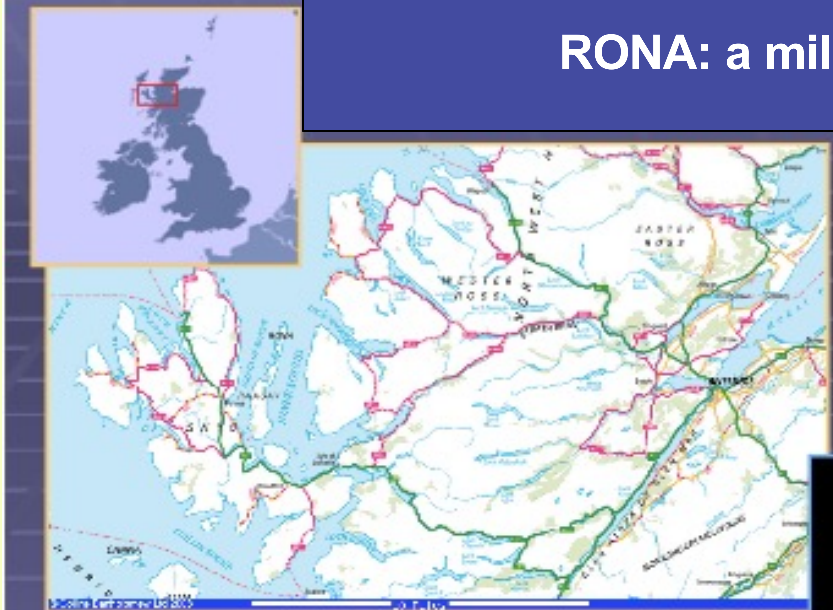

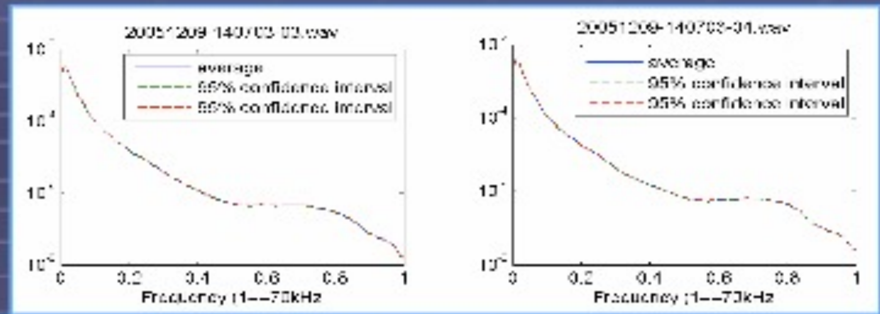

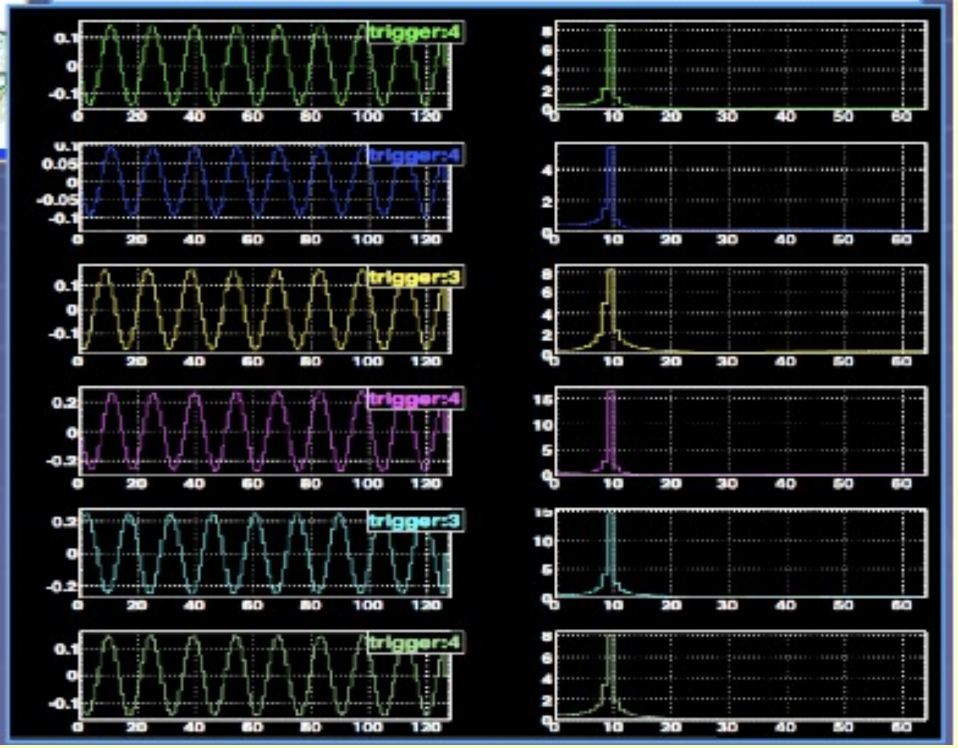

- Rona hydrophone array, a military array in Scotland used by the ACORNE collaboration
- *2 weeks of unfiltered data taking in December 2005, continuous since September 2006*
- 8 hydrophones read out continuously at 16bits,140kHz - a total of (~15Tb)
- *Data are passed through a number of triggers including a matched filter prior to analysis*
- Average spectra show hydrophones are well-balanced

Acoustic detection by INFN/NEMO site: OvDE

Neutrino Mediterrean Observatory

ONDE – Ocean Noise Detection Experiment

NEMO Test Site (Catania)

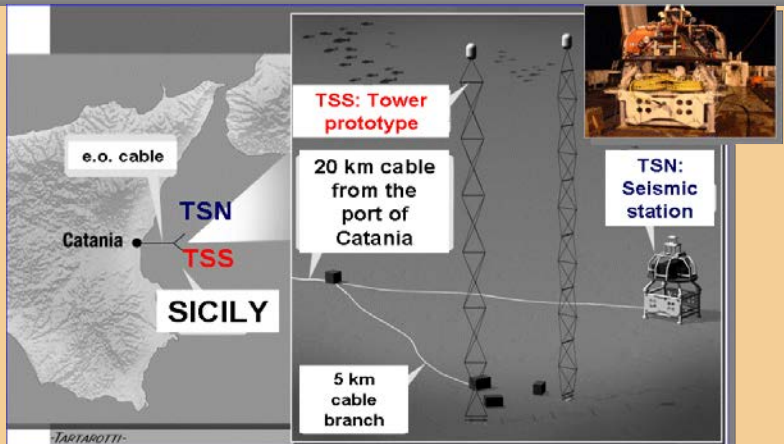

Lat: 37° 32.681' N
Long: 015° 23.773' E
Depth: 2050 m

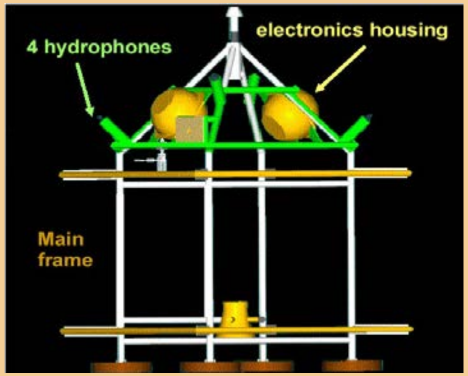

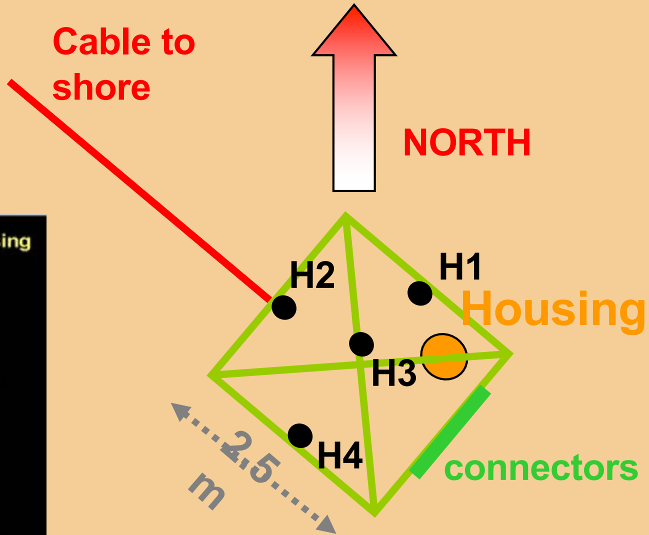

Height from seabed :
H1, H2, H4: ~ 2.6 m
H3: ~ 3.2 m

First noise spectra
Whales&Dolphins signals

OνDE: Ocean Noise Detection Experiment

4 hydrophones (10 Hz-40 kHz bandwidth) synchronized.
Acoustic signal digitization (24bit@96 kHz) at 2000m depth.
Data transmission on optical fibres over 28 km to the Catania lab on shore.
On-line monitoring and data recording on shore. Recording 5' every hour.
Data taking from Jan. 2005 to Nov. 2006 (NEMO Phase 1 deployed).

In collaboration with Uni-Pavia CIBRA

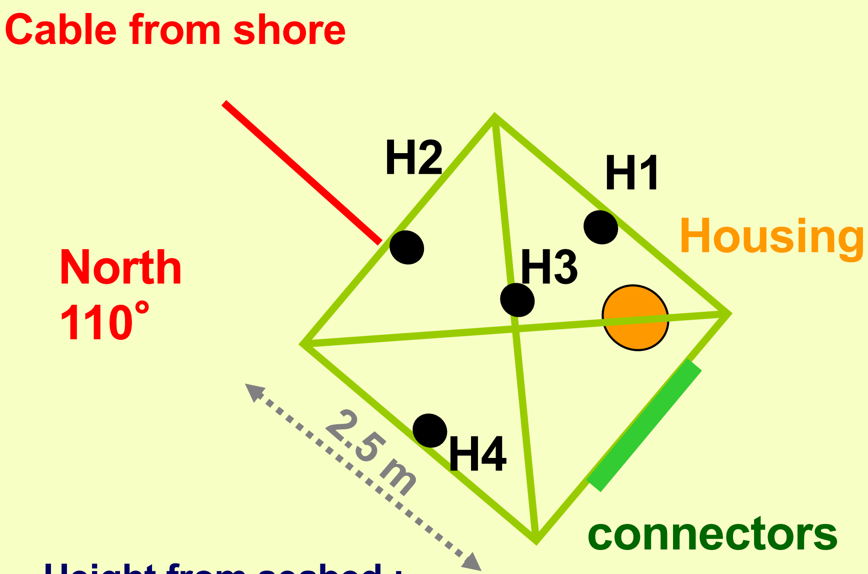

Height from seabed :
H1, H2, H4: ~ 2.6 m   H3: ~ 3.2 m

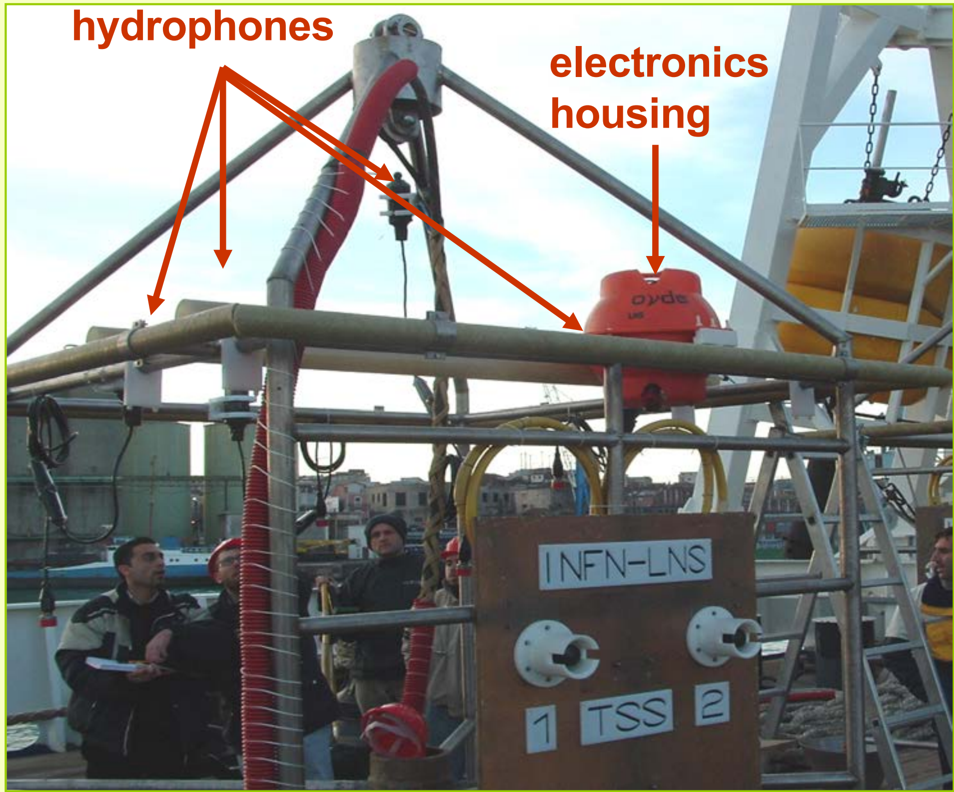

OνDE: Acoustic Noise measurement in the deep Sea

Ambient noise is generally made up of three constituent types:

- **Impulsive noise:** transient, wide bandwidth and short duration. Characterised by peak amplitude and repetition rate.
- **Continuous wideband noise:** Characterised by the SPD [dB re 1μPa^2/Hz]
- **Tonals:** narrowband signals, characterised as amplitude [dB re 1μPa] and frequency.

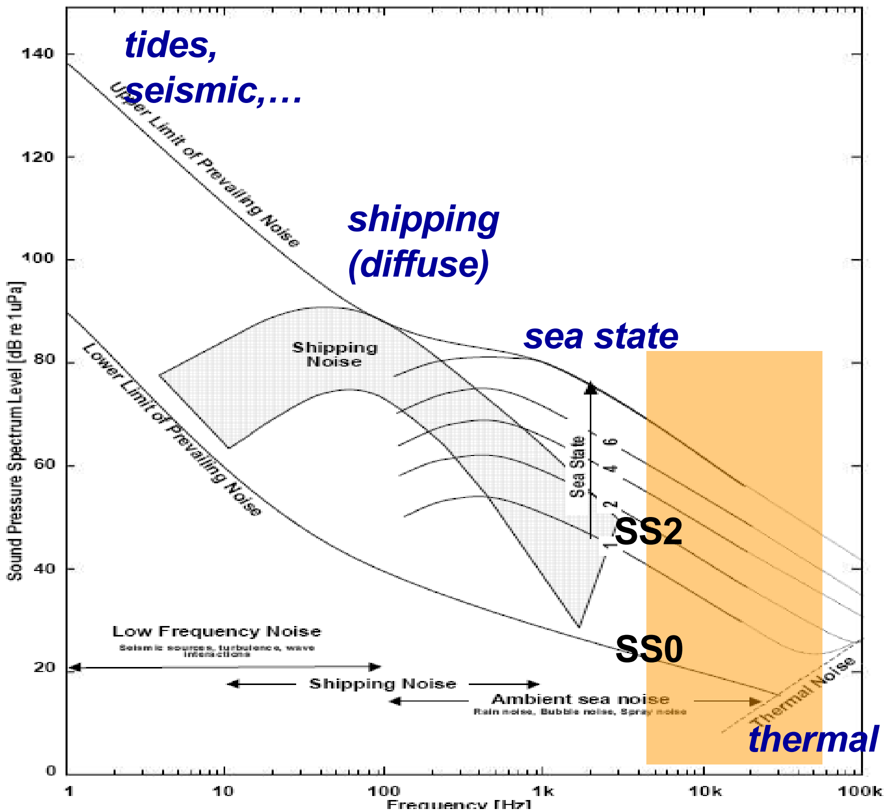

Major surces of noise

Diffuse noise: Seismic, surface waves (wind), rain, thermal noise

Impulisve Noise: Cetaceans, man made shipping (also diffuse!) and instrumentation

Man made noise is increasing (1 dB/year in densely inhabitated seas)

Knudsen's Formula

$$P(f_{Hz}, SS) = 10 \log f^{-5/3} + 94.5 + 30 \log(SS+1)$$

High Frequency Noise : Biological sources

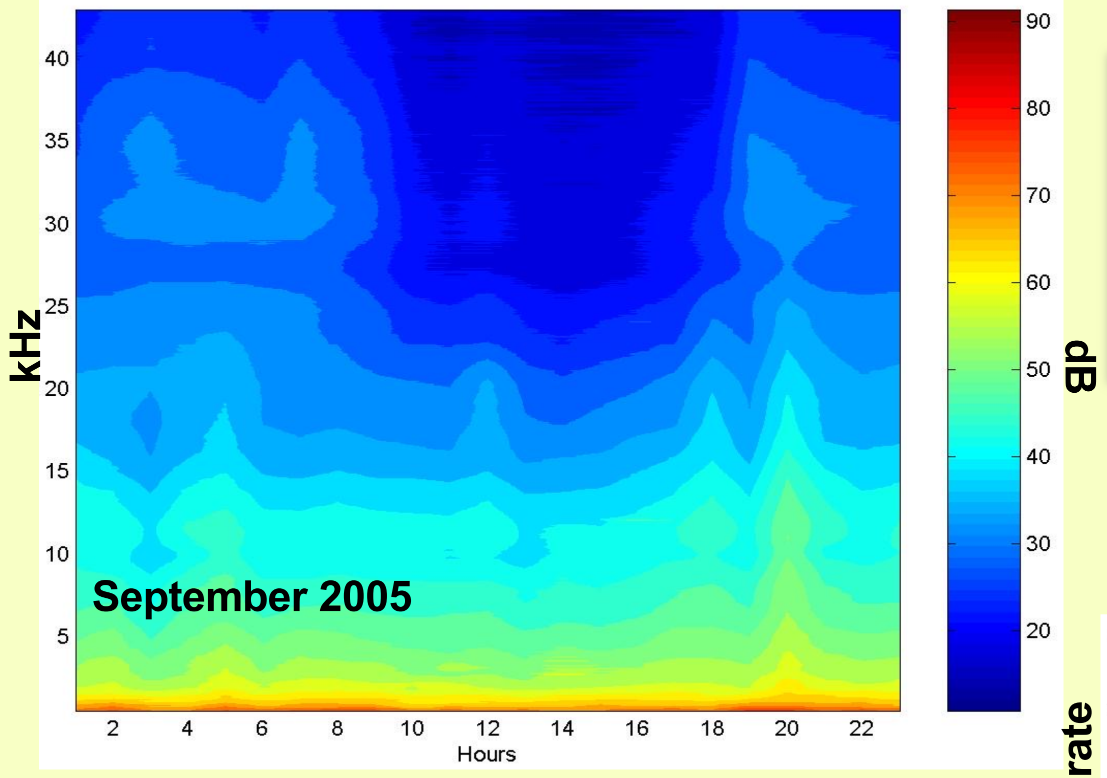

In the spectral region between 20 and 40 kHz we observe a day-night effect with upto 50% variations.

In this region dolphins give a strong contribution to noise

Preliminary

Independent CIBRA analysis:

Number of dolphins detected during day and night.

Night is the hunting time for dolphins

They emit both echolocalization clicks (>20 kHz) and whistles.

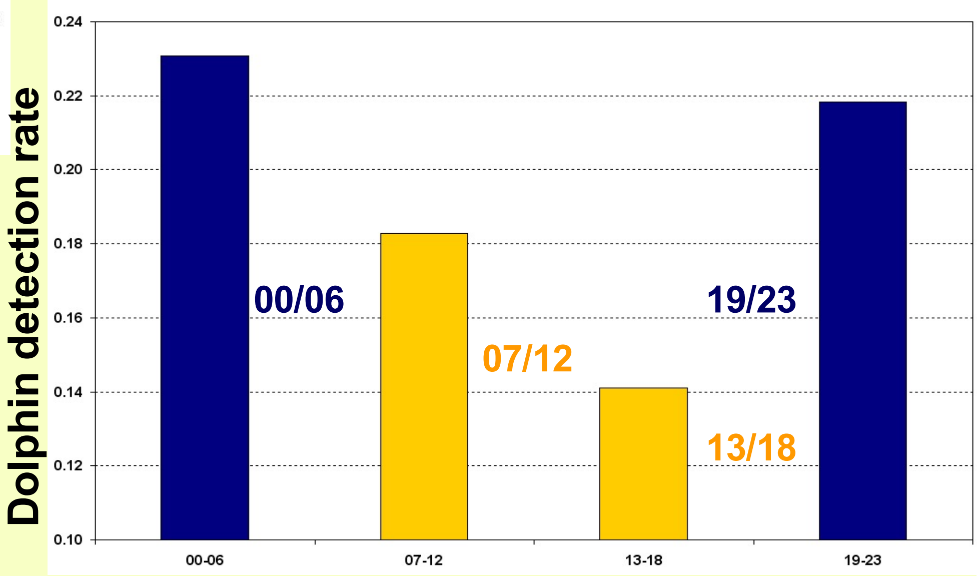

Bioacoustics: Sperm Whale detection in the Gulf of Catania

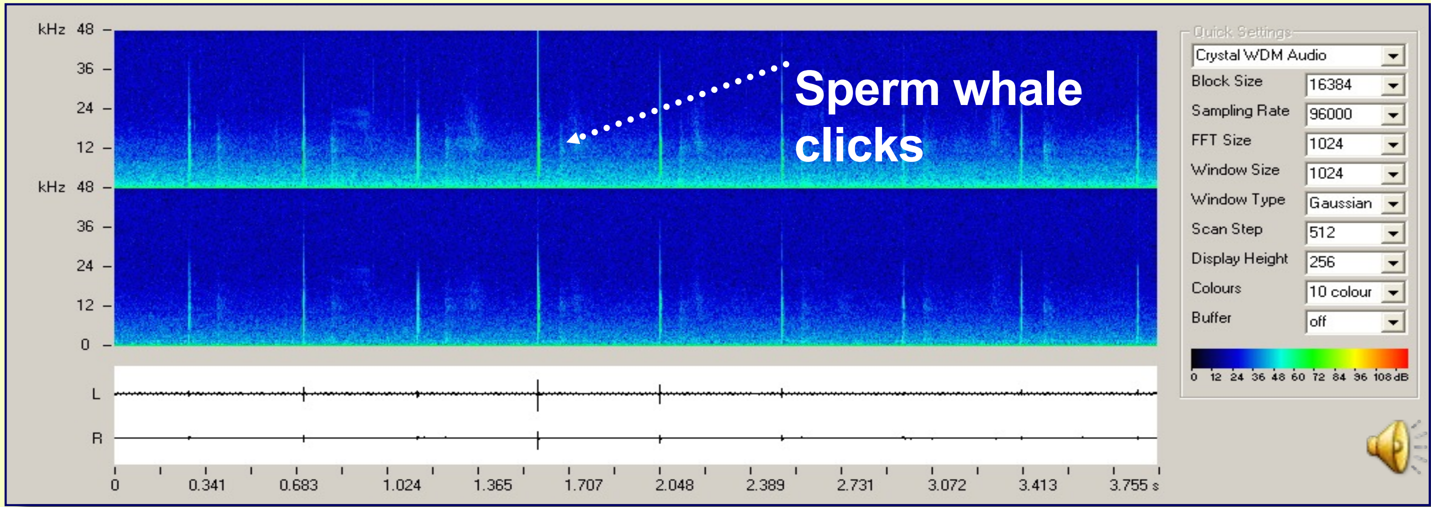

OνDE sensitivity allowed cetaceans detection over >40 km range.
The results indicate presence of sperm whales more frequent than previously observed.
Long term observation and source tracking is used to determine marine mammals presence and seasonal routes.

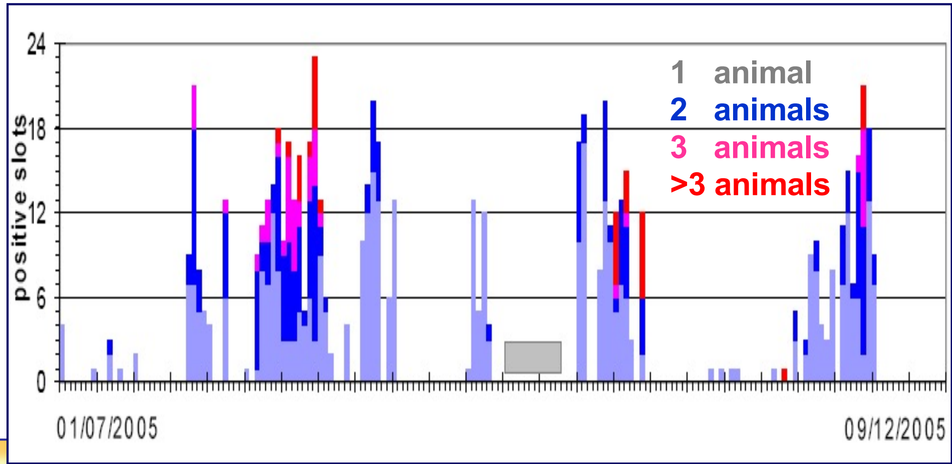

INFN and CIBRA

Science, March 2, 2007

Bioacoustics: Sperm-whale click analysis (a funny example)

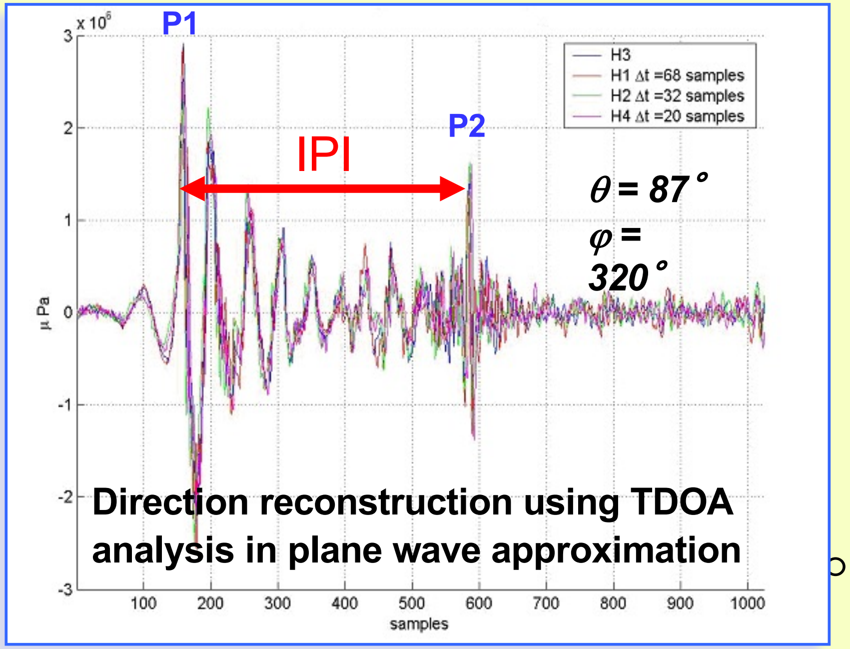

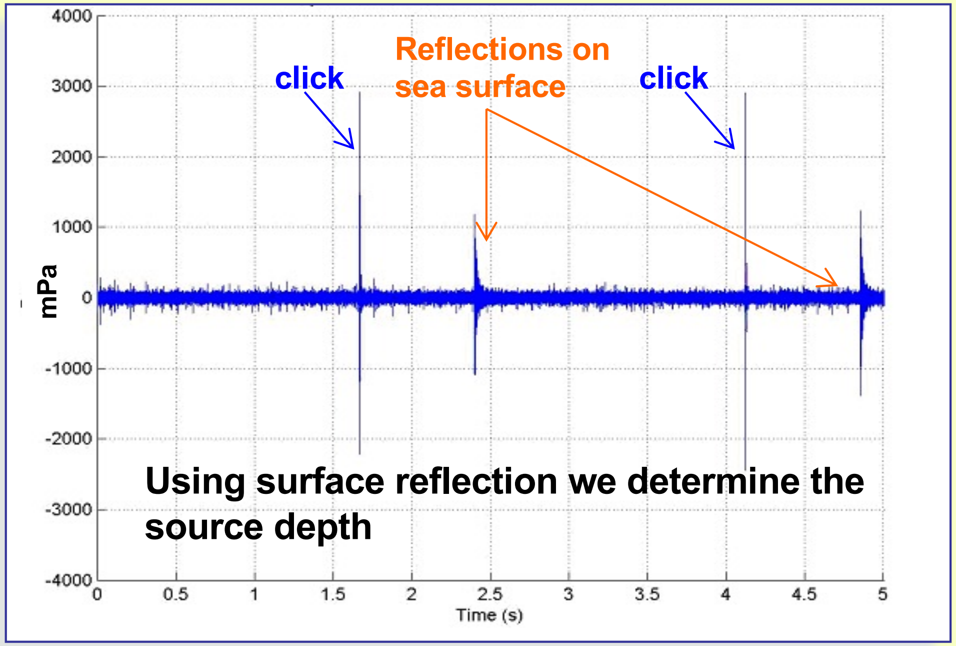

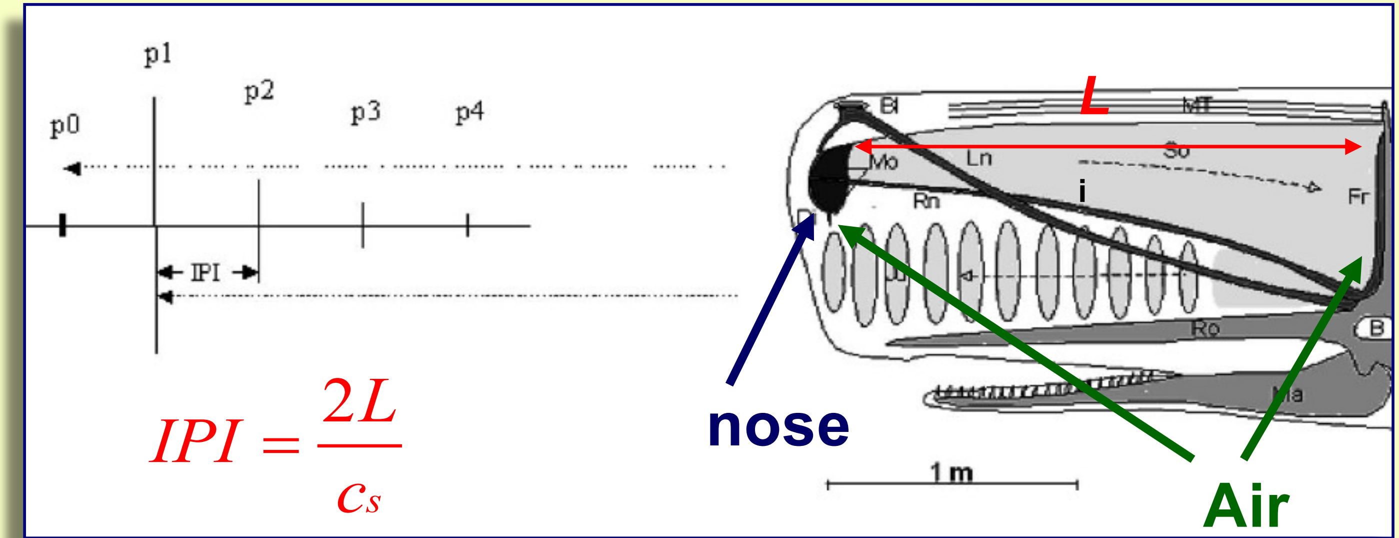

Depth = 560 ± 5 m

L = 3.41 ± 0.05 m

Size = 9.72 - 10.50 m

Young male or female

Acoustic - limits on UHE neutrino flux

Strategies:

- use standalone acoustic arrays (not always open science).
- Equip existing neutrino telescopes with test arrays:
  - Coincidences with conventional (optics) detection may help to study acoustic signal.
  - Particularly fits well with water Cherenkov – positioning system is acoustic-based.
  - Future hybrid detectors? Narrow “pan-cake” – great angular resolution for cascades.

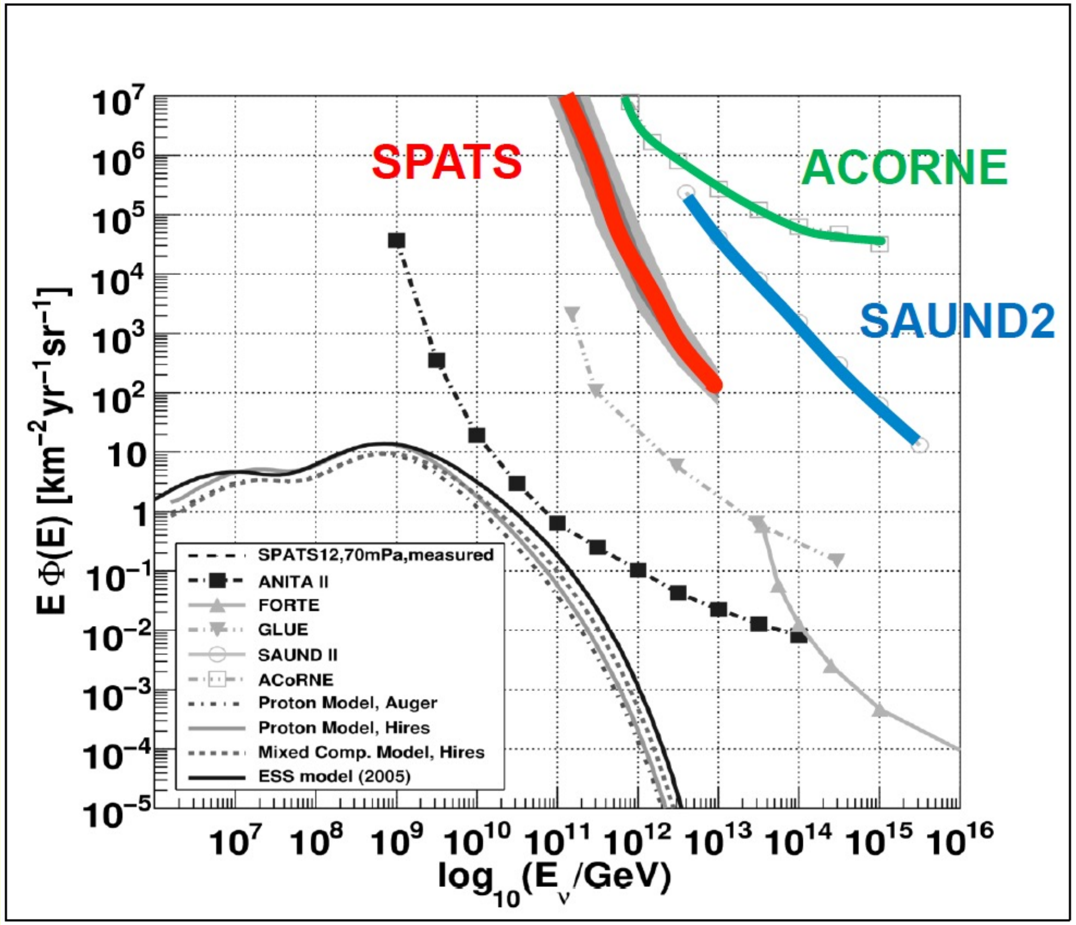

Currently only KM3NeT is active in this topic

Proposed/planned PeV-EeV radio neutrino detectors

~10 cosmogenic neutrino per km^2 per year + nu interaction length O(1000)km at 10^{18}eV

⇒ 0.005 detected neutrinos / km3 / year (considering half sky visibility since Earth is not transparent anymore).

⇒ We need 100's of km3 detection volumes

A. Connolly @ ARENA2018

running, planned

Air showers

- Radio (*interferometric*)
  - ***ANITA*** PoS(ICRC2019)867
  - *TAROGE* PoS(ICRC2019)967
  - *BEACON* PoS(ICRC2019)1033
  - GRAND PoS(ICRC2019)233
- Particles
  - **Auger** PoS(ICRC2019)979
- Cherenkov
  - **Ashra-1**, NTA (also fluorescence) PoS(ICRC2019)976
  - TRINITY PoS(ICRC2019)970
  - POEMMA PoS(ICRC2019)378

In-ice showers

- Radio
  - **ARA**, ARA5 PoS(ICRC2019)858
  - **ARIANNA**, ARIA PoS(ICRC2019)980
  - RNO PoS(ICRC2019)913
- Radar PoS(ICRC2019)986

Moon observations

- Radio
  - **NuMoon (WSRT, LOFAR)**
  - LUNASKA (**ATCA, Parkes**, SKA)
  - **RESUN (EVLA)**

Radio detection principle: the Askaryan effect

- EM shower in dielectric (ice) → moving negative charge excess
- Coherent radio Cherenkov radiation ($P \sim E^2$) if λ > Moliere radius

e^+, e^-, γ ⟶

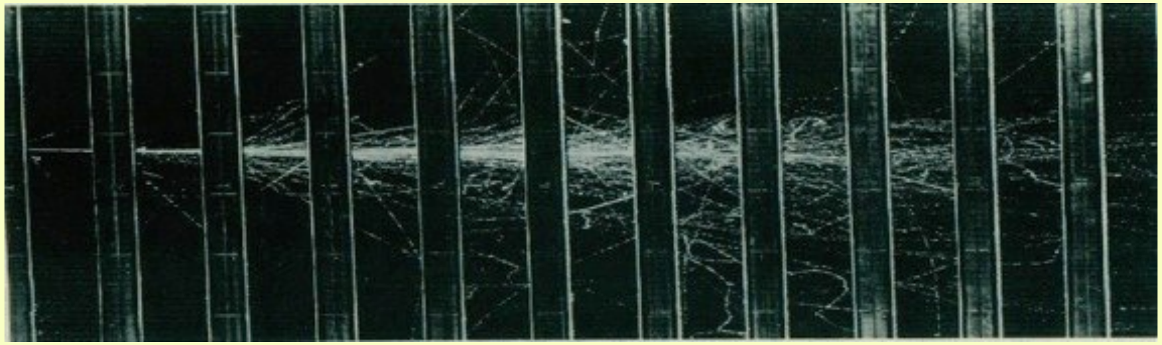

Typical Dimensions:
L ~ 10 m
$R_{moliere}$ ~ 10 cm

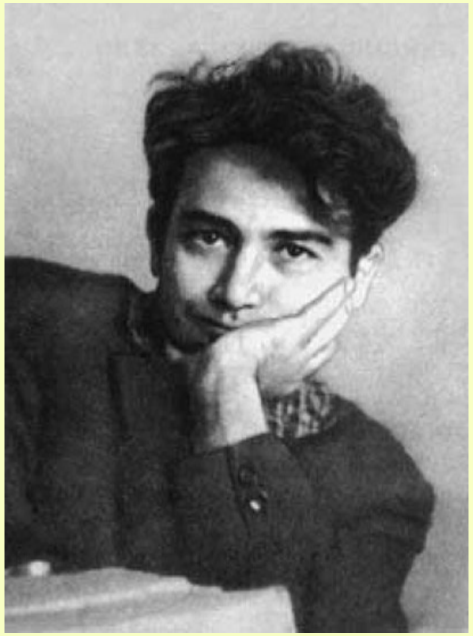

G. Askaryan

→ Radio Emission is much stronger than optical for UHE showers

Askaryan Effect Observed at SLAC

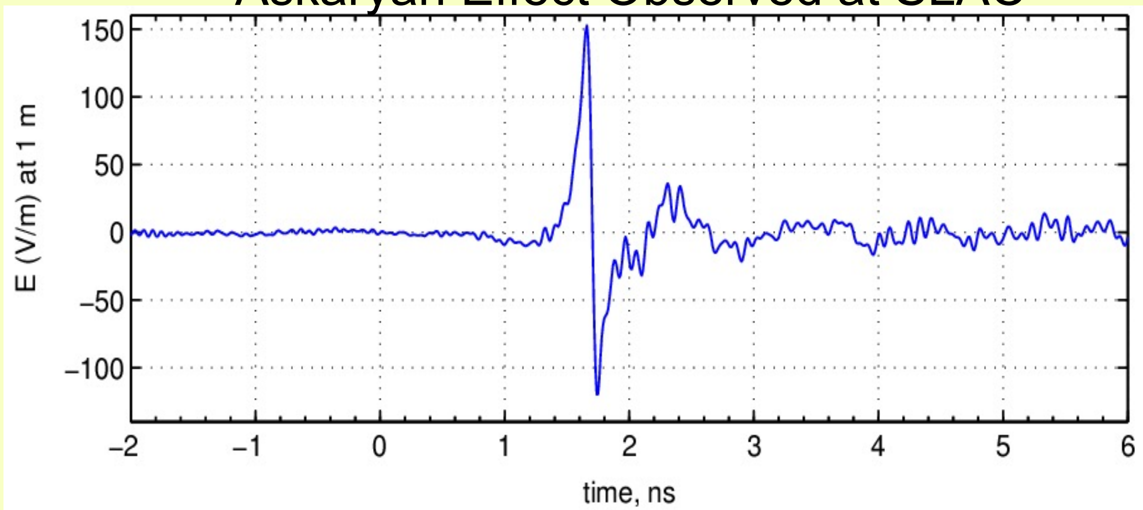

Radio signals from neutrino induced shower in ice

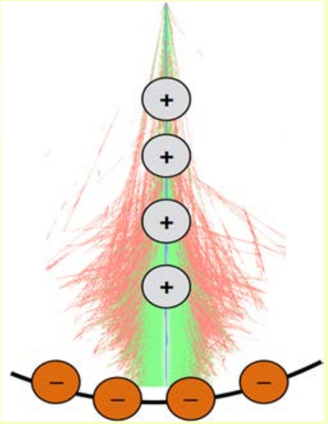

Any electromagnetic shower (component) creates radio emission.
- shower front accumulates negative charge from surrounding material
- macroscopically a changing current is induced (moving and changing net charge), this results in emission:
- emission is not caused by index of refraction, but
- emission is added up coherently for all observer angles at which the emission arrives simultaneously: emission strongest at the Cherenkov angle

Threshold: few PeVs.

Attenuation length: O(1 km).

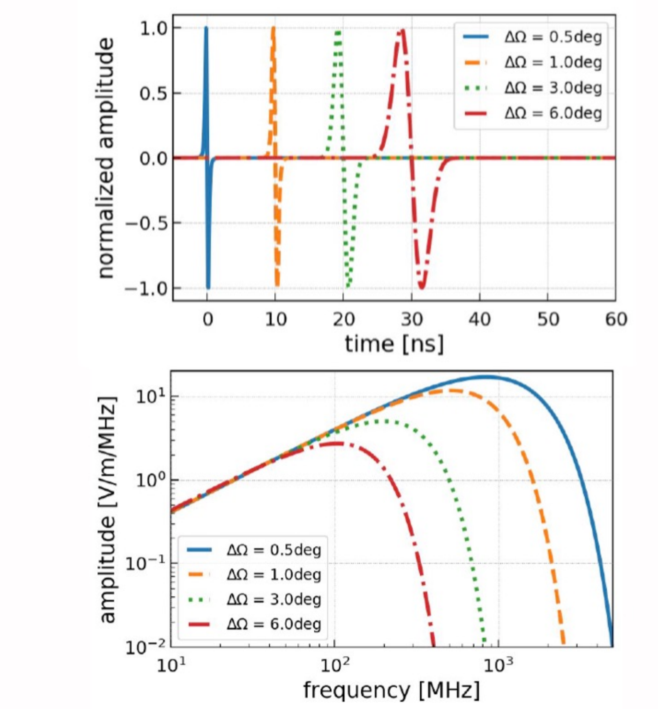

Askaryan radio emission properties in ice

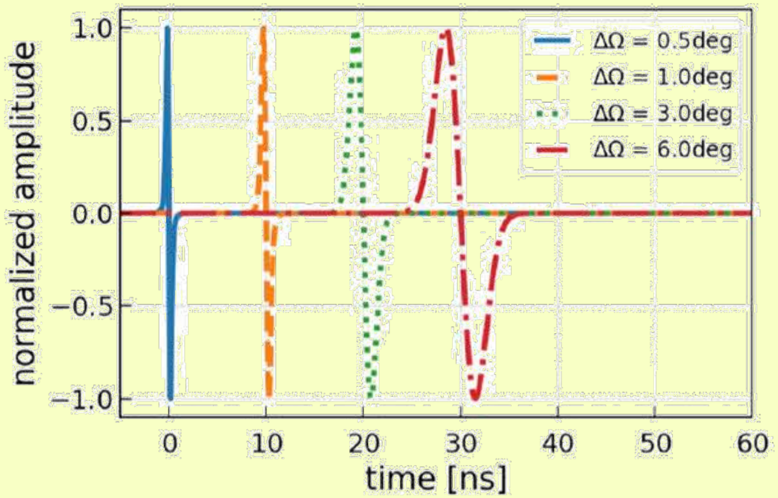

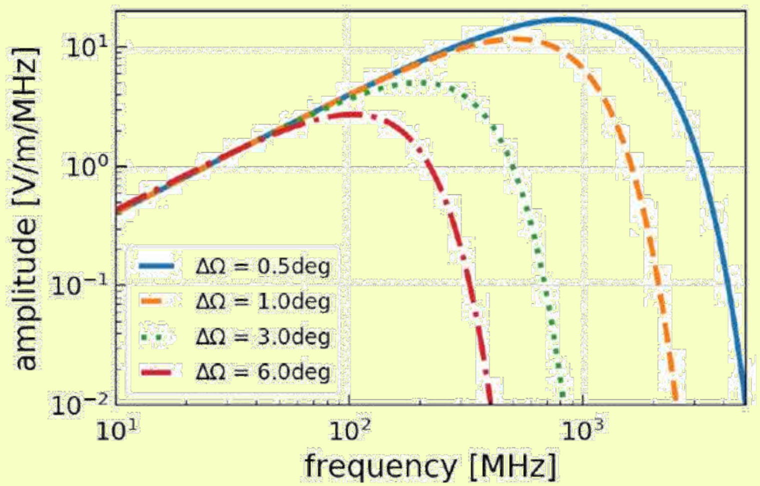

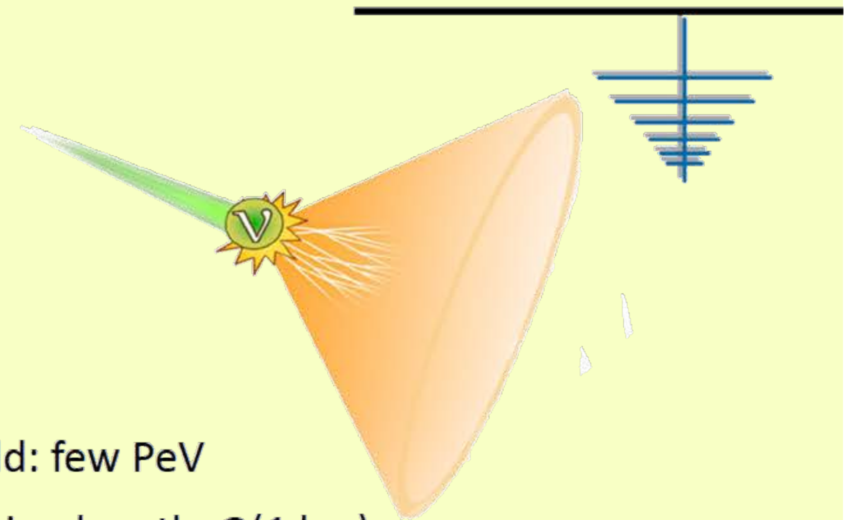

- Threshold: few PeV
- Attenuation length: O(1 km)

→ Cost-effective instrumentation for ultra-high energy (UHE) neutrinos (10^{16}-10^{20} eV)

C. Glazer @ ICRC20

Cone up to 56° (B. Price' webpage).

- Detection volume ~O(km^3) per modul

Radio detection in air

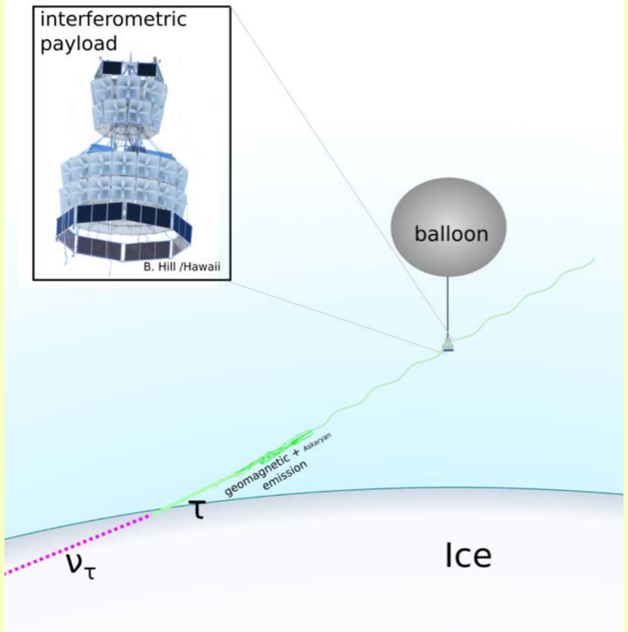

- Satellites:
  - ANITA
  - PUEO
- On mountain:
  - TAROGE
  - TAROGE-M
  - Grand
  - Beacon

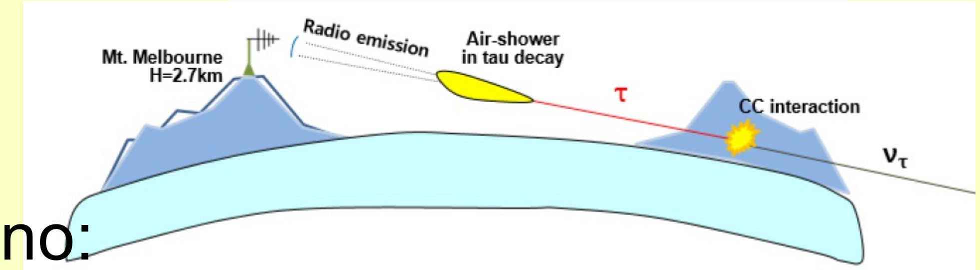

Sensitivity mostly to tau neutrino:

- Earth is not opaque to neutrinos for E>10 PeV.
- Signal is in the forward region.
  - Earth-skimming
  - Interacting in the mountains.
- Tau can escape the interaction medium (rock) and produce shower in the light propagating medium (air/ice).

ANITA

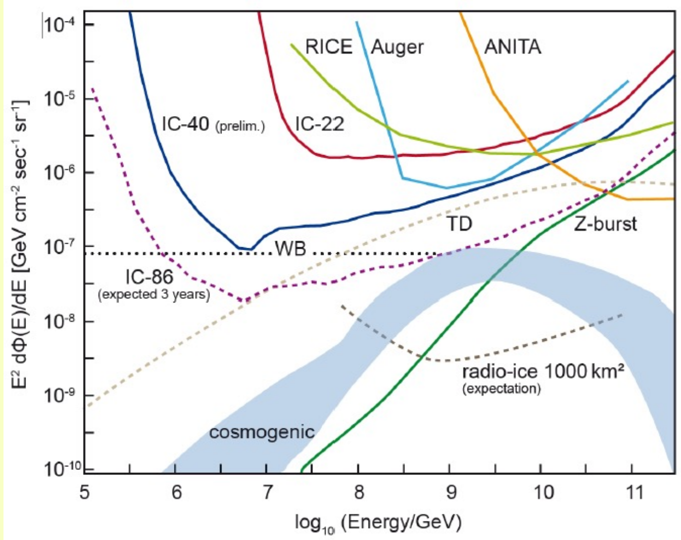

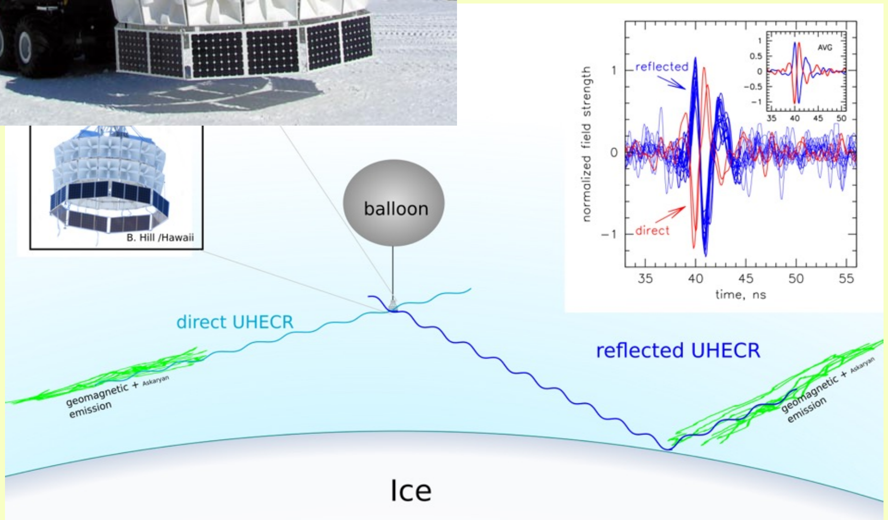

Signals are horizontally polarized

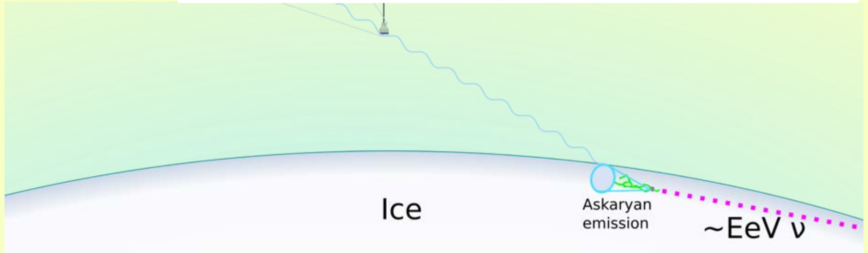

Signals are vertically polarized

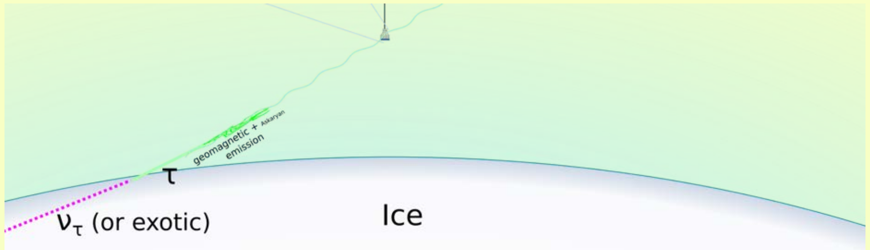

Signals are horizontally polarized
Comes from below the horizon

Polarity of reflected (below horizon) signal is inverted compared to direct (above-horizon) signal and tau neutrino (below-horizon) signal

Two of those are seen (ANITA-III, ANITA I
Background ~1.4.

ANITA-I & ANITA-II: best limit > 10^{19} eV

NASA Long Duration Balloon, launched from Antarctica

ANITA-I: 35 day flight 2006-07

ANITA-I: 30 day flight 2008-09

Instrument Overview:

- 40 horn antennas, 200-1200 MHz
- Direction calculated from timing delay between antennas
- In-flight calibration from ground
- Threshold limited by thermal noise

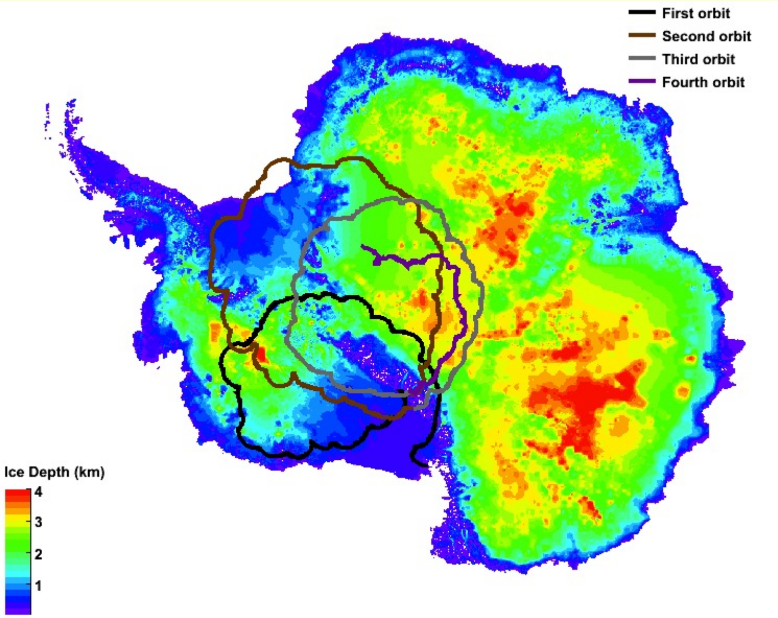

UHE Neutrino Search Results:

	ANITA-I	ANITA-II
Neutrino Candidate Events	1	1
Expected Background	1.1	0.97 +/- 0.42

ANITA- 2014

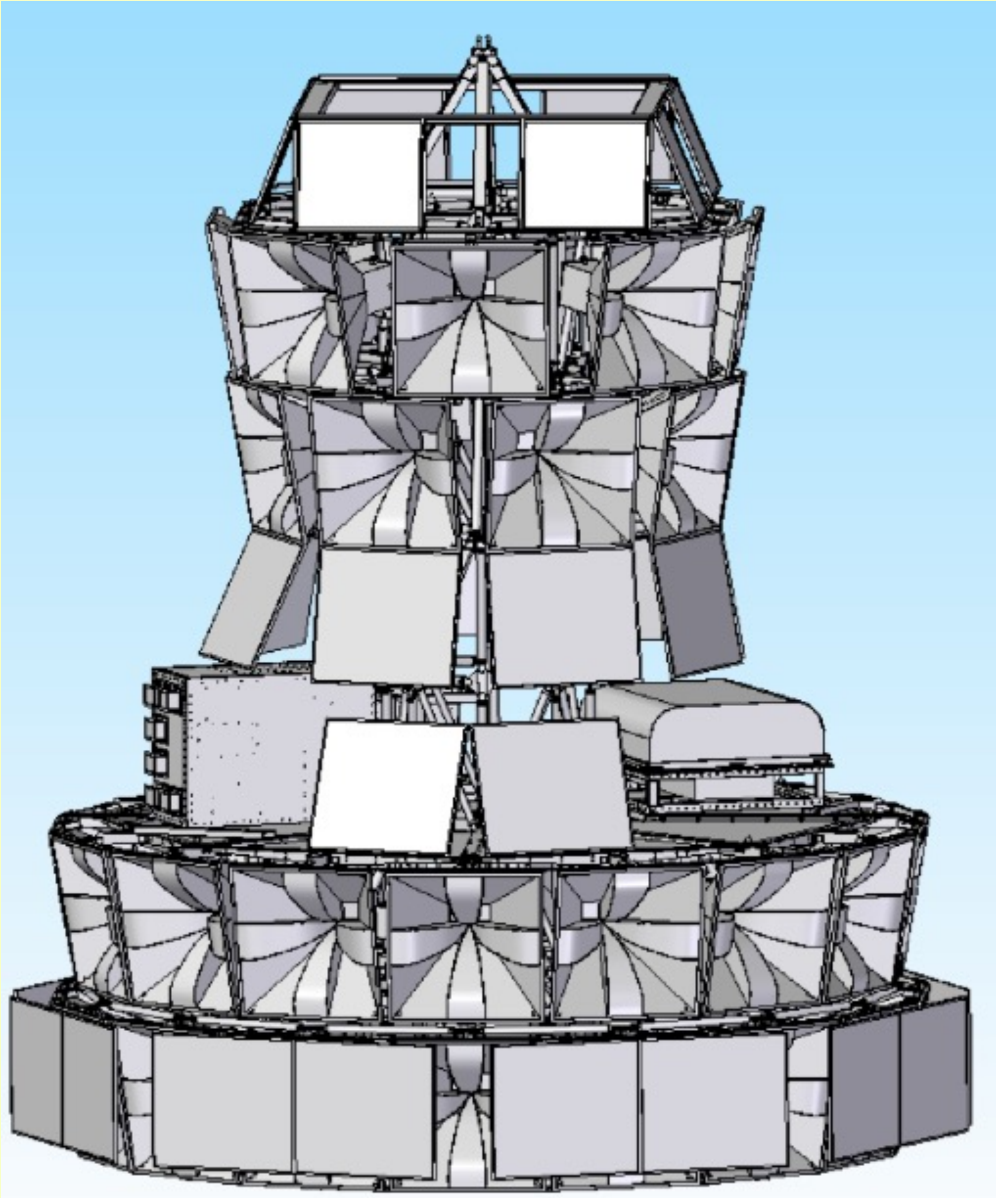

- Flight scheduled 2014
- More antennas
- Digitize longer traces
- New: interferometric trigger
- Lower noise front-end RF system

→ Factor of 5 improvement in neutrino sensitivity compared to ANITA-II

Result: arXiv:2010.02869v2:
»..there is no significant evidence for any source-associated neutrinos with ANITA- III ...»